Modeling Hydrodynamic Fluxes in the Nueces River Delta

Publication CBBEP – 75

October 2011

Prepared by:

Andrea J. Ryan, M.S.
Ben R. Hodges, Ph.D.

Center for Research in Water Resources
The University of Texas at Austin

Submitted to:
Coastal Bend Bays & Estuaries Program
1305 N. Shoreline Blvd., Suite 205
Corpus Christi, TX 78401

Modeling Hydrodynamic Fluxes in the Nueces River Delta

Andrea J. Ryan, M.S.
Ben R. Hodges, Ph.D.

Center for Research in Water Resources
The University of Texas at Austin

CRWR Online Report 11-7
Submitted to the Coastal Bend Bays and Estuaries Program
Nueces Delta Hydrodynamics Modeling, Contract #1001
October 10, 2011

Executive Summary

Municipal and regional water use has reduced freshwater inflows to the Nueces Delta. The flow reductions have lead to increased salinities that impair the marsh ecosystem's functionality. As part of a United States Army Corps of Engineers multi-agency collaboration to restore the Nueces River and its tributaries, we have developed a hydrodynamic model to analyze fate and transport of freshwater and tidal inflows to the Nueces Delta. The model's geographic basis is the LiDAR bathymetric data collected by the Coastal Bend Bays and Estuaries Program. Input data includes tidal, salinity, and wind data obtained from the Texas Coastal Ocean Observation Network and the Conrad Blucher Institute, pumping data from the Nueces River Authority, precipitation data from NOAA, and river flow from the USGS.

The model uses conservative finite-difference/volume discretization on a Cartesian rectangular grid to simulate the movement of water and salt fluxes across the delta. Sub-models to represent the hydraulic influence of flow constrictions (e.g. railroads trestles, culverts) have been developed. In this report, the model's response to forcing from wind, precipitation, boundary roughness, and freshwater pumping through the Rincon Pipeline Diversion are analyzed. The model validation analyses conducted to date are qualitative, but the overall tidal trends are in reasonable agreement with the limited available validation data. Quantitative model calibration and has not been possible as available data has insufficient spatial coverage. Additional data collection for calibration and validation is recommended to apply the model for operational water management.

Acknowledgments

This project was funded by the Coastal Bend Bays and Estuaries Program, with support of the City of Corpus Christi and the U.S. Army Corps of Engineers. Some work related to subgrid-scale roughness was developed under National Science Foundation Grant No. 0710901. Any opinions, findings, and conclusions or recommendations expressed in this material are those of the author(s) and do not necessarily reflect the views of the National Science Foundation or any other sponsor. This technical report is a modified version of the M.S. thesis submitted by the first author to the University of Texas at Austin (Ryan 2011); for clarity, further citations of the antecedent document are omitted.

Table of Contents

1 Introduction

1.1 Overview

This report presents results and analyses of the Nueces Delta Hydrodynamic Model (NDHM), which was designed to simulate the hydrodynamic conditions in the Nueces Delta near Corpus Christi, Texas. This model addresses the effects of freshwater pumping from the Rincon Diversion Pipeline, tidal inundation, wind-driven flows, and rainfall runoff from the nearby uplands. The model was built on the framework of the PC2 Hydrodynamic Code, v6.0, developed at the Center for Research in Water Resources (CRWR), University of Texas at Austin. The NDHM was created as part of a series of projects focused on restoring the Nueces Delta ecosystem and understanding the movement of fresh and saltwater through the system. This report demonstrates how the NDHM provides a framework for investigating the transport and fate of freshwater introduced in restoration projects.

1.2 Background

The Nueces River estuarine system includes the Nueces Delta, the Nueces River tidal segment, Corpus Christi Bay, Nueces Bay, Oso Bay, and Redfish Bay (Figure 1.1). The estuary is fed by the river systems impounded in the Choke Canyon Reservoir and Lake Corpus Christi (Figure 1.2). The former was completed in 1982, the latter in 1958 (Bureau of Reclamation 2000b). A smaller impoundment at Calallen near the upstream end of the Nueces Delta was constructed in the late 1800's by the Corpus Christi Water Supply Company to prevent saltwater from intruding upstream and contaminating the city's drinking water (Cunningham 1999).

This report focuses on the Nueces Delta, also known as the Nueces Marsh, covering approximately 75 square kilometers of vegetated marshes, mudflats, tidal creeks and shallow ponds (Bureau of Reclamation 2000b). A river delta is commonly the principal path through which a river enters into the broader embayments of an estuary. However, a combination of natural and anthropogenic alteration around Corpus Christi has left the Nueces Delta substantially cutoff from the main flow of the Nueces River into Nueces Bay by embankments that limit flooding (Heilman, et al. 2000). See Bureau of Reclamation (2000a) for a more detailed description of the Nueces Delta and its environs.

An estuary is the transition zone where salt water from the sea mixes with freshwater inflows from rivers, typically with low salinity where the river enters the estuary and increasing salinity towards the sea (Montagna, Merryl, et al. 2002). The balance of freshwater inflow working against tidal forcing generally determines the upstream estuarine salinity distribution (Alber 2002). However, high evaporation rates in hot climates, combined with limited rainfall and low freshwater inflows can create inverse estuary effects, where salinity patterns are reversed with hypersaline conditions upstream. Inverse estuary conditions have been documented in the Nueces Delta (Montagna, Kalke and Ritter 2002, Palmer, Montagna and Kalke 2002), arguably due to the combination of climate, landscape changes, and freshwater inflow reductions.

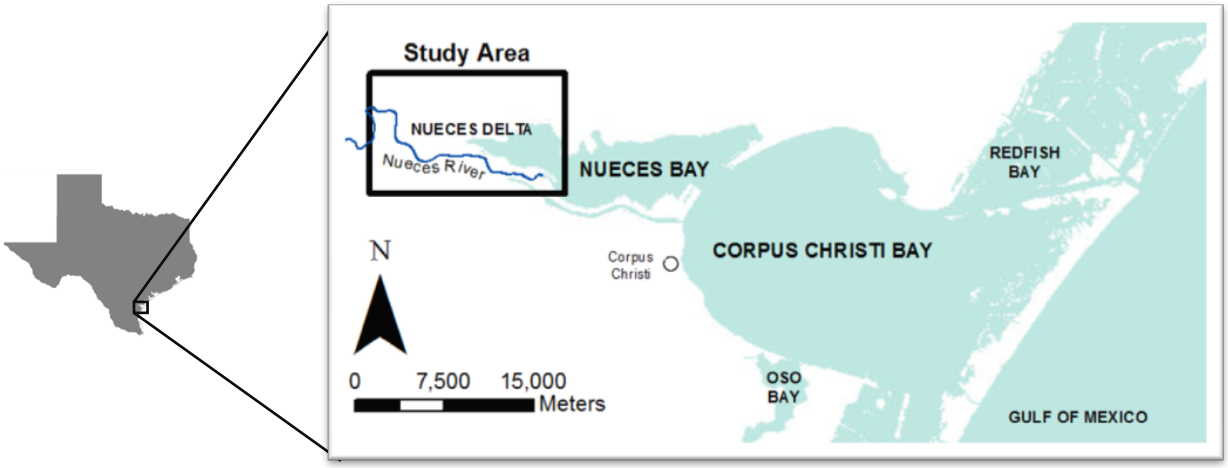

Figure 1.1: Location of the Nueces Delta

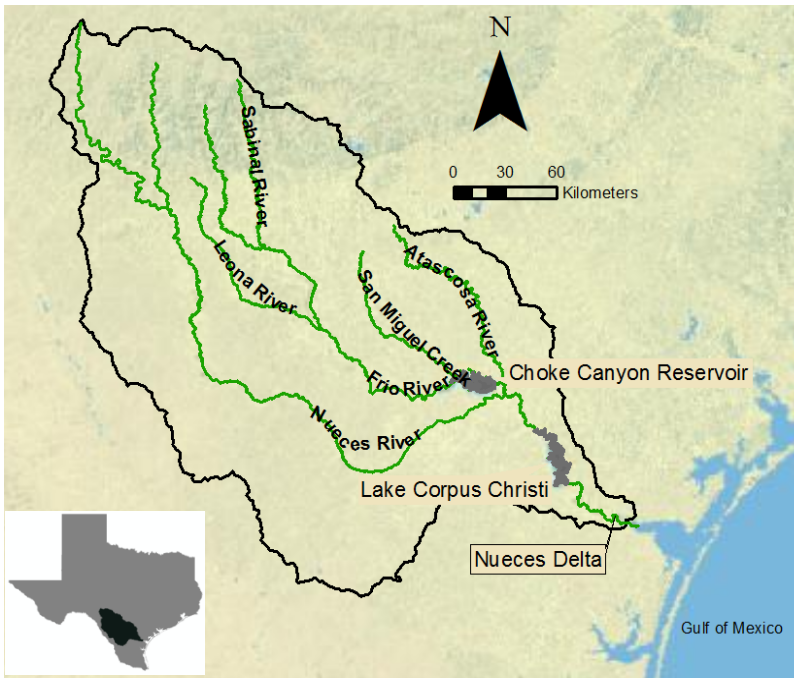

Figure 1.2: Major Rivers and Reservoirs in the Nueces Basin

Since the final dam was completed in 1982, the average annual freshwater inflow to the upper Nueces Delta has decreased by 99% compared to pre-impoundment conditions, i.e. before 1958 (Irlbeck and Ward 2000). Decreasing freshwater inflows often has a negative effect on estuarine ecology through increasing salinity (Copeland 1996), which has been documented for the Nueces Delta; the Rincon Bayou, a creek located in the upper Nueces Delta, has seen salinities ranging from 0 - 160 ppt and temperatures as high as 40^{o} C (Montagna, Kalke and Ritter 2002). The hypersaline conditions have had

demonstrable negative ecosystem effects (Alexander and Dunton 2002). From a simple heat and salt balance perspective, it can be argued that increasing hypersaline episodes will continue in the upper Nueces Delta unless the overbank flooding frequency is increased and/or sufficient freshwater can be introduced through the Rincon Pipeline Diversion.

1.3 Nueces Delta Projects

1.3.1 Introduction

Since 1987, several projects have focused on restoring aspects of the Nueces Delta ecology (Figure 1.3). The Nueces Delta Mitigation Project (§1.3.2) excavated an area to restore a salt marsh habitat in the lower delta. The Rincon Bayou Demonstration Project (§1.3.3), the reopening of the Rincon Overflow Channel (§1.3.4), and the Rincon Pipeline Diversion (§1.3.5) were each designed to increase freshwater inflows to the upper delta. The Allison Wastewater Treatment Plant Diversion (1.3.6) involved piping nutrient-rich water to the middle delta.

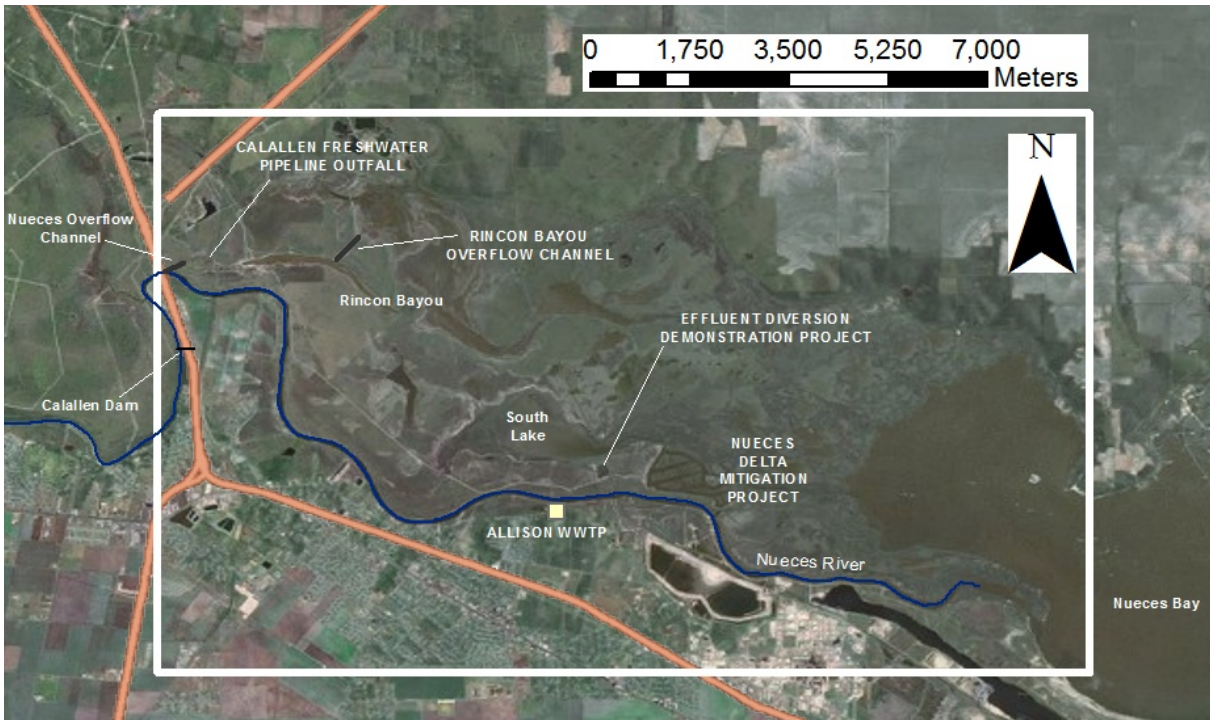

Figure 1.3: Nueces Delta restoration and mitigation projects

1.3.2 Nueces Delta Mitigation Project

The United States Army Corps of Engineers (USACE) and the Corpus Christi Port Authority conducted the Nueces Delta Mitigation Project in March 1987 as an effort to reduce wetland losses due to dredging in the Corpus Christi Ship Channel (Alan Plummer Associates, Inc. 2007). The objective was to create a salt marsh that could provide a

wetland habitat. An area of 198 acres was excavated to create a network of levees, channels and ponds simulating natural salt marshes (Nicolau, et al. 1996). While the Nueces Delta Mitigation Project did not provide new *Spartina alterniflora* habitat (an important marsh species in the delta), the project did produce significant non-vegetated bay bottom habitat (Nicolau, et al. 1996).

1.3.3 Rincon Bayou Demonstration Project

The U.S. Bureau of Reclamation conducted the Rincon Bayou Demonstration Project in October 1995 to increase freshwater inflows from the Nueces River to the Nueces Delta (Bureau of Reclamation 2000a). Within the demonstration project, the connection between the Nueces River downstream of the Calallen dam and the Rincon Bayou was excavated to form the Nueces Overflow Channel. The bottom elevation in the excavation was approximately mean sea level (Bureau of Reclamation 2000b). A second channel, the Rincon Overflow Channel, was excavated further downstream in the Rincon Bayou, providing a spillway to tidal mudflat areas located north of the bayou. The resulting increase in freshwater inflows had positive ecological effects in the Rincon Bayou and upper Nueces Delta. Over time, the freshwater inflows reduced salinities in the delta. However, the project did not have permanent easements over private property so the channel was closed in September 2000 (Montagna, Hill and Moulton 2009).

1.3.4 Reopening the overflow channels

Because of the success of the Rincon Bayou Demonstration Project (§1.3.3), a program to purchase property and obtain easements from property owners was undertaken, with the overflow channels from the Demonstration Project re-opening in October 2001. The overflow channels are now permanent features of the Nueces Delta (Alan Plummer Associates, Inc. 2007).

1.3.5 Rincon Pipeline Diversion from Calallen

Only two estuarine systems on the Texas Gulf Coast, the Nueces Estuary and the Colorado Estuary, have explicit bay and estuary freshwater inflow volume requirements attached to water rights (Tolan 2007). Based on the 1995 Agreed Order with the Texas Natural Resource Conservation Commission, the City of Corpus Christi is required to pass through freshwater to sustain the ecosystems (Adams and Tunnell 2010). To manage the Agreed Order freshwater inflows to the Nueces Delta, in 2008 the City of Corpus Christi constructed a pipeline and pumping station to divert water from the Calallen pool to the upper Rincon Bayou. Three pumps are installed, each capable of pumping approximately 1.5 m^3/s (109 acre-ft/day). Under normal operation only one or two pumps are typically in used (J. Tunnell, pers. comm.)

1.3.6 Allison Wastewater Treatment Plant Diversion Project

The Allison Wastewater Treatment Plant, located on the south bank of the Nueces River tidal reach, has historically discharged secondary treated municipal wastewater effluent to the Nueces River since the plant's construction in 1966 (Alan Plummer Associates, Inc. 2007). In an effort to provide high-nutrient freshwater to the delta, the City of Corpus Christi created a pipeline under the Nueces River to divert water from the

treatment plant to the delta. In August 1997, the City constructed three earthen cells to receive treated effluent in the Lower Nueces River Delta. The diversion began in October 1998, diverting approximately 2.0 MGD (Montagna, Hill and Moulton 2009). A study on the effects of the wastewater diversion project found that there were no detrimental impacts on the marsh, but that more wastewater must be diverted if substantial reduction in downstream salinity downstream is to be achieved (Alexander and Dunton 2006). The Allison Wastewater Treatment Plant Diversion Project was completed in August 2003 (Nicolau, et al. 2002).

1.4 Hydrodynamic model

1.4.1 Introduction

Prior to the present study, a comprehensive numerical model of flow and transport in the Nueces Delta using the shallow-water equations had not been attempted. The Bureau of Reclamation report for the Rincon Bayou Demonstration Project notes the opportunity for a numerical model to integrate the data components of the study and improve understanding of the marsh under various conditions (Bureau of Reclamation 2000b). The study presented here fills the need for a hydrodynamic model of the Nueces Delta to examine the impacts of changes in flow to the Delta, including inflows from the Rincon Pipeline, tidal flows, and rainfall.

1.4.2 Other estuarine models

A variety of numerical models have been used to simulate hydrodynamic conditions in estuaries (e.g. Table 1.1). For estuarine embayments and rivers without significant estuarine marshland the key modeling challenges are in representing tidal and river fluxes (e.g. Spillman et al 2008, Zhan et al 2004, respectively). However, marshland with significant wetting/drying of the landscape provides numerical challenges addressed in fewer models, most notably Yang and Khangaonkar (2009), Battjes (2006), Ji, et al (2001), Oey (2006), Casulli and Zanolli (2002).

1.4.3 PC2 Method

The estuarine models in Table 1.1 all use the hydrostatic Navier-Stokes equations (also known as the shallow water equations) to solve conservation of momentum and mass. A common numerical approach in several models is the semi-implicit algorithm using implicit discretization for the free surface (barotropic mode) and explicit discretization for the velocity and baroclinic forcing (internal wave), e.g. Casulli and Cheng (1992). This approach is generally implemented in a first-order accurate scheme for unsteady and baroclinic flows (Hodges 2004). By restructuring the semi-implicit algorithm for a predictor-corrector sweep, the semi-implicit θ-method (Casulli and Cattani, 1994) can be improved to 2nd order for both barotropic and baroclinic flow (Hodges and Rueda 2008). The PC2 Hydrodynamic Code used for the NDHM employs predictor-corrector methods using two time-levels of information (Hodges and Rueda 2008). It has volume-consistent discretization of both barotropic and baroclinic modes, along with mass-conserving scalar transport. The model can be implemented in either 2D or 3D, and using either first-order or second-order accurate numerical algorithms. During development of the NDHM, the PC2 Hydrodynamic Code was applied in 2D (depth-averaged) with first-order

algorithms. This approach ensured the fastest model simulation time, which is an advantage during model development.

1.5 Study objectives

The main objectives of this study were

1. Create a model of flow and transport through the Nueces Delta.
2. Examine the model sensitivity to different forcing conditions.

1.6 Organization of this technical report

This technical report provides documentation of the approach used in applying the NHDM to the Nueces Delta and an analysis of results. Section 2 presents the modeling methodology, including sources of input data, selection of modeled scenarios and analysis metrics. Detailed information on input sources and data analysis techniques are provided in Appendices A and B. Analysis of model results is provided in §3. Findings and recommendations for future work are provided in §4, with additional technical details in Appendix 0. The complete Matlab™ programming scripts used for data analysis are provided in Appendix C.

1.7 Caveat

Due to the lack of sufficient field data, the NDHM could be neither calibrated nor validated for the present study. Recommendations regarding the types of data needed for calibration and validation are provided in §4.2. However, because the model is mechanistic, the present uncalibrated results are still useful in model-model comparisons to investigate the system's sensitivity to different forcing conditions, which is the focus of this report.

Table 1.1: Prior numerical models created for simulating estuarine environments

Model	Area	Dimen-sion	Focus	Used by:
FVCOM	Skagit River Estuary, Puget Sound, WA	3D	Tidal circulation & transport processes	Yang and Khangaonkar 2009, Chen, Liu and Beardsley 2003
ECOM-si	Satilla River Estuary, Georgia	3D	Semi-implicit finite difference scheme; realistic vertical turbulent mixing parameters	Zheng, Chen and Zhang 2004
ELCIRC	Columbia River Estuary	3D	Turbulence closure schemes; includes terms for the tidal potential and atmospheric pressure gradients, and provides a detailed description of air–water exchanges	Zhang, Baptista and Myers 2004
Environmental Fluid Dynamics Code (EFDC)	Morro Bay, James River Estuary	3D	Provides a hydrodynamic model with water quality model, sediment transport model, and toxics model capabilities	Ji, Morton and Hamrick 2001
Princeton Ocean Model (POM)	Cook Inlet, Alaska	3D	Movable land-sea boundaries	Oey 2006
Delft-FLS	Polders of Tiel and Culemborg, Netherlands	2D	Specifically suited to simulate overland flow over initially dry land	Stelling, Kernkamp and Laguzzi 1998
TRIM	Barbamarco Lagoon, Italy	3D	A stable semi-implicit finite difference method of discretization computationally suitable for spatially fine grids with relatively large time steps	Casulli and Cattani 1994, Casulli and Cheng 1992
ELCOM-CAEDYM	Barbamarco Lagoon, Italy	3D	Provides a hydrodynamic model coupled with an aquatic ecosystem model; includes external environmental forcing	Spillman, Hamilton, Hipsey and Imberger 2008

This page intentionally left blank for two-sided printing.

2 Methodology

2.1 Introduction

This section provides: 1) an explanation of the types of input data required to run the NDHM, 2) a discussion and documentation of the scenarios modeled, and 3) details on the data analysis methods. The model input files are developed to reflect bathymetric, inflow, and meteorological conditions in the delta, but these are inherently limited by the availability of data and its spatial/temporal distribution. Hydraulic effects, such as overtopping of dikes or flow through bridge piers, are not readily represented by the shallow water equations at the practical model resolution and are handled by customized sub-models of the NDHM. Scenarios were selected to exercise a range of conditions to ensure NDHM responded appropriately to changes in forcing. Analysis methods were designed to compress the 3-dimensional data set (space, time, transported variables) into statistical representations that can be readily compared.

2.2 Model input data

2.2.1 Overview

There are several types of input: boundary data, forcing data, parameters, and initial conditions. Boundary data, such as land surface elevation (bathymetry) and surface roughness, vary across space but are constant over time for a model run. Forcing data accounting for wind, tide, precipitation and inflows vary in time, but are provided either at fixed points in space (e.g. tide) or are uniformly distributed over the entire domain (e.g. wind). Parameters are used to change the model representation of the physics, such as the time step and the wind drag coefficient. Initial conditions are the distribution of salinity and water depth across the delta at the start of the simulation.

The methodology for determining the boundary data, initial conditions, and forcing data for the Nueces Delta is outlined below in §2.2.2 - 2.2.4. Details for data preparation, are provided in Appendix A.

2.2.2 Data for land surface elevation (bathymetry)

A river delta is an intersection between wet and dry land, and thus where topographic descriptions of "land surface elevation" meet a bathymetric description of "water depth." Herein we will generally use the term "bathymetry" to indicate the elevation above the zero datum of the landscape (NAVD88), whether covered with water or dry.

The best available bathymetry for the Nueces Delta is a 1 x 1m raster data set prepared by J. Gibeaut at Texas A&M Corpus Christi from LiDAR data collected under a project funded by the Coastal Bend Bays and Estuary Program. This bathymetry was previously processed and validated against field measurements by J. Gibeaut (personal comm.). The 1 x 1 m data set consists of 105×10^6 elevations within the Nueces Delta and the nearby uplands. Extrapolating from recent experience, in its present configuration the PC2 Hydrodynamic Code running on a 3 GHz processor would require about 1500 GB of memory and 10 minutes of computer time for every second of model

simulated time (i.e. only 1/600th of real time so that 600 hours on the computer would model only one hour of flow and transport in the delta). By creating a coarser 15 x 15 m bathymetry data set for the NDHM, the computer memory requirements are more manageable (5 GB) and the computational time is 0.14 seconds for every second modeled in the delta (i.e. 7 times faster than real time, so that 1 hour of computation will model 7 hours in the delta).

Upscaling from the 1 x 1 m data to the 15 x 15 m data was accomplished as detailed in Appendix A.1.1. The result is shown in Figure 2.1. The upscaling method used the mean elevation value in a 15 x 15 m grid cell with adjustments for subgrid scale features. Channelization effects along grid cell diagonals for subgrid features was approximated using a statistical analysis to identify affected cells in the 15 x 15 m data set and adjust to the cell elevation to the mean of the lowest 15 data points in the 1 x 1 m grid. The PC2 Hydrodynamic Code has cell edge features to represent for subgrid-scale blocking topography that is otherwise lost in the upscaling process for a grid cell. The two railways crossing the Nueces Delta are 3 to 4 m wide would be lost in the mean elevation of a 15 x 15 m grid, so they are represented by PC2 cell edges. Where piers allow flow under the railways, the computed mean elevation in the grid cell was used without cell edge elevations; a hydraulic model applied to represent the drag associated with the piers.

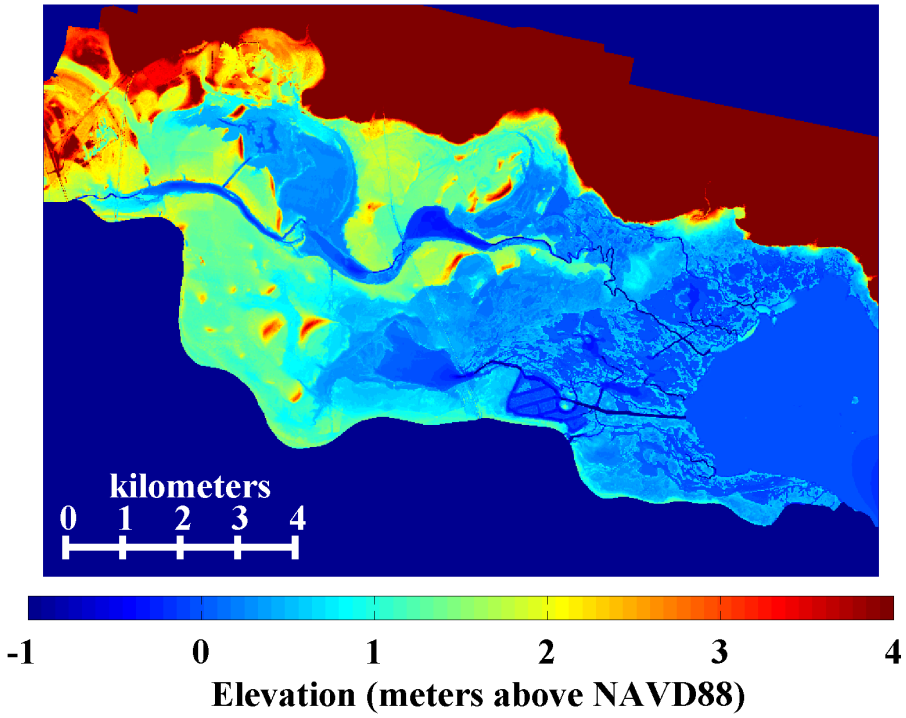

Figure 2.1: Image of the bathymetry used in the model. The color scale is selected to show details in the marsh lowlands, however the uplands higher than 4 m are also well-resolved in the data set (q.v. Figure A.1)

2.2.3 Data for surface roughness

The 2D shallow water flow equations in NDHM require a drag coefficient (C_D) or an equivalent Manning's 'n' to model frictional losses in the depth-averaged water column. For NDHM, we used a Manning's 'n' approach, where the roughness coefficient was developed from the 2001 National Land Cover Dataset using the approach developed by Hossain, Jia and Chao (2009) for remotely-sensed data. The baseline result is shown in Figure 2.2 and explained in more detail in Appendix A.2.7. The impacts of piers and culverts under barriers are incorporated into the land cover matrix as adjusted Manning's roughness coefficients.

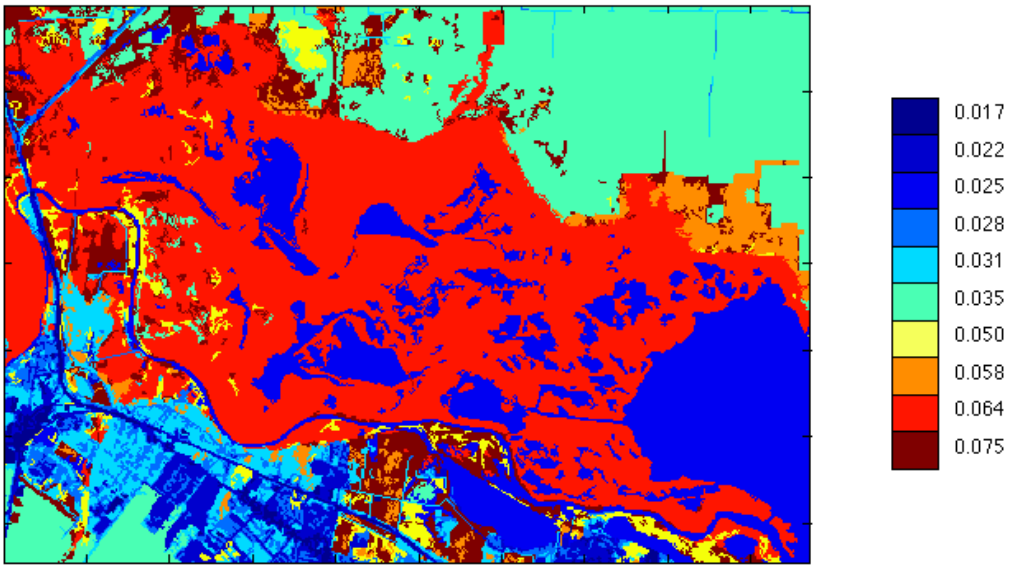

Figure 2.2: Manning's 'n' based on land-cover

The methodology described above is fairly common in the modeling literature, usually described as applying a grid-cell average elevation with surface roughness based on accepted literature values. However, as technology improves our data, we are faced with increasing evidence of shortcomings in this traditional approach. Because the 15 x 15 m grid was rasterized from the 1 x 1 m grid, we can analyze the subgrid-scale topography, which shows that topographical roughness can dominate the surface roughness developed from landcover in the Nueces Delta. Figure 2.3 gives an example of two 15 x 15 m grid cells, each containing two-hundred and twenty-five 1 x 1 meter data values. The two grid cells have the same mean elevation of 2.1 m, but the cell on the left has a standard deviation of 0.70 m whereas the cell on the right has a standard deviation of 0.02 m. Given the same free surface gradient and antecedent conditions, it seems obvious that the flow across these two grid cells should be different because of the different subgrid-scale topography within the cell. Clearly, cell with the higher variability in elevation should have greater subgrid-scale frictional effects for flows through the upper face of the cell, although the lower elevations along the lower and right faces of the cell might provide a preferential low-friction path. However, no one has

developed a method for representing known subgrid-scale topological roughness in terms of either an effective Manning's 'n' or a drag coefficient for this type of modeling. This issue is a subject for future research as discussed in §4.2.

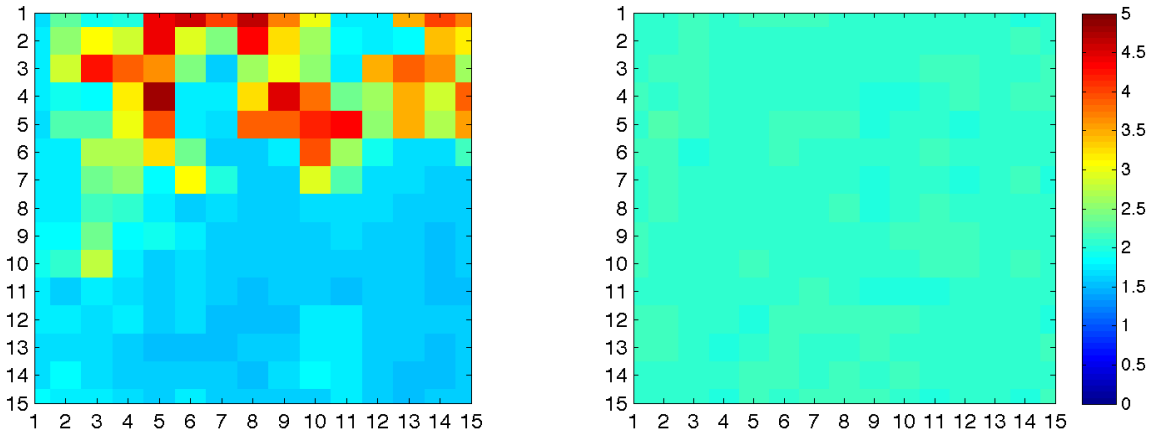

Figure 2.3: Examples of two 15 x 15 m grids and their subgrid-scale topography.

Nevertheless, we can gain some insight into how subgrid topography might affect the flow field by changing the roughness in grid cells having a relatively large standard deviation in the subgrid elevation. Localized and global changes to the baseline surface roughness set (R_B) are used to evaluate model sensitivity. The different surface roughness sets tested to date are outlined in Table 2.1. For local changes, we adjust the roughness only in grid cells having a large standard deviation in subgrid scale elevation, using twice the baseline surface roughness ($R_{\sigma 2}$) and ten times the baseline surface roughness ($R_{\sigma 10}$). As a comparison to this localized affect, in the global approach the baseline surface roughness for every cell is multiplied by a factor of ten (R_{10}) and one hundred (R_{100}).

Table 2.1: Roughness sets; $n_B(k)$ is the baseline Manning's n roughness for k={1...N} grid cell, i.e. the 15 x 15 m cells in Figure 2.2; $\sigma_Z(k)$ is the standard deviation of the subgrid elevation, c_σ is the standard deviation cutoff value (set at 10 cm, see Appendix A.1.1)

Surface roughness set identifier	Roughness algorithm
R_B	$n_B(k)$
$R_{\sigma 2}$	$n_{\sigma 2}(k) = \begin{cases} 2n_B(k) & : \ \sigma_Z(k) \geq c_\sigma \\ n_B(k) & : \ \sigma_Z(k) < c_\sigma \end{cases}$
$R_{\sigma 10}$	$n_{\sigma 10}(k) = \begin{cases} 10n_B(k) & : \ \sigma_Z(k) \geq c_\sigma \\ n_B(k) & : \ \sigma_Z(k) < c_\sigma \end{cases}$
R_{10}	$n_{10}(k) = 10n_B(k)$
R_{100}	$n_{100}(k) = 100n_B(k)$

2.2.4 Data for initial conditions

The NDHM requires the spatial distribution of water depth, salinity and velocity across the entire simulation domain as initial conditions. A model approximation of the initial conditions must be made from the limited available data. For velocity, the initial velocity is set to zero. For salinity, data from Conrad Blucher Institute (CBI) observation stations SALT and NUDE (Figure 2.4) are used as discussed in Appendix A.1.2. For water depth, the initial tidal elevation at the Nueces Bay boundary is applied as a uniform water surface across the entire delta. As discussed in §3.2, the uncertainty associated with these approximations of the initial conditions are reduced by using an extended model spin-up time.

Figure 2.4: Locations of TCOON salinity monitoring stations in the delta

2.2.5 Forcing data

The model forcing data are tidal elevation, wind speed and direction, inflows, salinity, and precipitation. Data sources, time periods of data availability, and data manipulation are discussed in Appendix A.2. Table 2.2 gives the data sources for the years simulated. Section 2.3 below describes how forcing data were modified for different scenarios.

Of the salinity observation stations in Figure 2.4, only SALT03 is used as forcing data, providing the salinity for inflows through the open tidal boundary of Nueces Bay. The other stations are used for both initial conditions (§2.2.4) and for analysis of model results (§3.3)

Table 2.2: Data sources for model forcing for the scenarios

Forcing Data	Source
Tide	TCOON
Salinity	CBI
Precipitation	NOAA
Wind	NOAA
Inflow	USGS
Rincon Pipeline Pumping	Nueces River Authority

2.3 Simulation scenarios

Different model scenarios with different sets of initial, boundary, and forcing conditions were selected to test and evaluate various aspects of the model. Forcing data that were *not* altered were tidal elevation, initial and inflow salinity, and the USGS gauged inflow inflows from the Nueces River into the delta; measured values for these data were used in all simulations. Using measured data as a baseline, additional forcing data sets were created for rain, wind speed, surface roughness and the Rincon Diversion pumping. Development of these data sets is discussed in detail in Appendix A.2.

Based on data availability, the model was run for 7 to 17 days for simulations using data from the first half of April in years 2008, 2009 and 2010. Table 2.3 provides an overview of the scenarios. In this table "baseline" conditions use only observed values from field data. For sensitivity testing, three wind speed conditions were considered: zero, baseline, and twice the baseline. Similarly, three rain conditions were considered, zero, baseline, and a heavy rain; the latter corresponding to a week of severe rainfall (computed as described in Appendix A.2.7). Five surface roughness conditions were modeled, as outlined in Table 2.1. Four different flow conditions for the Rincon Diversion Pipeline were modeled, corresponding to a single pump operating, reduced flow conditions of 2/3 and 1/3 of a single pump capacity, and zero flow[1]. Using three baseline years, these data sets provide 324 different possible combinations. The selected 17 scenarios are considered screening scenarios that evaluate the change of a single variable from the baseline.

[1] Note that the Rincon Diversion pumps cannot be run at 1/3 or 2/3 of their normal capacity, so these scenarios only examine the relative effects of different flow conditions. The original intent was to model 0, 1, 2 and 3 pumps operating. However, miscommunication with the Nueces River Authority over the units used in their online data set resulted in NDHM being applied with flow rates that were 1/3 of the intended conditions.

Table 2.3: Conditions used in the simulations of the Nueces Delta

Scenario		Year			Wind			Rain			Days simulated				Roughness					Pump Capacity				
		2008	2009	2010	no wind	baseline wind	2x wind	no rain	baseline rain	heavy rain	7	10	14	17	R_B	$R_{\sigma 2}$	$R_{\sigma 10}$	R_{10}	R_{100}	0	1/3	2/3	1
Pump	1	X				X			X		X				X					X				
	2	X				X			X		X				X						X			
	3	X				X			X		X				X							X		
	4	X				X			X		X				X									X
Rain	5		X			X		X			X				X					X				
	6		X			X			X		X				X					X				
	7		X			X				X	X				X					X				
Wind	8		X		X				X		X				X					X				
	9		X			X			X		X				X					X				
	10		X				X		X		X				X					X				
Spin Up	11		X			X		X				X			X					X				
	12		X			X		X						X	X					X				
Roughness Scenarios	13			X		X			X				X		X					X				
	14			X		X			X				X			X				X				
	15			X		X			X				X				X			X				
	16			X		X			X				X					X		X				
	17			X		X			X				X						X	X				

2.4 Analysis methods

2.4.1 Overview

The analysis of model results focuses on a few metrics: inundated area, total volume of water in the system, volume of freshwater in the system, volume of brackish water in the system, mean difference in depth between two simulations, and the mean depth across the delta from north to south.

2.4.2 Computing the inundated area

The inundated area (A_i) is used to integrate the model behavior over all space into a single metric that evolves through time and has practical meaning for water management. However, the wetting and drying algorithms in the hydrodynamic model will include infinitesimally thin layers (e.g. 10^{-6} m), which may not represent important inundated area and should not be included. As a practical measure, the inundated area can be defined as a sum over the N grid cells with individual cell areas $a_k = 225\,m^2$ for the evolution of the water depth over time $d_k(t)$ as

$$A_i(t) = \sum_{k=1}^{N} a_k H\left\{d_k(t) - c_i\right\} \tag{2.1}$$

where $H\{\}$ is the Heaviside step function and c_i is a cutoff, chosen as 0.02 m for the present study. The methodology for setting the cutoff is presented in Appendix B.1.

For computing the inundated area affected by pumped water, only those cells containing a significant fraction of pumped water should be used. The computation is

$$A_{pi}(t) = \sum_{k=1}^{N} a_k H\left\{d_k(t) - c_i\right\} H\left\{P_k(t) - c_p\right\} \tag{2.2}$$

where $P_k(t)$ is the fraction of pumped water in the k^{th} grid cell and c_p is a cutoff for the minimum water fraction that is considered significant. The cutoff choice affects the computation of A_{pi}, as discussed in §3.7.

2.4.3 Computing the total volume

The evolution of the total water volume V_T in the delta is computed without a cutoff, as small depths will not significantly distort the computation:

$$V_T(t) = \sum_{k=1}^{N} a_k d_k(t) \tag{2.3}$$

Changes in V_T and A_i provide two slightly different ways to evaluate the amount of water in the delta.

2.4.4 Computing the freshwater volume

The water volume can be divided into saline and fresh, which is helpful for isolating the effects of pumping. At grid cell k, the fraction of the local volume that can be considered

fresh water, F_k, diluting salt water of with reference salinity S_R to the local salinity, $S_k(t)$, is

$$F_k(t) = \frac{S_R - S_k(t)}{S_R} \tag{2.4}$$

The total volume of freshwater in the system, V_{FW}, is then

$$V_{FW}(t) = \sum_{k=1}^{N} a_k F_k(t)\, d_k(t) \tag{2.5}$$

2.4.5 Computing the brackish water volume

The natural complement to a freshwater volume would be a saltwater volume, which we could define simply as $V_T - V_{Fw}$. However, of more interest is the volume of brackish water in the system, V_B , i.e. the water with reduced salinity. Herein, V_B can be defined as sum of the volume of brackish water in the individual cells v_{Bk}

$$V_B(t) = \sum_{k=1}^{N} v_{Bk}(t) \tag{2.6}$$

where the cell brackish water is calculated with reference to a salinity cutoff, c_s. The volume of brackish water in a cell, v_{Bk}, is calculated as

$$v_{Bk}(t) = \begin{cases} a_k d_k(t) & : \quad S_k(t) \le c_s \\ 0 & : \quad S_k(t) > c_s \end{cases} \tag{2.7}$$

For the present study we use 15 ppt as the cutoff for defining brackish water; this selection is illustrative only, and does not reflect salinity levels that might be important for ecological concerns.

2.4.6 Depth statistics for cross-delta slices

The spatially-averaged depth over the entire delta does not provide any more information than computation of V_T and A_i. However, we can use a more refined depth metric to evaluate how the model represents wind-forced transport from Nueces Bay into the upper delta (§3.5). The wind is typically from 120 to 150 degrees during the modeled periods, which roughly coincides with the main flow axis of the delta. Ideally, a depth metric should compute the mean depth and standard deviation in slices perpendicular to an axis of 135 to 315 degrees, i.e. providing the characteristic depth at cross-sections moving upstream in the delta. However, as the model grid is aligned north-south, it is convenient to define a metric based on slices perpendicular to an east-west axis as shown in Figure 2.5, which provides reasonable cross-sections for analysis. The delta is divided into 48 slices, each 300 m wide (20 grid cells) along the east-west axis and containing the entire domain (up to 600 grid cells) along a north-south axis. The mean and standard deviation of the depth for slice p are computed from the set of depths D_j (without any minimum cutoff) as

$$\mu_{300D}(p) = \frac{1}{N}\sum_{j=1}^{N} D_j(p) \tag{2.9}$$

$$\sigma_{300D}(p) = \frac{1}{N-1}\sqrt{\sum_{j=1}^{N}\left[D_j(p) - \mu_{300D}(p)\right]^2} \tag{2.10}$$

2.4.7 Metrics for depth comparison across scenarios

Comparing the local difference between the depths in two different scenarios provides insight into how different forcing conditions affect the modeled response. Such metrics are particularly useful in evaluating when two models produce similar responses, which is necessary for evaluating model spin-up (§3.2). The mean difference in depth between to simulations can be defined as

$$\mu_{\Delta D}(t) = \frac{1}{N}\sum_{k=1}^{N} \Delta D_k(t) \tag{2.7}$$

where $\Delta D_k(t)$ is the local difference between the k^{th} grid cell depths in two simulations at time t. The standard deviation is

$$\sigma_{\Delta D}(t) = \frac{1}{N-1}\sqrt{\sum_{k=1}^{N}\left[\Delta D_k(t) - \mu_{\Delta D}(t)\right]^2} \tag{2.8}$$

2.4.8 Computing spin-up time

Spin-up time is the interval from the model start until some time when the model results are sufficiently independent of the initial conditions. We can think of this as the time it takes to clear the system's memory. The initial conditions for velocity, depth and salinity are approximations of the unknown real values, with uncertainty that affects results over the spin-up time. However, as tidal, wind and inflow forcing move water through the delta, by the end of the spin-up interval the effects of the initial conditions will be washed out of the system. Beyond the spin-up time, the modeled results are principally determined by the modeled forcing. Thus, estimating the model spin-up time is a necessary exercise in determining the time range over which model result should be compared to field data for calibration and validation. A comprehensive evaluation of spin-up time requires comparison of depth, velocity and salinity metrics. The present study has focused spin-up time on the water depth, using the V_T, A_i , $\mu_{\Delta D}$, and $\sigma_{\Delta D}$ metrics described in §2.4.2, 2.4.3, and 2.4.7. Spin-up is analyzed by starting simulations at two different physical times and evaluating convergence of statistical metrics. Results for spin-up analysis are presented in §3.2.

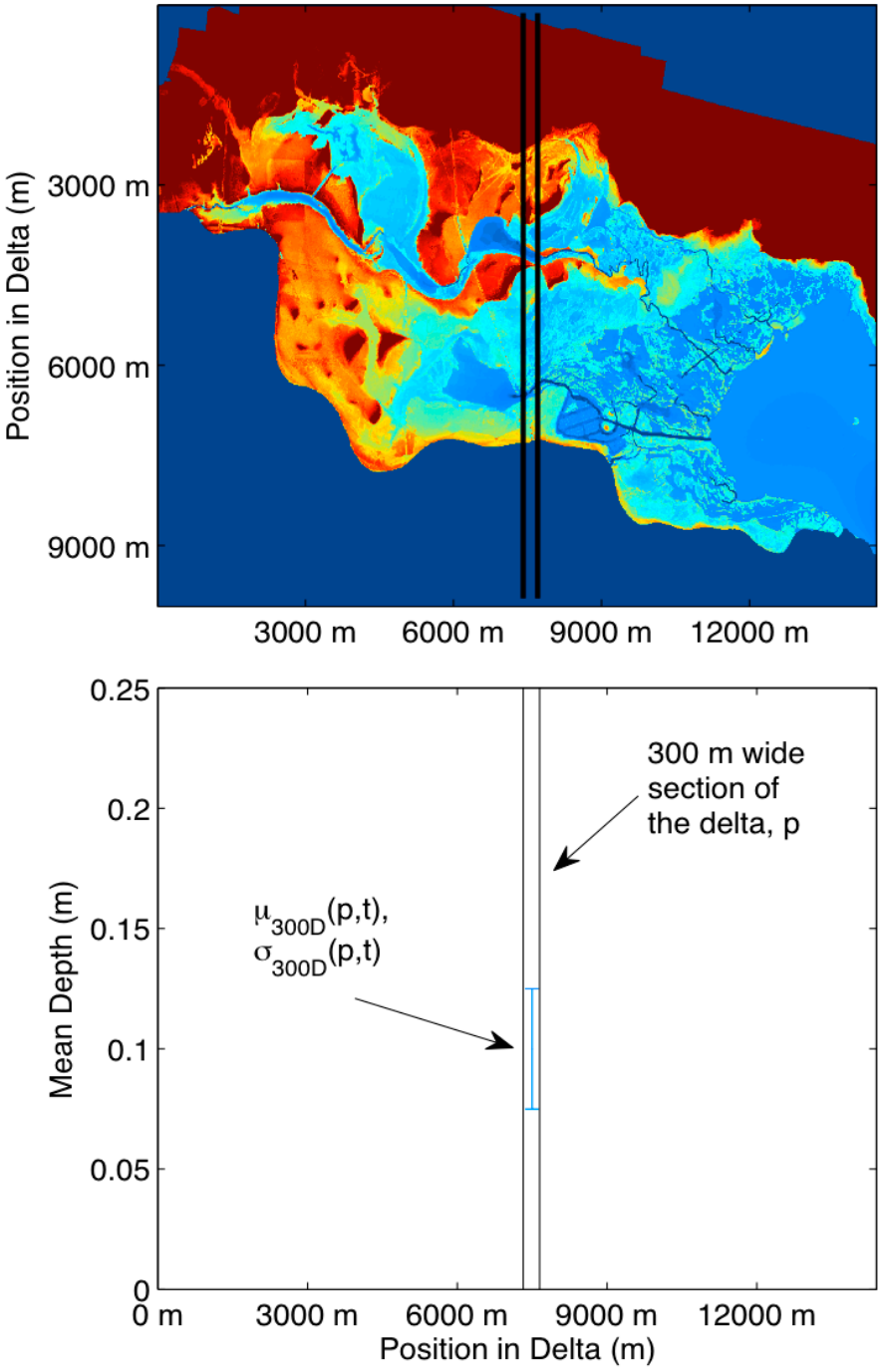

Figure 2.5: Slices of 300m width for computing mean depth (μ300D) and standard deviation (σ300D)

2.4.9 Methods for comparison to field data

For insight into model behavior, in §3.3 the water surface elevations are compared with data from the SALT and NUDE stations (q.v. Fig. 2.4). Unfortunately, these stations are not benchmarked to a vertical geodetic datum. Without a vertical reference datum, the depth measurements cannot be quantitatively compared to the model. That is, we do not know the exact height of the sensor relative to the model bathymetry so we cannot diagnose either magnitude or direction of any error in water surface elevations. Thus, calibration becomes impossible. However, we can obtain an estimate of sensor elevations by neglecting the mean horizontal gradient in the surface elevation as discussed in Appendix B.2. Using this estimated datum, we can make qualitative comparisons of the water surface behavior between the model and observations.

3 Results and discussion

3.1 Overview

The NDHM was run to simulate scenarios outlined in §2.3. The model spin-up time (§3.2), comparison to field data (§3.3), response to different forcing conditions (§3.4, 3.5, 3.6) and effects of pumping (§3.7) are analyzed below. Details on metrics for these analyses are found in §2.4.

3.2 Spin-up results

Scenario 12 (q.v. Table 2.3) was run for 17 days, beginning from 3 April 2009. Scenario 11 commenced on 10 April 2009, seven days into the Scenario 12 run, but using initial conditions developed from measured field data (i.e. without reference to Scenario 12 results).

In Figure 3.1 the daily mean depth difference between these two scenarios, $\mu_{\Delta D}$, and standard deviation, $\sigma_{\Delta D}$, are computed for the time period when both simulations were running (see §2.4.7 for definitions). When Scenario 11 begins $\mu_{\Delta D}$ is of the order of 10 cm with similar variability across the domain. However, after Scenario 11 has computed 9 days (i.e. day 16 of Scenario 12 in Figure 3.1), the $\mu_{\Delta D}$ is reduced to 1.32 mm and $\sigma_{\Delta D}$ is 2.62 mm, indicating that the different initial conditions for the two scenarios are causing only minor differences in the water surface elevations across the entire delta.

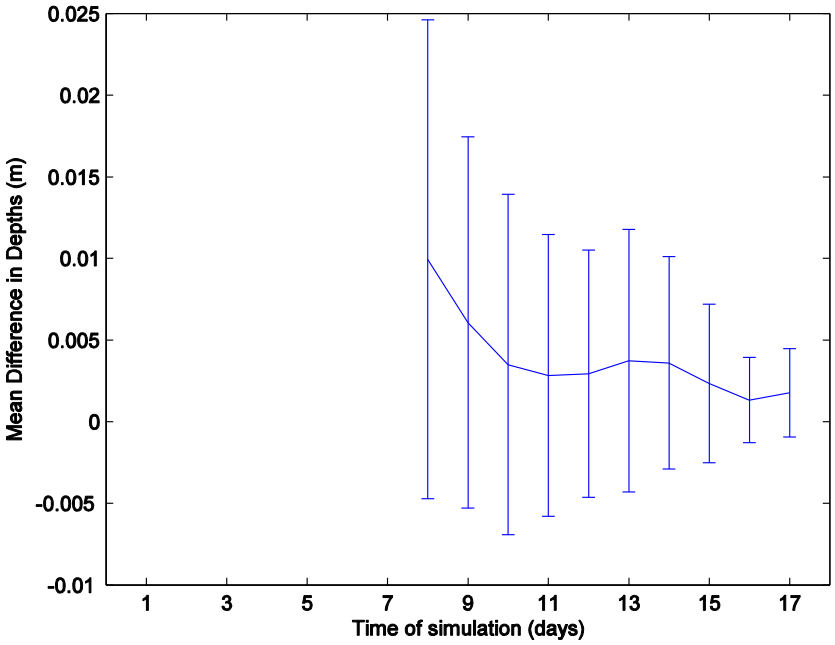

Figure 3.1: Mean depth difference ($\mu_{\Delta D}$) with error bars of $\sigma_{\Delta D}$ for 10 day (Scenario 11) and 17 day (Scenario 12) simulations. The X-axis is simulation days for Scenario 12.

A more qualitative comparison of convergence between the 10 day and 17 day simulation results can be obtained using the inundated area (A_i) and total volume (V_T) metrics defined in §2.4.2 and §2.4.3. As shown in Figure 3.2, after day 14 of Scenario 12 (i.e. the 7th day of Scenario 11) the inundated area and total water volume have converged, indicating that there are no large-scale differences between the models. Thus, the spin-up time for water surface elevation is estimated to be on the order of 7 to 9 days. Spin-up times associated with salinity and velocity have not yet been analyzed.

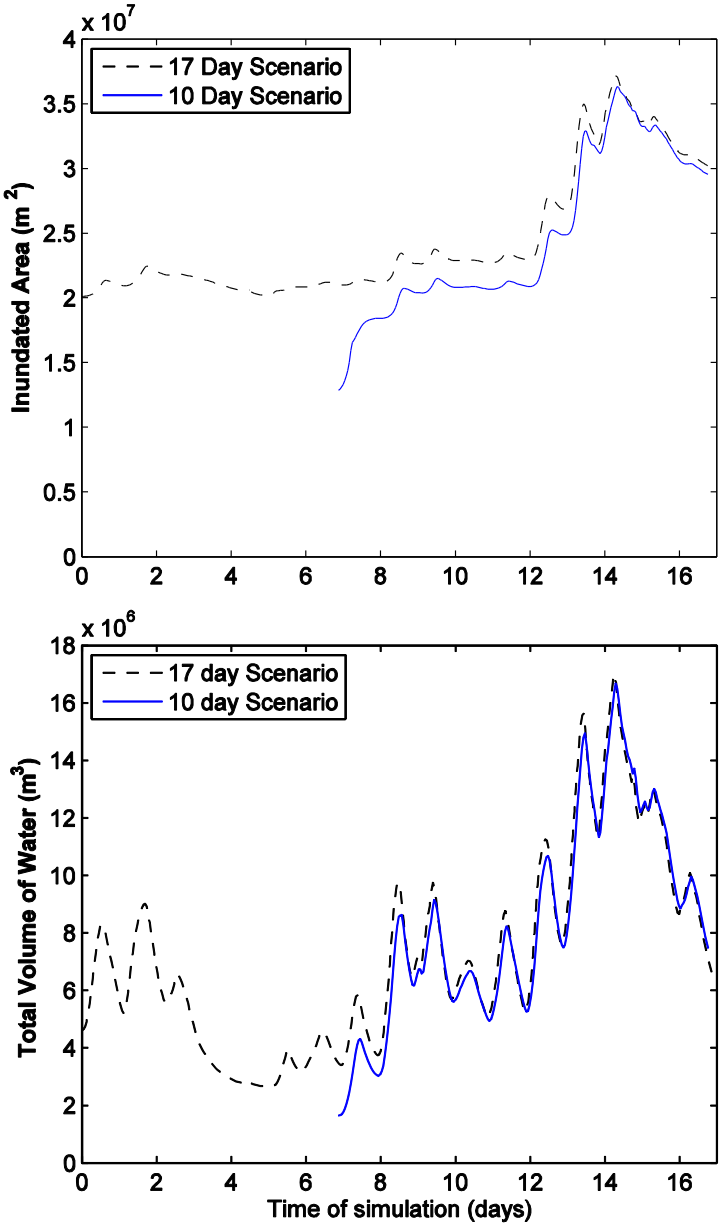

Figure 3.2: Comparison of A_i (upper panel) and V_T (lower panel) for 10 day (Scenario 11) and 17 day (Scenario 12) simulations. The X-axis is simulation days for Scenario 12.

3.3 Comparison to field data

Field data comparisons are made to 2010 observations using Scenario 13 (q.v. Table 2.3) with the baseline roughness R_B described in §2.2.3 and a total of 14 simulation days. Allowing for 7 days of spin up, the field and model free surface elevation data can be compared for days 7 through 14 as shown in Figure 3.3.

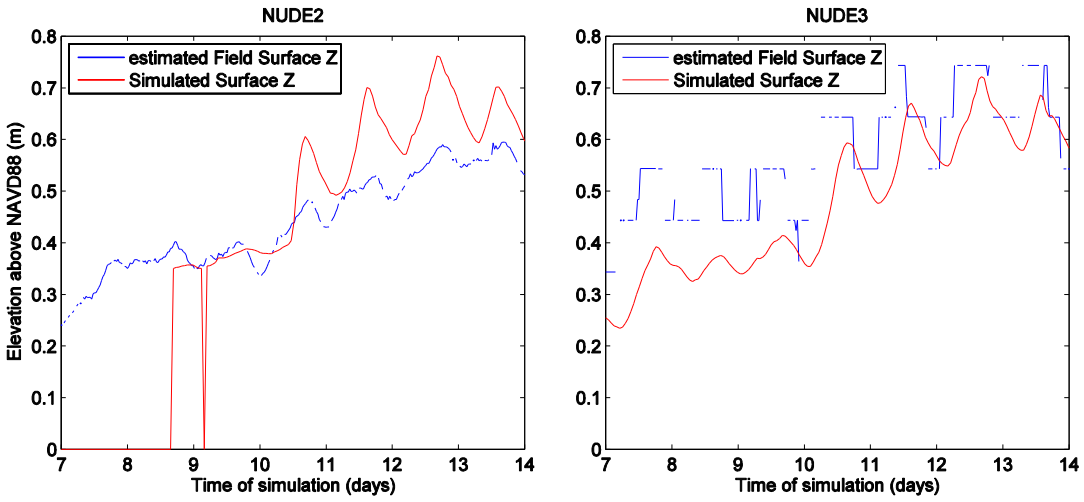

Figure 3.3: Comparison of simulated surface elevations with field data estimated elevations.

The overall increasing trend appears to be in reasonable agreement at both stations, indicating that the lowest frequency forcing of the tide and wind are correct. The sharp behavior change at day 10 for NUDE3 is apparent in both field and model data, indicating the model is capturing the transitional features. However, at NUDE2, which is further upstream in the delta compared to NUDE3 (q.v. Figure 2.4) the field data daily tidal amplitude is less than 5 cm, but is more than 15 cm in the model. In contrast, the tidal amplitudes appear reasonable at NUDE3 in the lower delta. Thus, it appears that the model surface roughness between the NUDE2 and NUDE3 stations is not sufficiently damping the daily tidal motions. Better agreement could likely be obtained through comprehensive calibration (see §4.2). See §2.4.9 for a discussion of the qualitative comparison between model and field data and Appendix B.2 for methods used in estimating the surface elevation for field data from the observed depth with unknown vertical datum.

3.4 Model response to rainfall

Rainfall effects on inundated area (A_i) for Scenarios 5, 6, and 7 (q.v. Table 2.3) are shown in Figure 3.4. The baseline rainfall (Rain) increased the A_i by only 7.29×10^2 m^2 (0.180 acre) over the zero-rain (0) simulation, whereas the heavy rainfall scenario (HR) increased the inundated area by over 1.56×10^4 m^2 (3.85 acre). Although the increase in inundated area is negligible for the baseline scenario and only 0.1% of the flooded marsh for the heavy rain scenario, the effects are more dramatic as measured by total water volume, V_T shown in Figure 3.5. The baseline rainfall increases V_T by 2%, whereas the heavy rainfall increases V_T by 24%.

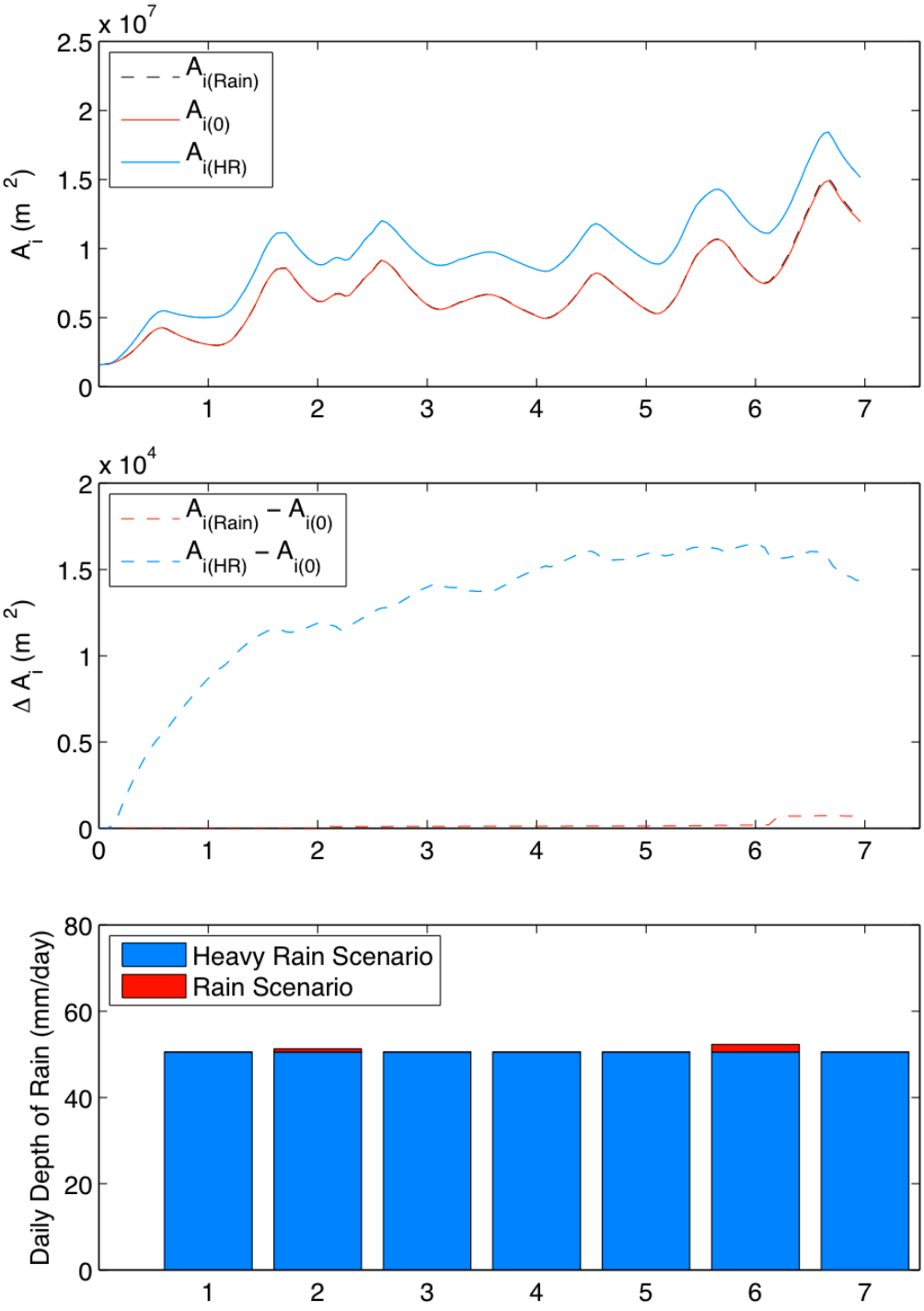

Figure 3.4: Rainfall comparisons of inundated area for the seven days of rainfall simulations in Scenario 5 (0 = no rainfall), Scenario 6 (Rain = baseline rainfall) and Scenario 8 (HR = heavy rainfall). Inundated area (A_i) evolution in upper panel; difference between scenarios ΔA_i in middle panel; depth of rainfall on each of seven simulation days in lower panel.

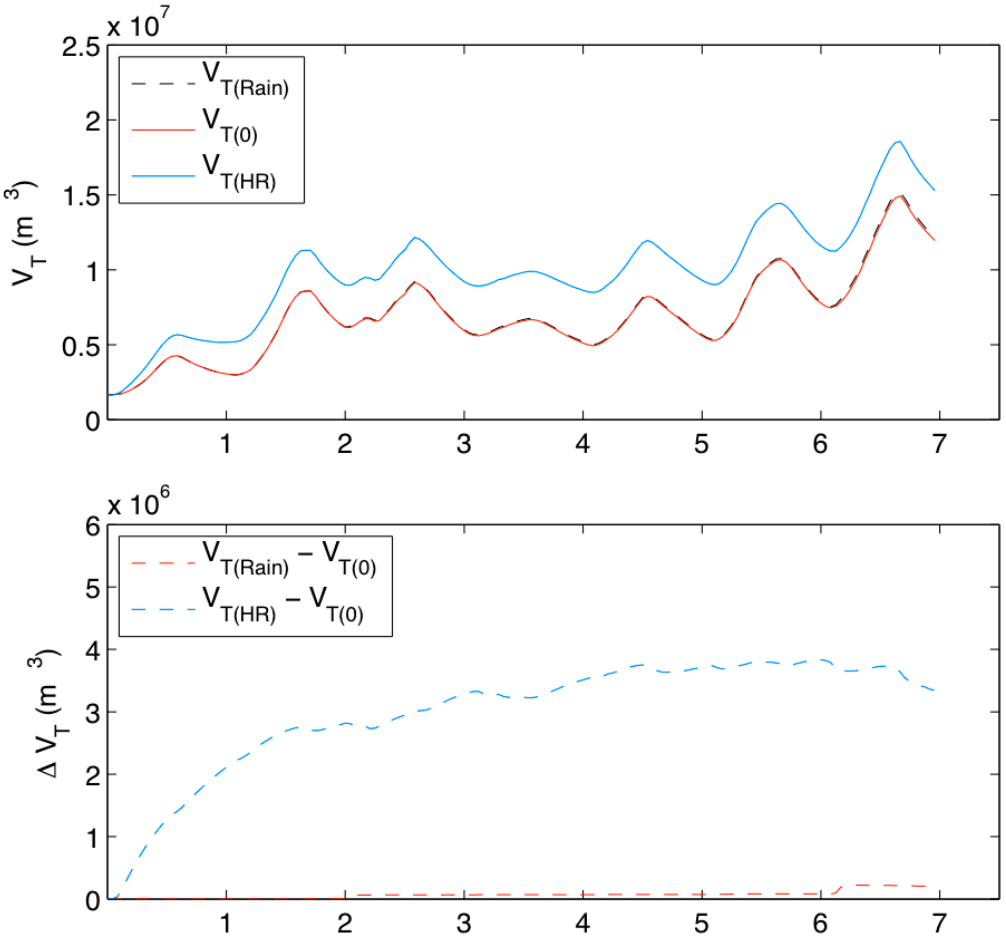

Figure 3.5: Rainfall comparisons of total water volume for the seven days of rainfall simulations in Scenario 5 (0 = no rainfall), Scenario 6 (Rain = baseline rainfall) and Scenario 8 (HR = heavy rainfall). Total Volume (V_T) evolution in upper panel; difference between scenarios ΔV_T in lower panel.

These scenarios demonstrate that the NDHM represents the collection of sheet flow from dry-land runoff into stream flow, which is a computational challenge for hydrodynamic models. Rainfall in the dry uplands of the Nueces Delta is channelized into streams and rivulets as it flows down to join the flooded marsh (Figure 3.6). Because the cutoff depth for defining an inundated grid cell was 2 cm (see Appendix B.1), the A_i computation does not represent areas temporarily wetted by the rain, but reflects the collection of rainfall into streams and rivulets in the uplands, as well as increased flooded area in the marsh. A portion of the rainfall onto dry landscape is absorbed through infiltration (Appendix B.3), so the baseline Rain Scenario in Figure 3.6 shows negligible contributions in the uplands that is above the depth cutoff for computing A_i. In contrast, the Heavy Rain Scenario shows significant ponding and stream formation deeper than 2 cm, which contributes to calculated A_i.

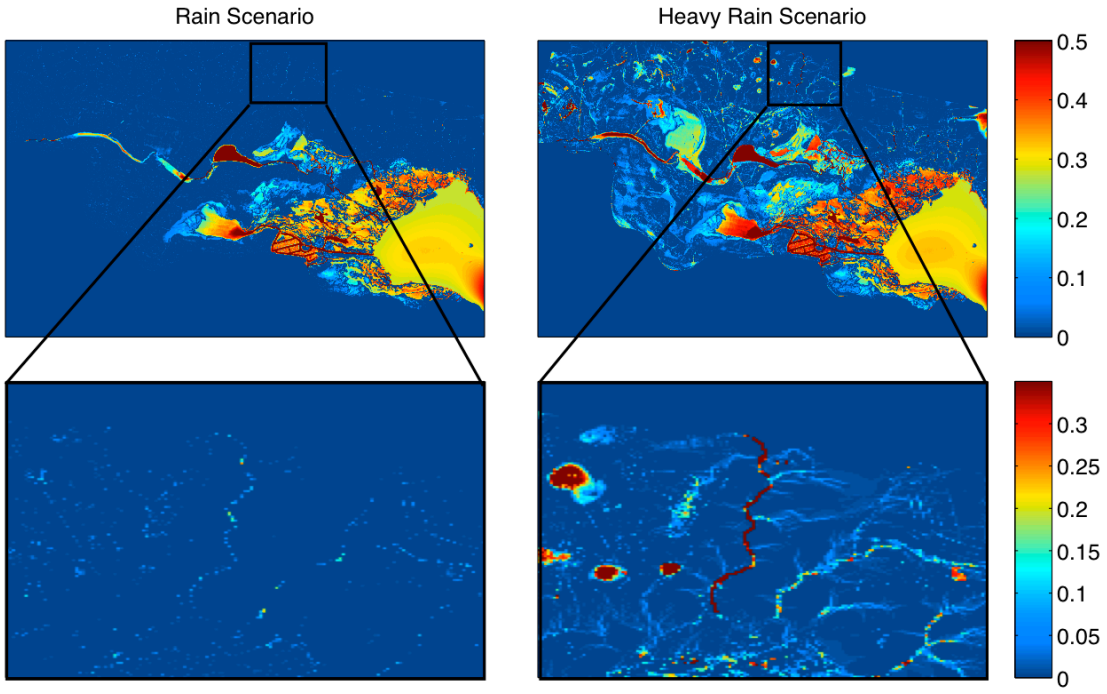

Figure 3.6: Modeled water depth during a rainstorm for the baseline Rain Scenario (Scenario 6) and the Heavy Rain Scenario (Scenario 7).

3.5 Model response to wind

Simulations 8 through 10 (q.v. Table 2.3) use zero wind speed (No Wind), the observed wind speed (Normal Wind), and twice the observed wind speed (2x Wind), respectively. Observations of the Nueces Delta (J. Tunnell, pers. comm.) indicate that steady winds from the south-southeast tend to push water further up into the delta, an effect that the NDHM must be able to capture. Modeling wind-driven flows over shallow marshland is a computational challenge (see §4.2). A comparison of the different wind scenarios in Figure 3.7 and 3.8 indicates the model is able represent wind-driven flows into the upper Nueces Delta. In Figure 3.7, both the Normal Wind scenario and the stronger 2x Wind scenario show increased depths through both the lower and upper marsh as compared to the No Wind scenario. This result is echoed in Figure 3.8, which shows the total volume of water in the delta after 7 days of simulation is 12% greater for the Normal Wind scenario and 49% greater for the 2x Wind scenario compared to the No Wind scenario.

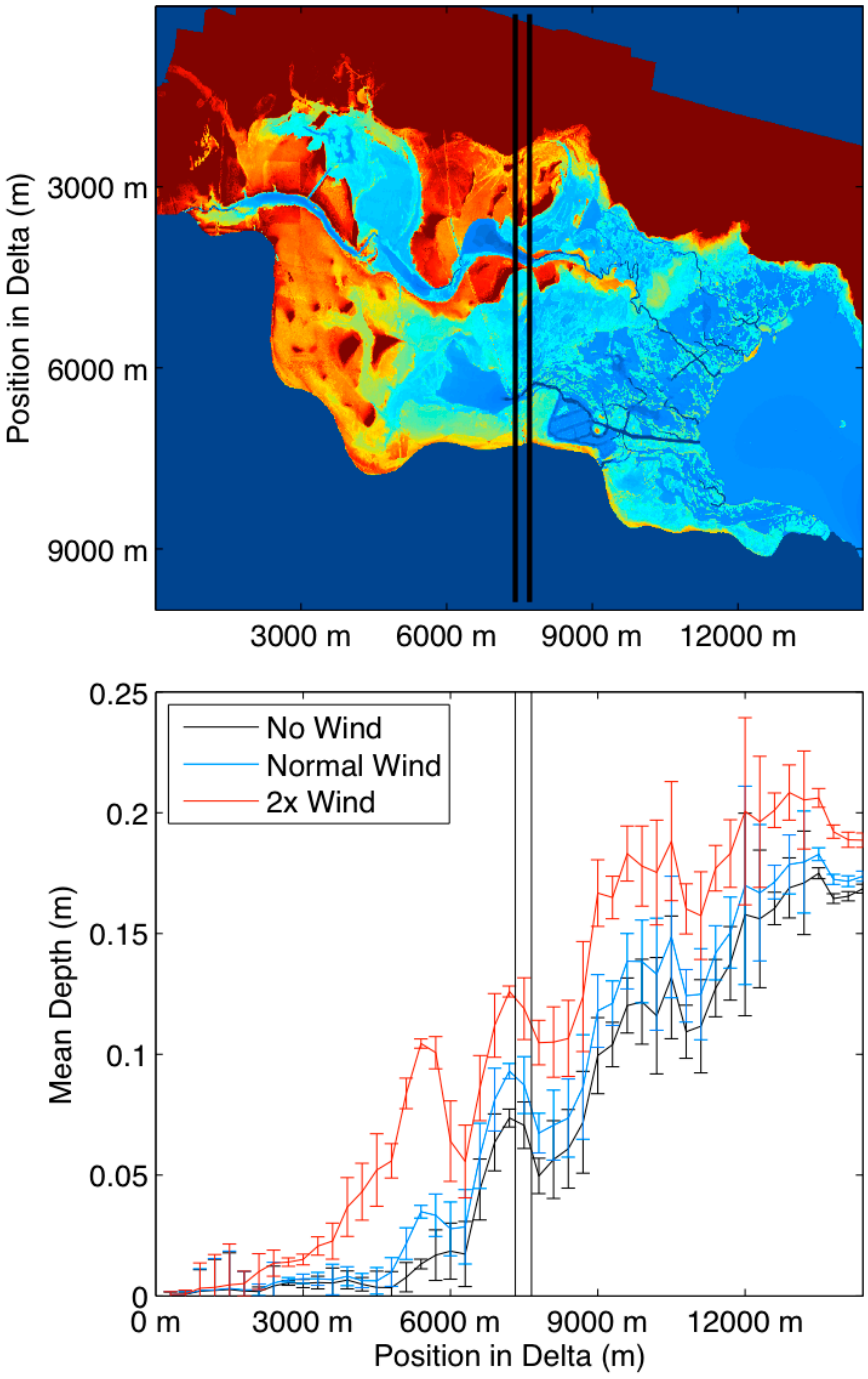

Figure 3.7: Wind speed effects on depth from positions upstream in delta to Nueces Bay. Mean depth (μ_{300D}) with error bars of one standard deviation (σ_{300D}) for north-south cross-delta slices (see §2.4.6) after 7 days of simulation for Scenario 8 – No Wind, Scenario 9 – Normal Wind (baseline), and Scenario 10 – Twice the observed wind speed.

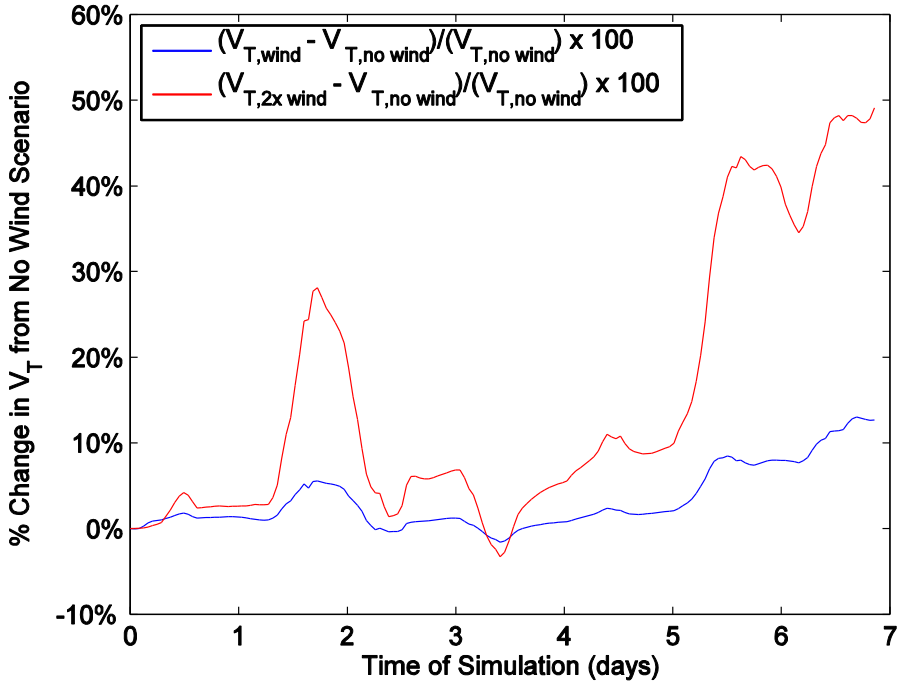

Figure 3.8: Total water volume (V_T) change caused by wind forcing for Scenario 9 (Normal Wind) and Scenario 10 (2x Wind) compared to Scenario 8 (No Wind)

3.6 Model response to surface roughness

Surface roughness affects the flow rate of water through the delta. Higher surface roughness values should result in slower water motion and should damp tidal oscillations, particularly in the upper Nueces Delta. The evolution of total water volume (V_T) over a seven-day simulation, shown in Figure 3.9, indicates that increasing roughness does result in damping tidal oscillation and reducing fluxes through the delta. Comparing these results with Figure 3.3, a logical conclusion is that the model's exaggerated tidal oscillations at the NUDE2 observational station is likely caused by surface roughness values that are set too low. Correctly setting roughness values is a challenge for future calibration efforts (§4.2).

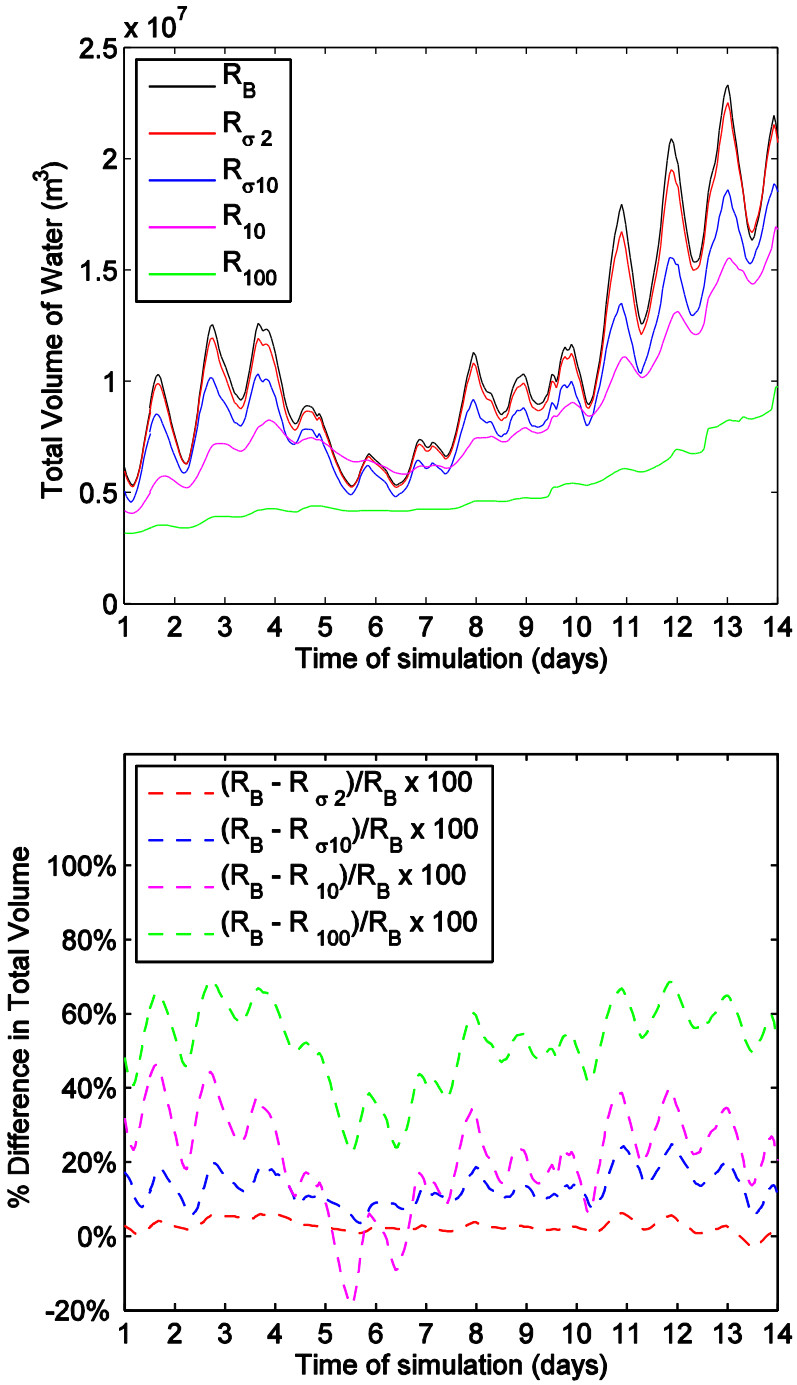

Figure 3.9: Effect of surface roughness on total water volume (V_T) for Scenarios 13 through 17 (see Table 2.1 for nomenclature)

3.7 Model response to freshwater pumping

Scenarios 1-4 are used to evaluate the model's response to freshwater pumping from the Rincon Diversion Pipeline (q.v. Table 2.3). The simulations begin from April 14, 2008 using all baseline conditions with the exception of the pumping flow rates. A tracer was used in the model to track the time-space evolution of water that enters the delta from the pipeline. The tracer concentration in any model grid cell reflects the fraction of that grid cell containing pumped water.

In Figure 3.10, the total volume of freshwater in the delta is graphed for the pumping scenarios, indicating that the model performs as expected with increases in freshwater volume proportional to the increases in the pump flow. The volume of brackish water, Figure 3.11, shows fairly similar proportionality in the first three days; however a sharp reduction in brackish water volume for the low flow (1/3 pump capacity) scenario occurs midway through day 3, followed by a much slower increase in brackish water volume. Further analysis is necessary to understand these phenomena, but initial review of simulations indicates that the lower flow rate is less successful in pushing fresh water out of the Rincon Bayou.

For further insight, Figure 3.12 shows the computed pumped water inundated area (A_{pi}) of eq. 2.2 for Scenario 3 using a range of cutoff values to define the significant fraction of pumped water in a grid cell. The results show a transition in computed A_{pi} where the cutoff changes from 0.4 and 0.5, indicating that the cutoff may dramatically affect the pumped water inundated area computation. Arguably, either 40% or 50% of the water in a model grid cell being pumped water would seem to be a reasonable definition of significant, but they result in quantitatively different computations. Because the higher cutoff value may understate A_{pi}, we use 0.4 as the cutoff for the analyses below.

Figure 3.13 shows the pumped water inundated area for the pumping scenarios. Similar to Figure 3.11, these graphs indicate that the relationship between the pumped water area inundated and the pumping rate may not be linear. With 1/3 the flow rate, the inundated area is roughly 10% of the area inundated by the full pump flow rate. In contrast, 2/3 of the pump flow rate provides roughly 80% of the same area. The sharp feature midway through day 3 in the 1/3 flow scenario is similar to that observed in Figure 3.11.

Further studies will be necessary to analyze how the inundated area changes with 2 and 3 pumps operating. However, caution must be used in considering with any of these results until the model has been calibrated and validated.

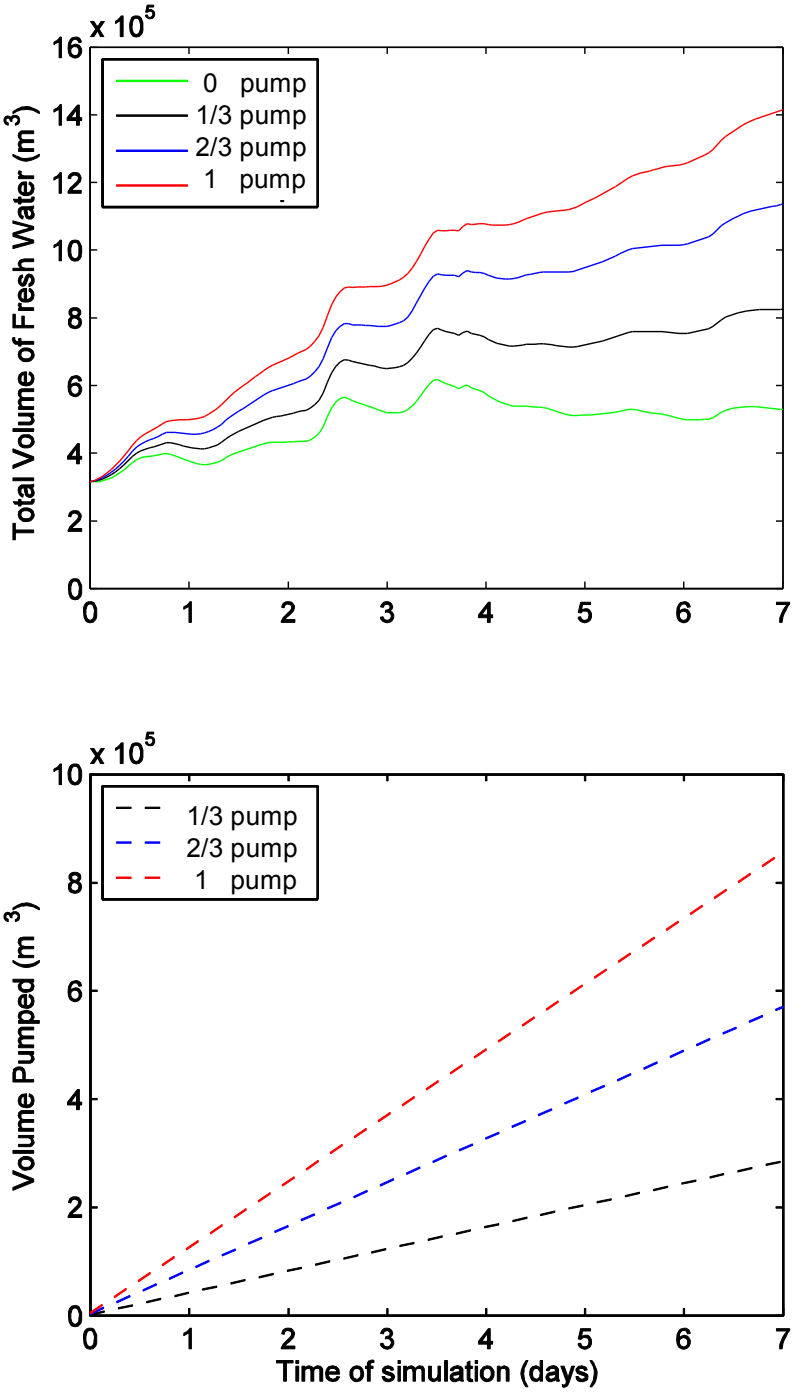

Figure 3.10: Fresh water volume (upper frame) and total volume pumped (lower frame) for Scenarios 1 (0 pump), 2 (1/3 pump), 3 (2/3 pump) and 4 (1 pump).

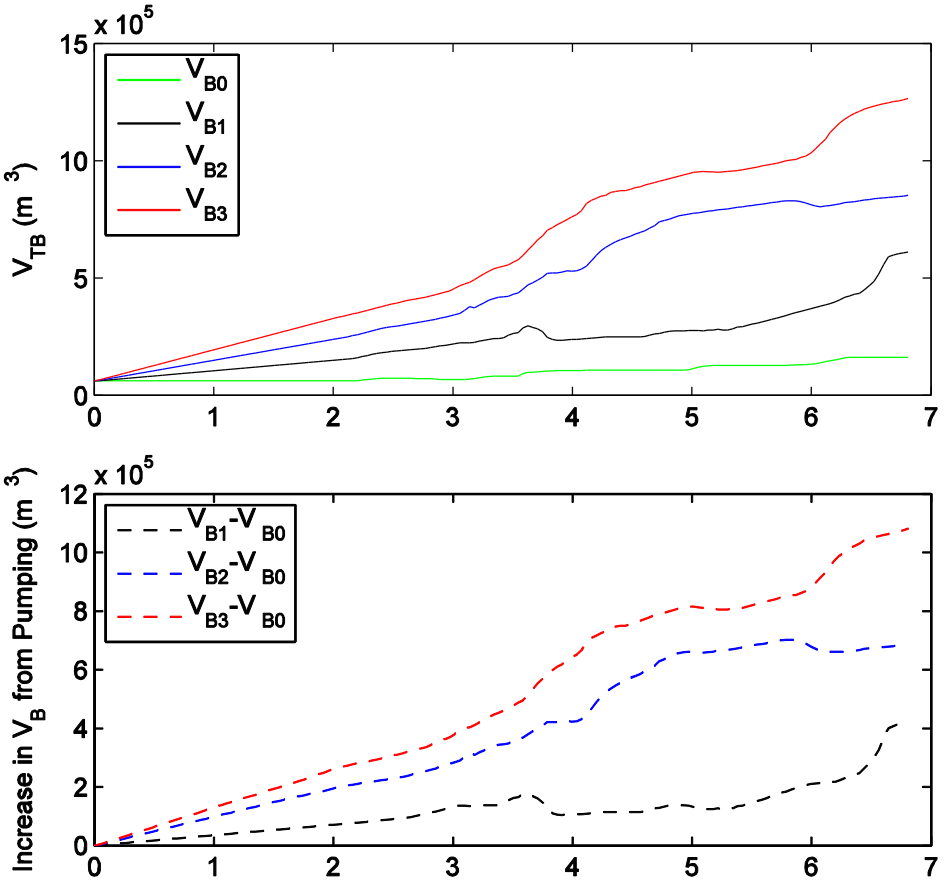

Figure 3.11: Brackish water volume (upper frame), difference between brackish water volume in pumping scenarios and baseline (lower frame). B0 = Scenario 1 (0 pump), B1 = Scenario 2 (1/3 pump), B2 = Scenario 3 (2/3 pump) and B3 = Scenario 4 (1 pump).

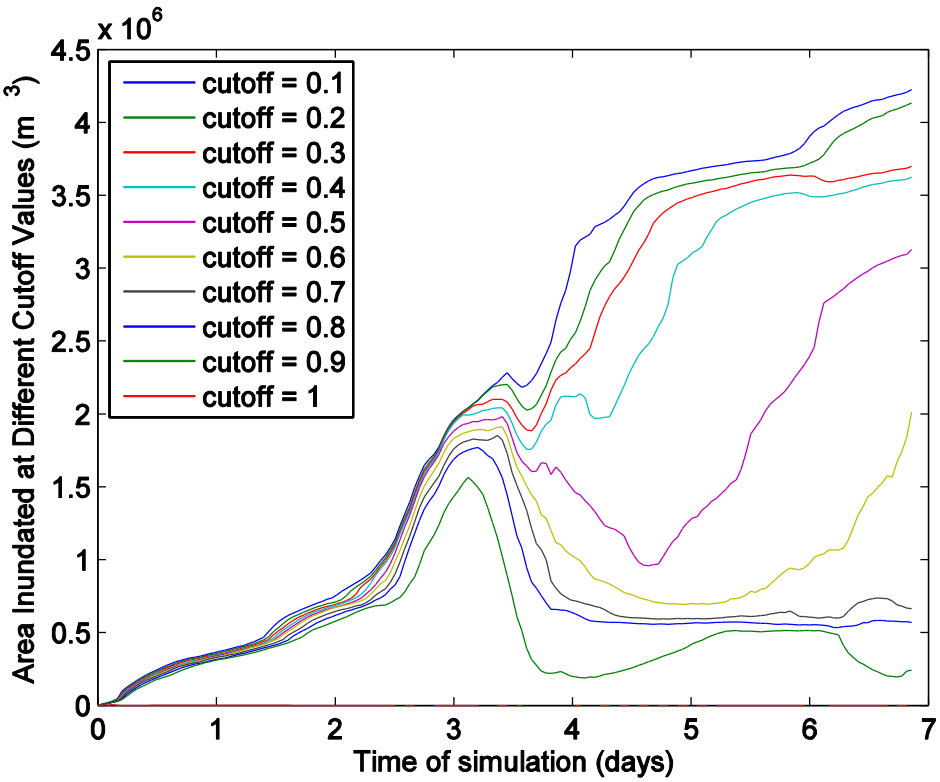

Figure 3.12: Pumped water inundated area (A_{pi}) for Scenario 3 over seven days with varying cutoffs for minimum fraction of pumped water in a cell.

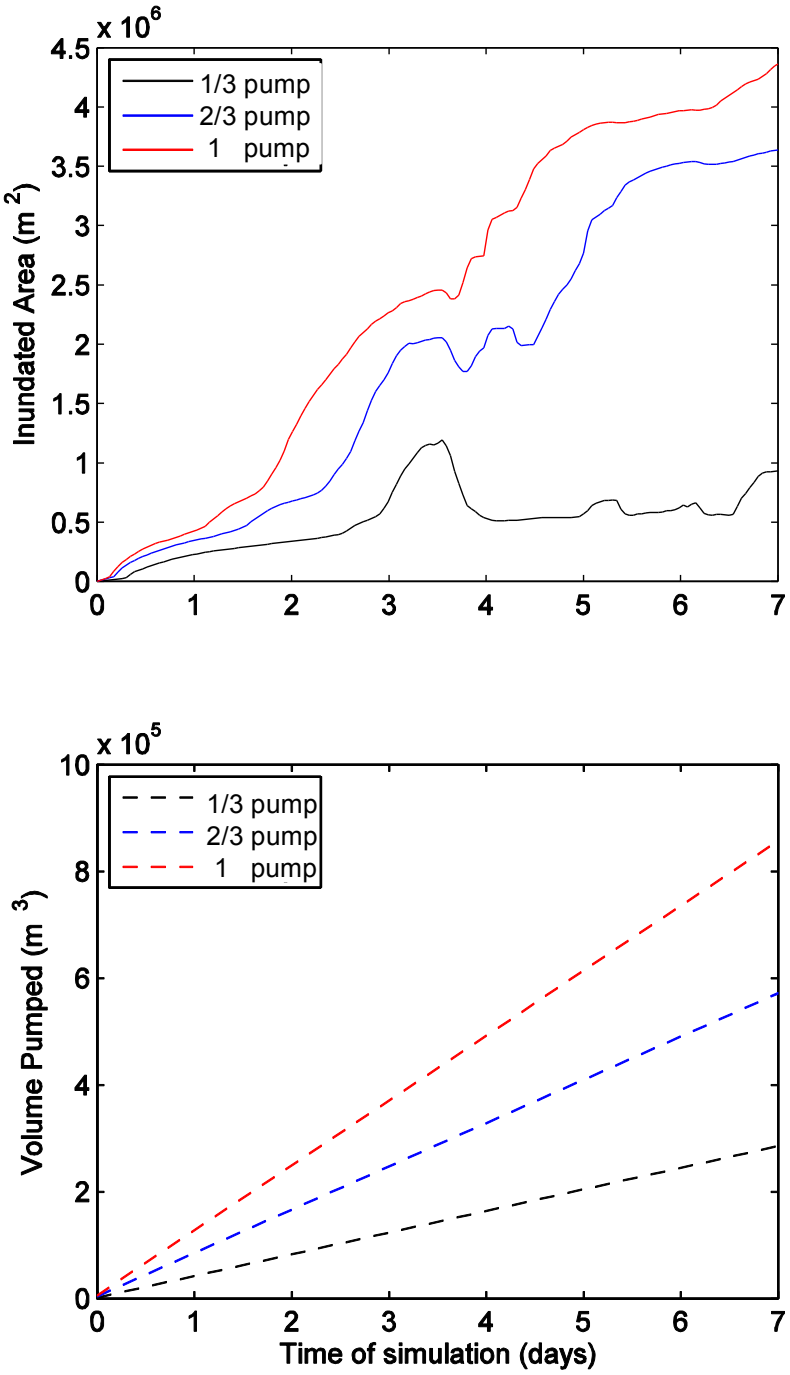

Figure 3.13: Pumped water inundated area (upper frame) and total volume pumped (lower frame) for Scenarios 2 (1/3 pump), 3 (2/3 pump) and 4 (1 pump).

4 Conclusion

4.1 Findings

The preliminary model validation was only qualitative; however, results indicate the model approximates the overall observed trends for the available data during the time period tested. In this report, the model's response to changes in wind, rainfall, and roughness on inundated area, total volume of water in the system, and mean depths across the delta were investigated.

Overall, the results indicate the model algorithms controlling the underlying hydrodynamics are working as expected. The model is able to capture tidal propagation from Nueces Bay up through the marsh and freshwater fluxes down the Rincon Bayou. Mixing conditions where salt and fresh water meet show the typical turbulent features expected in a 2D flow. The railroad dike is seen to block water movement except through trestles. The wind model creates upwind flows that push water into the West Lake area. The rainfall and runoff algorithms can handle heavy rainstorms that create rivulets gathering into streams in the uplands. The model shows nonlinear behaviors in inundation area as the pump flow rate is changed, which is expected if higher flow rates allow water to move further out of the Rincon Bayou.

Specific findings of the present model must be used with caution, and are subject to revision with further studies and analyses. Based on water depth, the model appears to need a week of spin-up time from starting conditions. The model for surface roughness has a significant impact on the timing and amplitude of tidal propagation through the lower marsh; baseline values derived using standard methodology appear to understate the topographic roughness effects thereby allowing a greater tidal range in the marsh than observed. Wind forcing appears to create the fluxes into the West Lake region that have been observed (J. Tunnell, pers. comm.), but the relationship between the wind forcing and transport volume cannot presently be validated.

4.2 Recommendations for future work

Calibration and validation of the model is incomplete, so further work is essential to improve our understanding of the model's capabilities and limitations. However, the available field data from the existing monitoring systems is inadequate to calibrate and validate the model. There are three principal projects required:

Project 1: Collect new data on salinity and water surface elevation throughout the delta under a variety of flow/tidal/wind conditions,

Project 2: Collect new data required for flow/velocity conditions through key choke points in the system,

Project 3: Collect new data regarding wind effects over shallow depths.

Project 1 requires emplacement of new Conductivity-Temperature-Depth (CTD) sensors and surveying existing sensors against the NAVD88 vertical datum. Approximately one year of data at 15-minute time intervals is needed with 14 or 15 new sensors distributed

throughout the delta. Projects 2 and 3 require short-term field studies that could be conducted by using Acoustic Doppler Velocimeter (ADV) instruments. These projects would each require 3 or 4 emplacements of equipment for 2 or 3 days each.

A key focus for future work should be in representing subgrid-scale effects that cannot be captured at the 15 x 15 m grid scale. In particular, there are several choke points narrower than 15 m in the Rincon Bayou that are likely to play a key role in controlling the flow. To calibrate these choke points over a wide range of conditions we need the data from Project 2 above. Baseline calibration can be accomplished using data from Project 1; however, our understanding of how best to model these subgrid-scale features is relatively poor so the modeled representation is likely to be a key limitation on the model accuracy. That is, using data from Project 1, the model would be calibrated to capture the correct flux through the choke points at the calibrated conditions, but our confidence in the model's performance outside the calibrated conditions would be limited. Project 2 collects velocity and topographical data at several choke points, providing the basis for a better mechanistic model of the flow at these key places. The result would be a model with a wider range of validity and less uncertainty.

The conditions in the Nueces Delta, with strong wind forcing over water depths less than 20 cm, have not been studied by any research team. The NDHM started with the wind model used for deeper systems, but this proved to significantly overestimate the wind-driven fluxes. The model used in NDHM provides a means of damping the wind momentum transfer to the water. However, we need a study of the water velocities in West Lake to determine how to correctly parameterize the model. It appears likely that the wind forcing from the Rincon Bayou into West Lake delivers more water into that system than the Rincon Overflow, so we need a better understanding of the wind-driven fluxes to gain a better understanding of the inundation of this large area.

For simplicity and minimizing computational requirements, the present NDHM excludes the tidal segment of the Nueces River. Future work should add this segment to the model and test the effects of overbanking from the river into the delta.

Future studies should develop more sophisticated approaches to analyzing freshwater inundated area. The channelized nature of the Nueces Delta and distribution of freshwater near the channels affects the vegetation species composition. Two of the principal species in the delta, *Borrichia frutescens* and *Salicornia virginica*, have very different conditions for ideal growth. *B. frutescens* is not hindered by flooding and has a positive growth rate only under low salinity conditions. In contrast, *S. virginica* is unaffected by increased salinity and has inhibited growth from waterlogged soil (Rasser 2009). In the present study, we examined inundated area as a one-dimensional metric, but the model data could be readily analyzed to provide species-specific values. Such an approach might improve our understanding of the impact of different pumping scenarios.

Future work might include developing a management tool for operating the Rincon Diversion Pipeline. This effort might incorporate output from or automatic operation of the hydrodynamic model to determine the most effective pumping scenario associated for existing conditions.

A Appendix: Input data preparation

A.1 Initial Conditions

Initial conditions are broadly discussed in §2.2. In this appendix, details are provided for bathymetric processing, developing the initial salinity distribution in the delta, and implementation of the flow barriers (e.g. railroad dike).

A.1.1 Bathymetry

The available bathymetry was received as the 2007 DEM (Digital Elevation Model) combined with the bathymetric data in ASCII format measured for the Coastal Bend Bays & Estuaries Program (CBBEP). In its original format (Figure A.1), the bathymetry is in a 1m x 1m grid gathered using Light Detection and Ranging (LiDAR). LiDAR systems send pulses of laser energy to surfaces that reflect energy to measure distance (Gibeaut 2003). The bathymetric data is relative to the North American Vertical Datum of 1988 and is given in meters. The North American Vertical Datum of 1988 (NAVD88) was developed by the National Geodetic Survey in 1991 and is the most recently developed vertical datum (Veilleux 2011). NAVD88 is the reference datum for all inputs in the model.

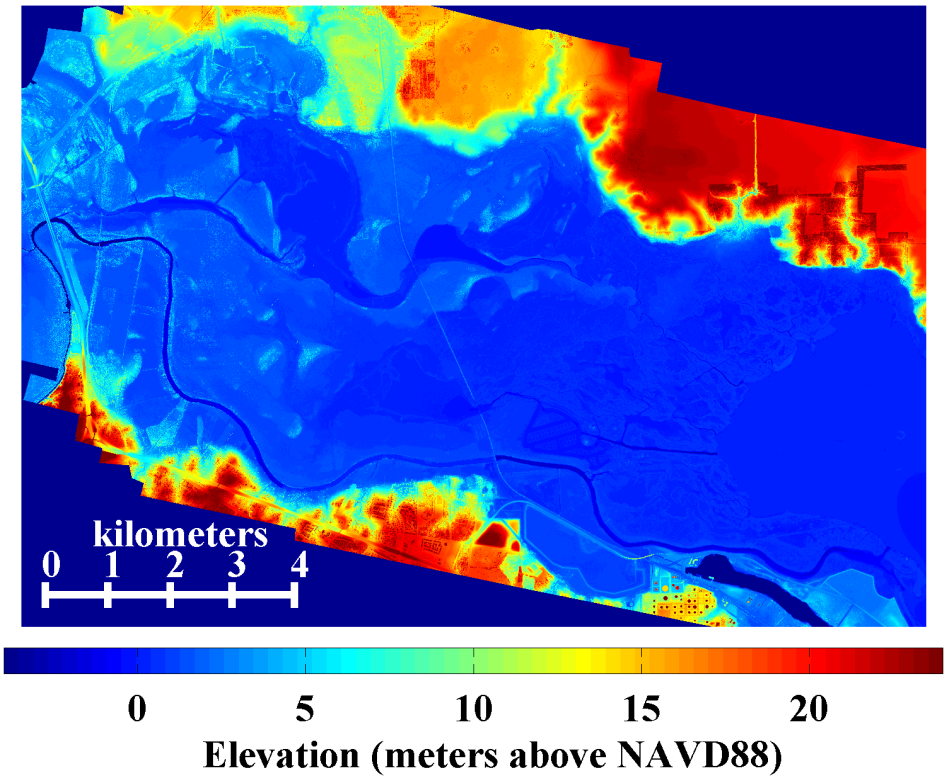

Figure A.1: The CBBEP (Gibeaut) 1 x 1 m bathymetry with a color scale from -5 to 25 m

The elevation color scale in Figure A.1 covers the entire range of data, from -5 to 25 m relative to NAVD88. This scaling shows the detail in the uplands but washes out the fine detail in the marsh. Figure A.2 displays the same bathymetry with a truncated color scale from -1 to 4 m. This image creates solid color blocks in the uplands, but shows greater detail in the lower marsh elevations. Note that the deep channel connecting Nueces Bay to the Nueces Delta Mitigation Project (q.v. Figure 1.3) is not an error in the bathymetry set, but reflects a historic access channel dredged for oil exploration (Pulich 2006).

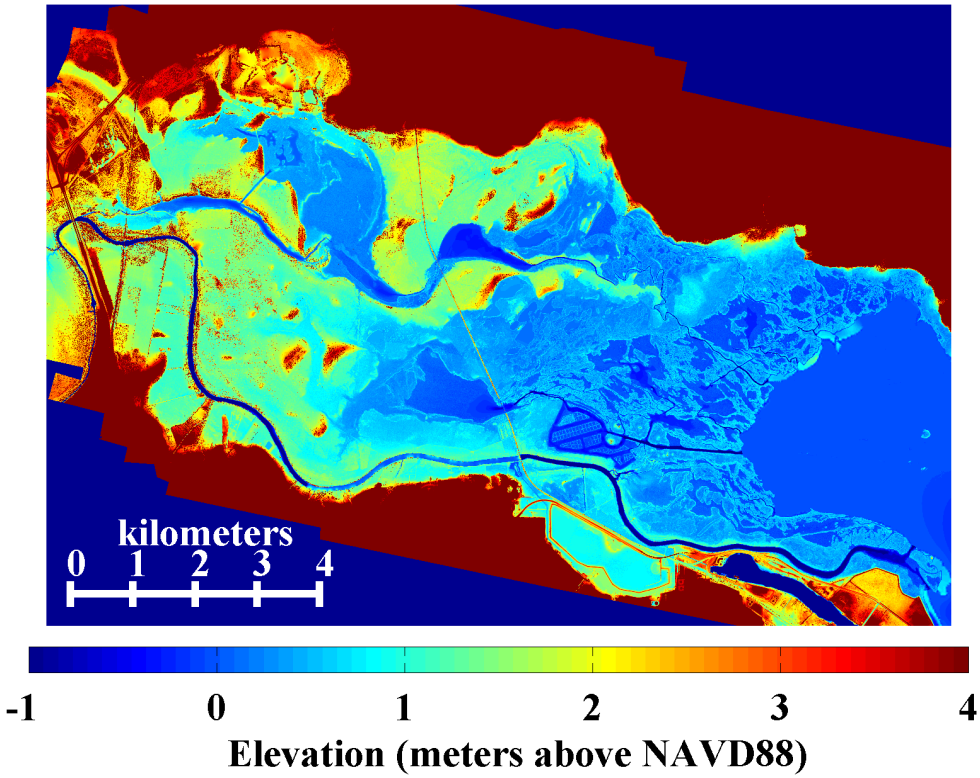

Figure A.2: The CBBEP (Gibeaut) 1 x 1 m bathymetry with a color scale from -1 to 4 m

The 1m x 1m data contains "not a number" (NaN) values in pixels where no LiDAR data were recorded. We handled these data points by filling the holes with the average of the non-NaN neighbor values. The algorithm is applied recursively to obtain values for NaN cells that are initially surrounded by all NaN cells.

The original bathymetric data does not include elevation data for Nueces Bay, which is needed to model the tidal boundary conditions. A 10x10m bathymetry data set from the National Oceanic and Atmospheric Administration (NOAA) is used complete the bathymetric data set. To obtain consistent grid specification in any future project, 10x10m grid was rasterized to a 1x1 meter grid using direct injection, i.e. setting all 1x1m data points within a 10x10m cell at the single value. This approach does not develop any significant discontinuities when the data is interpolated to the 15x15m grid used for the model.

The CCBEP 1x1m data set is 10,012 by 14,564 pixels. This fine data set does not allow for the model to be run at faster than real time. Rasterizing this data to a 15m x 15m grid provides a data set of 667 by 971 grid cells, which is more amenable to computation (approximately 7 times faster than real time on a single CPU core). The data is transferred from the fine pixels to the coarse grid using the mean of the 225 elevation values within each 15x15m grid cell. To visualize the effect of this on the bathymetry, it is useful to examine a small section of the bathymetry, labeled A in Figure A.3.

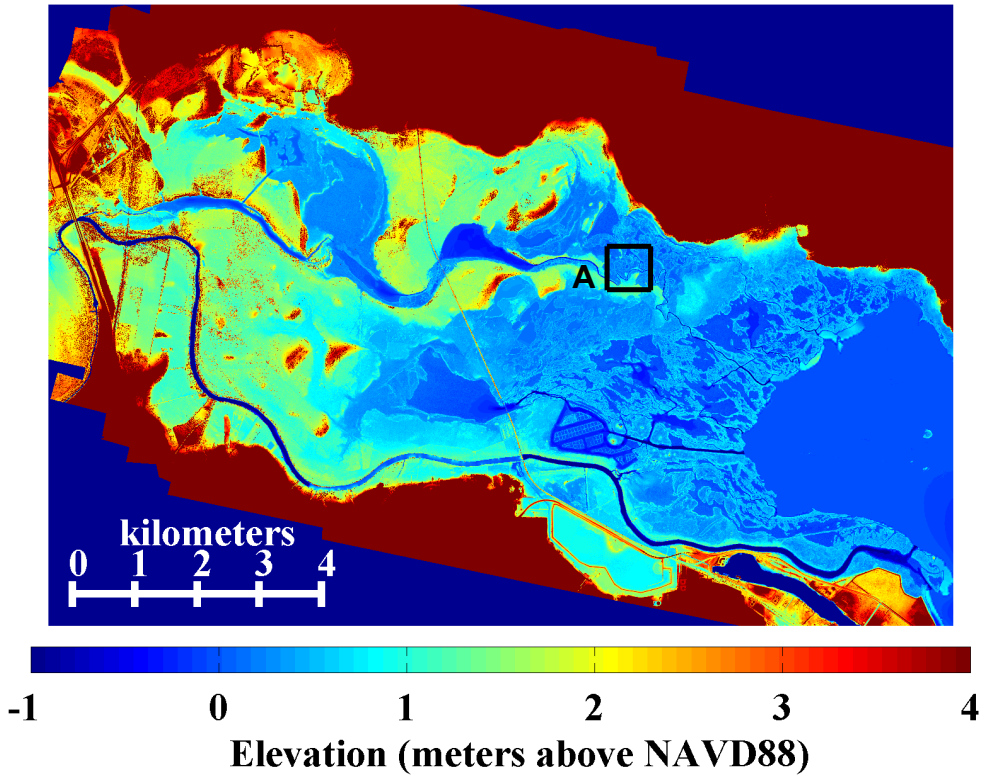

Figure A.3: CCBEP 1x1m bathymetry w of Section A in the delta

Box A in Figure A.3 is shown at the 1x1m resolution in Figure A.4 and for a 15x15 m grid in Figure A.5. In some areas of the bathymetry, averaging the 1x1m pixels to a 15 x 15 m grid caused artificial channel blockages, which distorted the flow patterns. As a remedy, we processed the data to find the 15x15 m grid cells whose standard deviation in the 225 elevation pixels exceeded a cutoff value. For these cells, we use the mean of the lowest fifteen 1x1m pixels in that grid is used as the value for that grid. The bathymetric data was tested with six different high cutoff values to examine the channel effects. Plots of the 15x15m bathymetry with high cutoffs ranging from 5 - 30 cm are provided in Figure A.6, which shows no large-scale effects of any choice. Detailed analysis indicated a high cutoff of 20 cm was the largest value ensuring free flow paths through the key choke points along the Rincon Bayou.

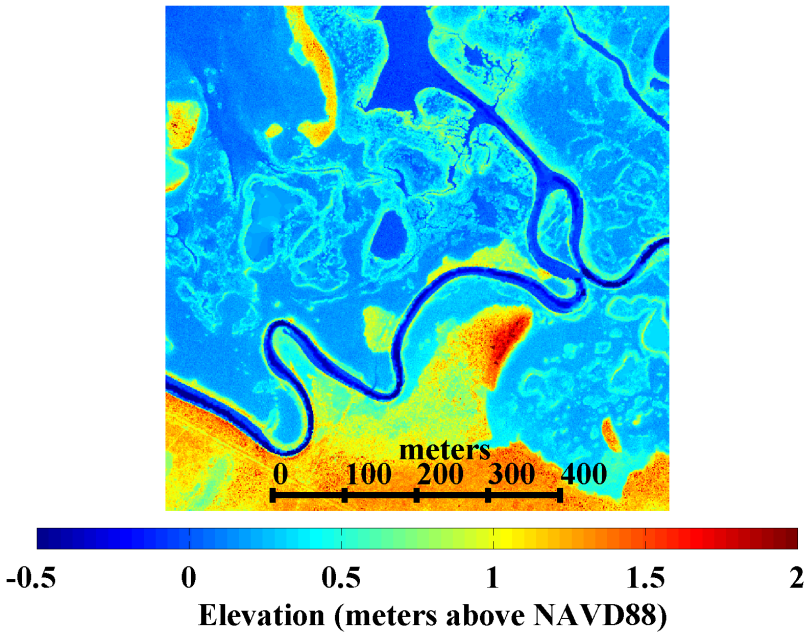

Figure A.4: Box A from Figure A.3 at the native 1x1m resolution

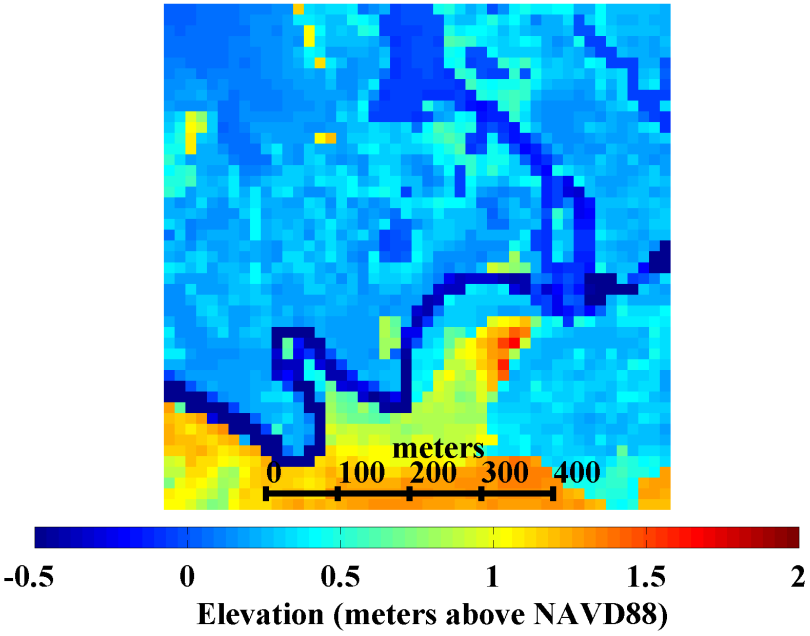

Figure A.5: Box A from Figure A.3 averaged to a 15 x 15 m grid

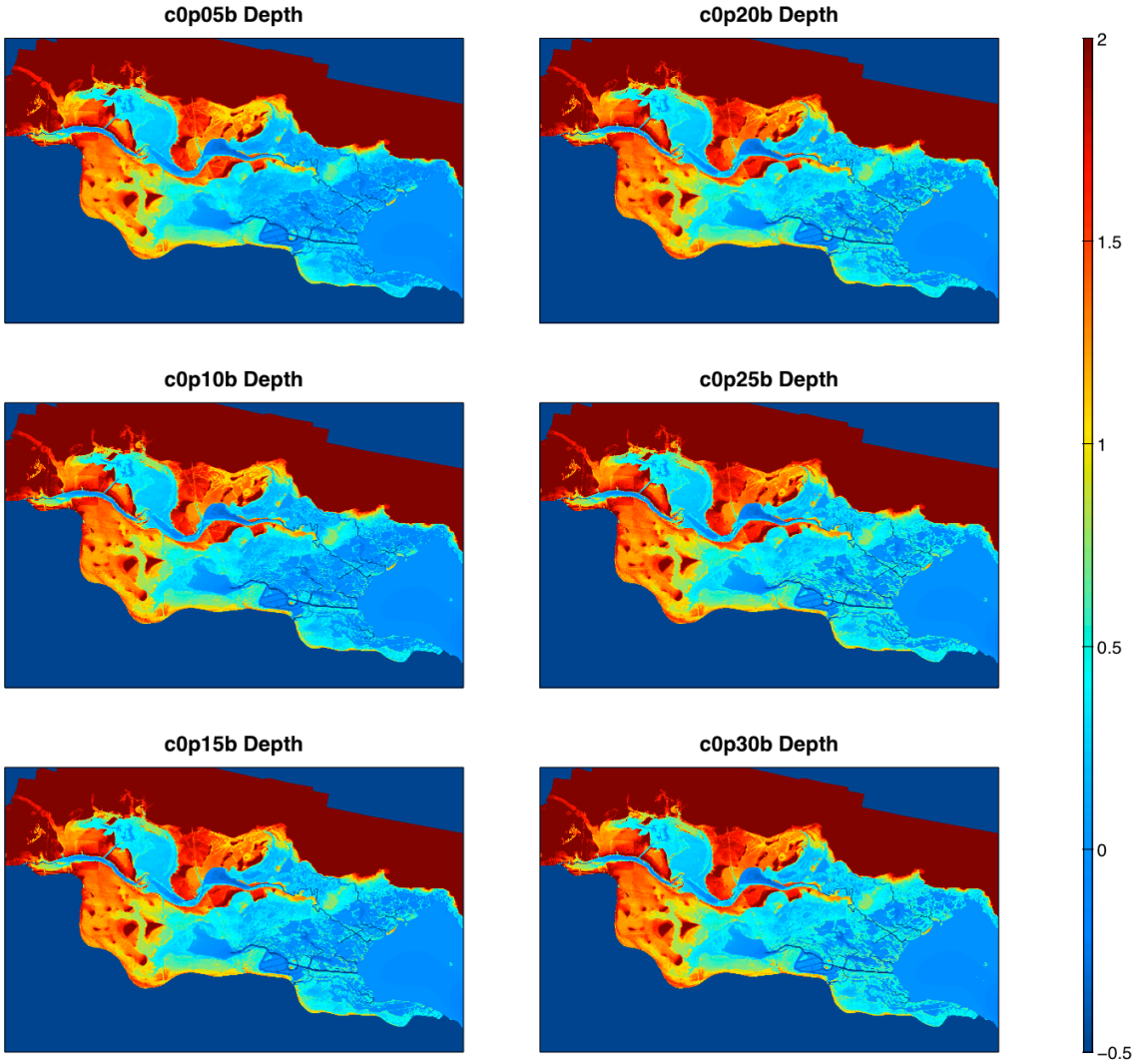

Figure A.6: Images of the 15x15m bathymetry with varying standard deviation cutoff used for channelization.

A further difficulty in representing channels that are poorly represented on the 15x15m grid (e.g. Figures A.4 and A.5) is the development of diagonal blockage on the coarse grid. The Cartesian-grid hydrodynamic model allows flow only through the four faces of any grid square, but in some places a channel occurring diagonally across the grid is blocked by higher elevations on the rectilinearly-adjacent cells. Adjusting the bathymetry to remove diagonal blockage requires testing for blocked diagonal flow paths based on elevation data and replacing the elevation in a rectilinearly-adjacent cell with the average of the two diagonal cells.

The CBBEP 1x1m data set (Figures A.1, A.2) includes bathymetry of the Nueces River tidal segment, which adds to the model computational time. During initial model development, keeping computational time to a minimum is desirable so that a large number of model scenarios can be run. Because the focus of the present effort is on the pumped freshwater flow rather than overbanking, the Nueces River sections were removed from the data set (q.v. Figure 2.1).

A.1.2 Salinity

Salinity data for CBI monitoring stations NUDE1, NUDE2, and NUDE3 were only available for 2010, so the initial conditions developed for 2010 were used for 2008 and 2009 simulations. The initial conditions for the salinity in the delta were calculated by interpolating between the salinity monitoring stations and extrapolating to zero salinity at the upper end of the Rincon Bayou. The value used for the initial condition at each station was found using the mean of all salinity values at that station from the day previous to the start of the simulation. Because the salinity is only known at points where there is monitoring data, the interpolation for the initial condition assumes uniform salinity across the delta from north to south, with salinity varying from east to west. The weaknesses associated with the initial condition become less important as the model simulates longer time periods. The spin-up time to remove the effects of the uncertain initial salinity conditions requires further investigation.

A.1.3 Railroad dikes, roads and culverts

Because the bathymetric data was gathered using LiDAR technology which measures surface elevation data using remote sensing from an airplane, the elevation of the bathymetry at the 1x1m resolution includes all railroads and roads forming flow barriers that are 1 m or wider. The bathymetric processing discussed in §A.1.1 will effectively eliminate these features, so the elevations are added into the model as a "cell edge" feature that applies as "sill" elevation higher than the surrounding grid cell elevations. Sill elevations were determined by isolating the barriers and averaging the elevation of the barrier within each cell, neglecting the surrounding bathymetry. The sill model allows flow higher than the sill elevation to pass over the sill (through the grid cell edge) but block any flows when the water surface elevation is less than the sill elevation. At this time, creating the sill data set is a laborious process that requires careful cross-checking to ensure continuity of the flow barriers.

Where railroad dikes and roads have piers or culverts to allow flow below the LiDAR elevation, the model bathymetry must be adjusted. In the present approach, the cell edge (sill) feature is eliminated at this point and the grid cell elevation is replaced by averaging the lowest fifteen values at the 1x1 m resolution. To model the effects of bridge piers and culverts, the surface roughness coefficient is increased in these grid cells. The change in Manning's n from bridge piers in subcritical flow was determined in Equation A.1 (Charbeneau and Holley 2001).

$$\frac{\Delta n}{n} = \sqrt{1 + \frac{\varphi^2 K y^{4/3}}{g L n^2}\left(K + 5Fr^2 - 0.6\right)\left(\alpha - 15\alpha^4\right)} - 1 \qquad \text{(A.1)}$$

where:

L = reach length (the flow length under the bridge)

φ = 1 for SI units

y = depth of flow

n = the original Manning's n value

K = coefficient depending on the pier shape (e.g. for three circular piers in a row = 1.11)

$Fr = V\left(gy\right)^{-1/2}$ = the Froude number downstream of the pier

α = ratio of the area of the submerged part of the piers to the total flow area.

Future work to improve the representation of culverts and railroad trestles should be considered (see §C.1)

A.2 Forcing Input

A.2.1 Overview

The model is run to simulate wet, dry, and average conditions for the Nueces Delta. The input data was collected for April 2008, April 2009, and April 2010. Sources, preparation and graphs of the forcing data are provided below.

A.2.2 Tidal Data

Tidal data was obtained from the Texas Coastal Ocean Observation Network (TCOON) platform at White Point, located on the northern shore at the outlet of Nueces Bay, Figure A.7.

Figure A.7: Location of the monitoring station at White Point

The tidal data is available thirty-minute increments as the "primary water level" variable at White Point. The downloaded data was provided in elevation (in meters) relative to the NAVD88 datum, shown in Figures A.8 – A.10. Missing data points were replaced by taking the linear average of the surrounding data, which is valid as long as the missing points are few and discontinuous (which is valid for the downloaded data set). The tidal data at White Point is used in the model for the entire eastern boundary of Nueces Bay south of White Point. Although the bay may have a surface slope in this direction (Ward 1997), the effect of this slope is negligible compared to the tidal range (Ward, Irlbeck and Montagna 2002).

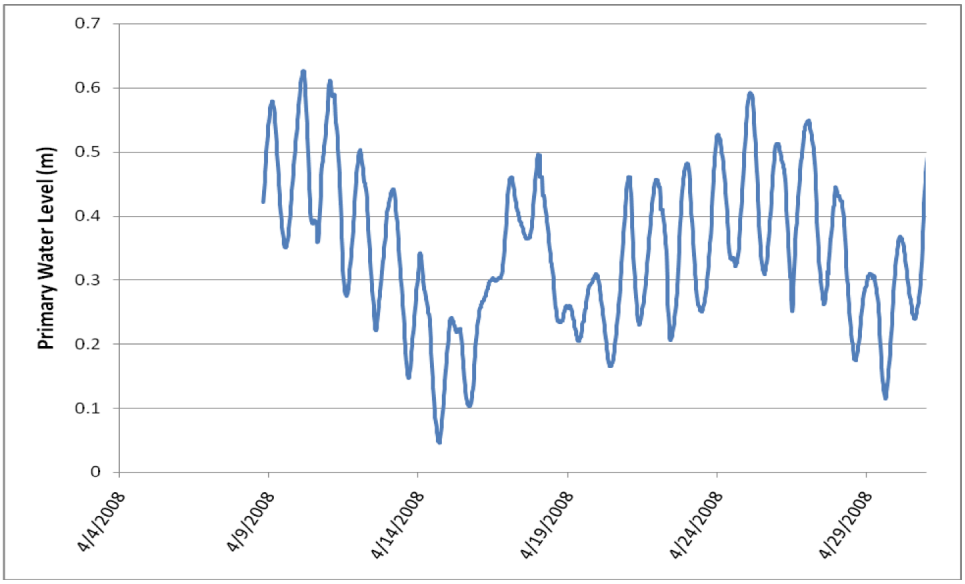

Figure A.8: Tidal boundary condition in April 2008

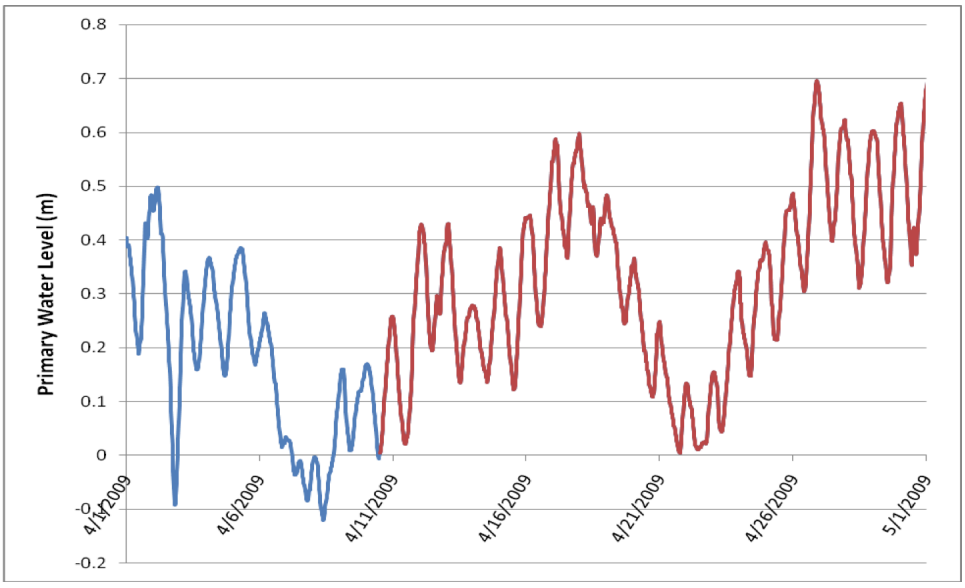

Figure A.9: Tidal boundary condition in April 2009

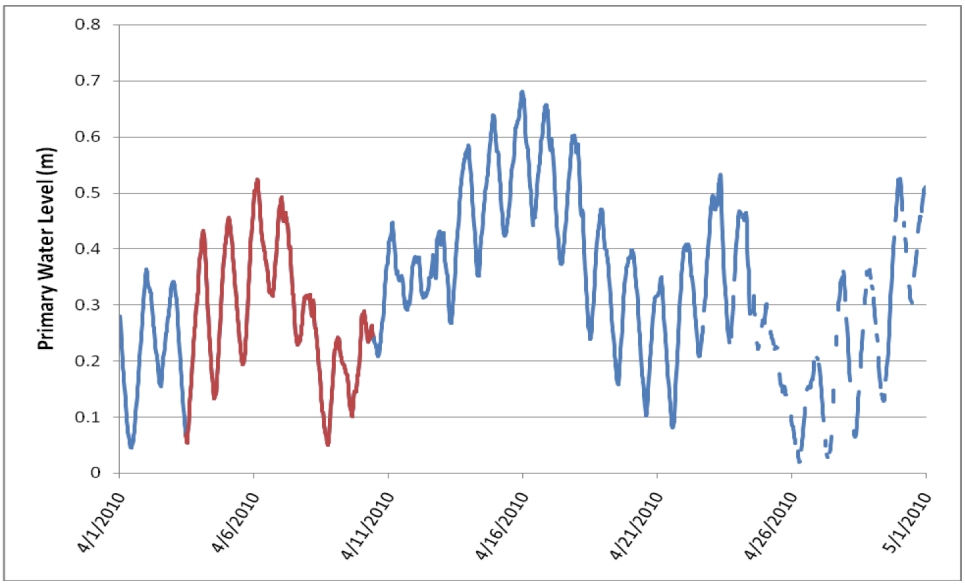

Figure A.10: Tidal boundary condition in April 2010

A.2.3 Inflow Data

The Nueces River Authority monitors the volume of water pumped into the Nueces Delta through the Rincon Pipeline Diversion Project. This inflow modeled as entering vertically from the bottom of six grid cells. Spreading the inflow over multiple grid cells prevents numerical stability problems cause by the high flow rates developed at the pipe terminus. The actual inflow is in a significantly smaller area developing flow conditions that cannot be readily represented by a 2D hydrostatic model such as the NDHM. Spreading the flow over a larger region is a reasonable approximation that does not impact downstream modeling of the pumped freshwater. The pumping data is provided online at hourly intervals at http://www.nueces-ra.org/CP/CITY/rincon/ . The data is supplied in millions of gallons per day and is converted to cubic meters per second for the model.

The Nueces River splits just downstream of the Calallen Dam and upstream of where the Rincon Pipeline Diversion Project outfall. At this split, the majority of river flow runs south of the delta through the Nueces River tidal segment, with a minority of the flow continues east into the delta through the Nueces overflow channel. The locations of the Rincon Pipeline Outfall and the USGS gage in the study area are shown in Figure A.11, and in detail in Figure A.12. USGS Gage 08211503 monitors the flow continuing into the delta. The discharge at this point in the river is measured by USGS in cubic feet per second in 15-minute increments. For the model, this data is converted to cubic meters per second. At times, the discharge is measured as a negative value, representing that the direction of flow at those times is reversed. This change in the direction of flow is caused by saltwater from the Nueces Bay moving up the Nueces River into the Rincon Bayou through the Rincon Bayou Channel during high tide (Ockerman 2001). The negative values in the inflow are removed and replaced with zeros so that the point where this inflow is defined does not become a sink for water at times of reverse flow. The reversed direction of flow is accounted for in the model by the tide coming up into that portion of the delta, pushing the flow inward.

Figure A.11: Locations of the USGS Gage and the Rincon Pipeline Outfall in the Study Area

Figure A.12: USGS Gage and the pipeline outfall.

A.2.4 Wind Data

Wind data was obtained from NUDEWX for 2009 and 2010. The weather station at NUDEWX was not functional during April 2008. To choose the most appropriate weather station to gather wind data for the April 2008 simulation, wind speed and direction values were compared at various stations for April 2009. The weather stations used for comparison were the National Estuarine Research Reserve System station located in the Mission-Aransas Reserve, the TCOON station at Port Ingleside, and the weather station at the Corpus Christi Airport (Figure A.13). Data from these weather stations were compared to NUDEWX (Figure A.14). The Corpus Christi Airport station was chosen as the best match for the April 2008 simulations. Wind speed and direction applied in the models is shown in Figures A15 – A20.

Figure A.13: Locations of the weather stations measuring wind data

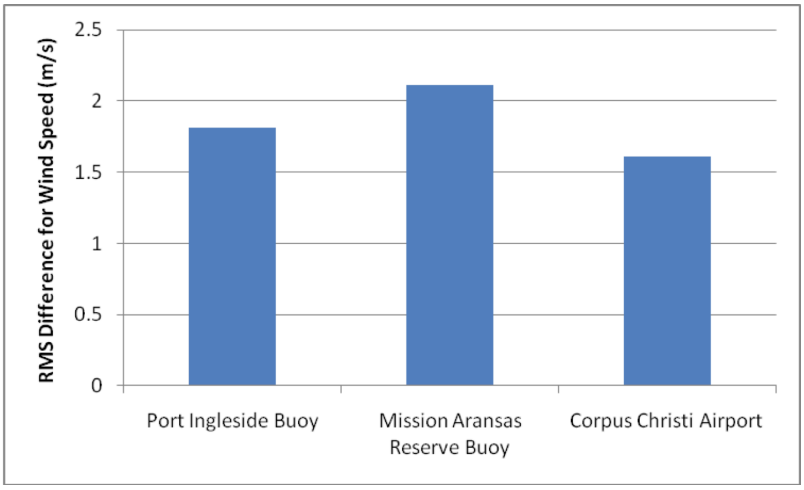

Figure A.14: Comparison of wind data from various weather stations with NUDEWX

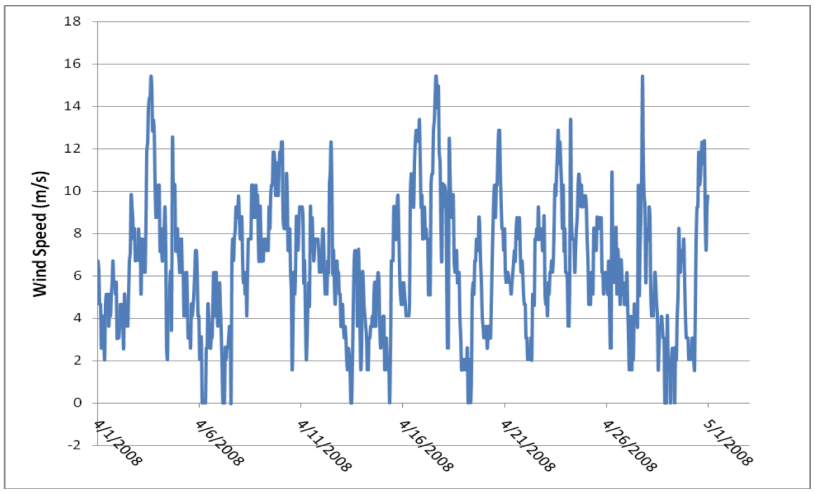

Figure A.15: Wind speed in April 2008

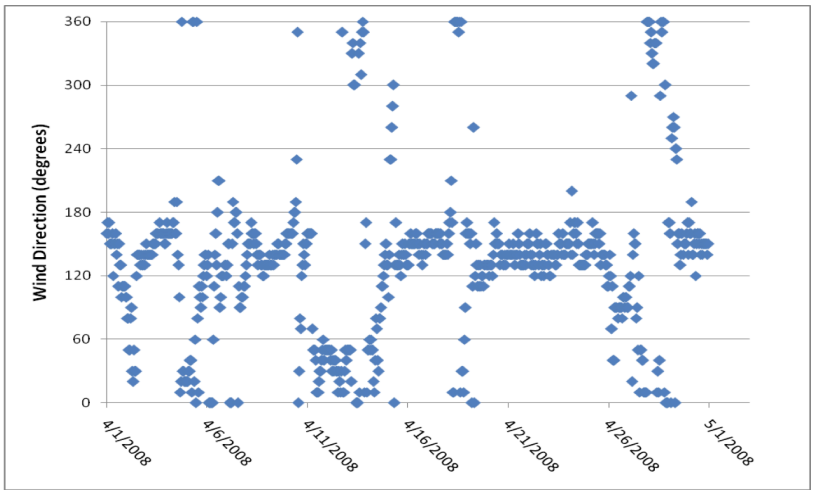

Figure A.16: Wind direction in April 2008

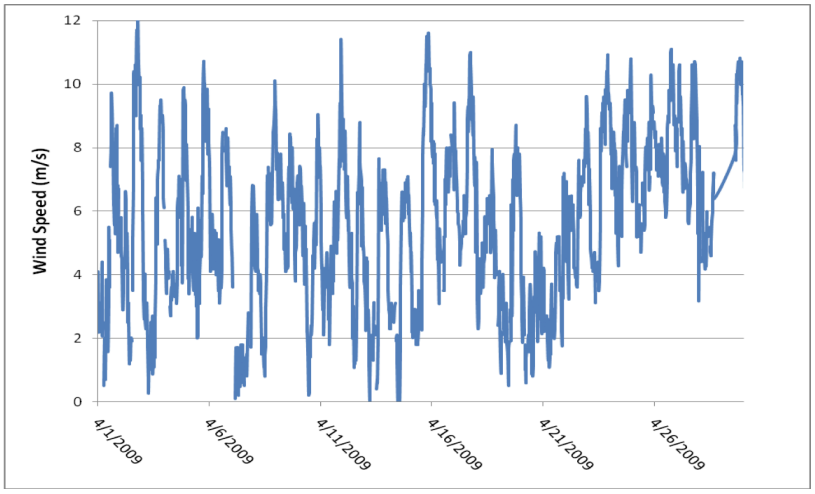

Figure A.17: Wind speed in April 2009

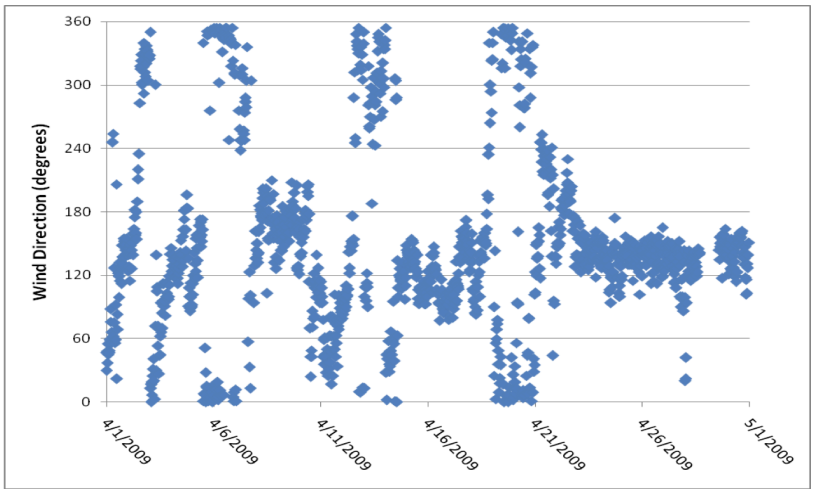

Figure A.18: Wind direction in April 2009

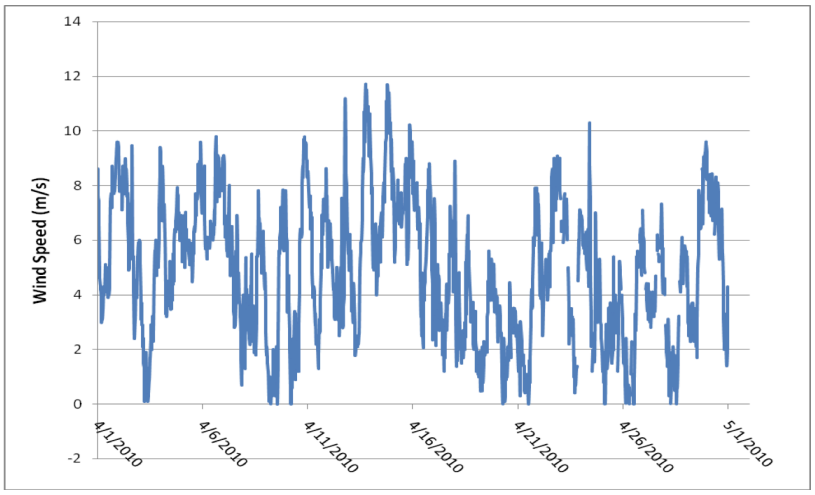

Figure A.19: Wind speed in April 2010

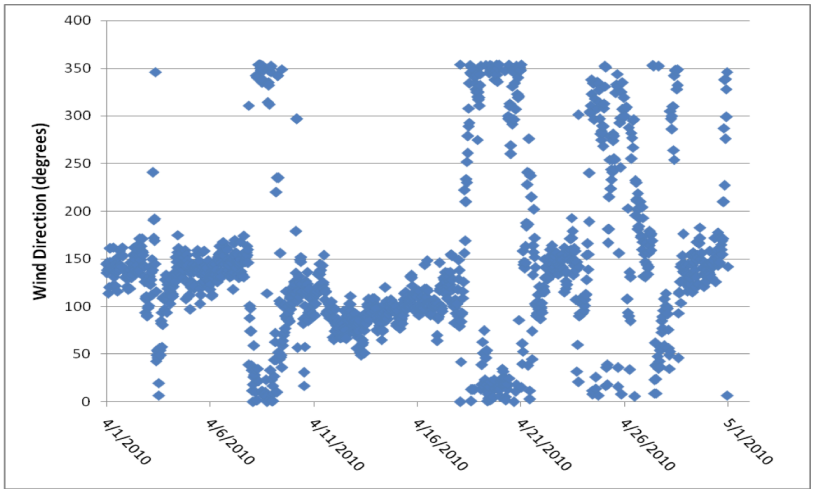

Figure A.20: Wind Direction in April 2010

A.2.5 Precipitation Data

The precipitation data was collected by NOAA at the Corpus Christi Airport, located approximately 7 miles from the delta at 27°46'N 97°31'W. The simulation periods were chosen to test varying conditions. The average precipitation in the Nueces Delta area for April of 2000 – 2010 was approximately 3.8 inches. April 2008 represents a wet condition with 6 inches of rain, April 2009 was dry with less than one inch of rainfall, and April 2010 was slightly above average with 4.85 inches of rain. The precipitation data was obtained in hundredths of inches of rainfall per hour and converted to mm/h for model input. All "trace" precipitation values were converted to zero precipitation.

Scenarios (q.v. Table 2.3) were run for April 2009 with no rain, the actual measured rainfall, and a heavy rainfall. The heavy rainfall scenario is an artificial construction based on the measured rainfall at the NOAA rain gage at Corpus Christi Airport for the last ten years. The highest month of precipitation occurred in July 2007, with the highest consecutive seven days of rainfall of 353 mm. This rainfall was distributed uniformly over time as 2.10 mm/h.

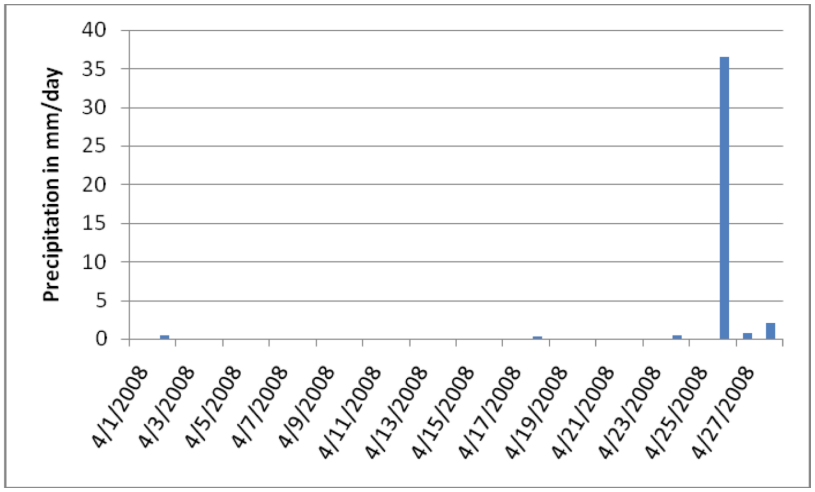

Figure A.12: Rainfall in April 2008

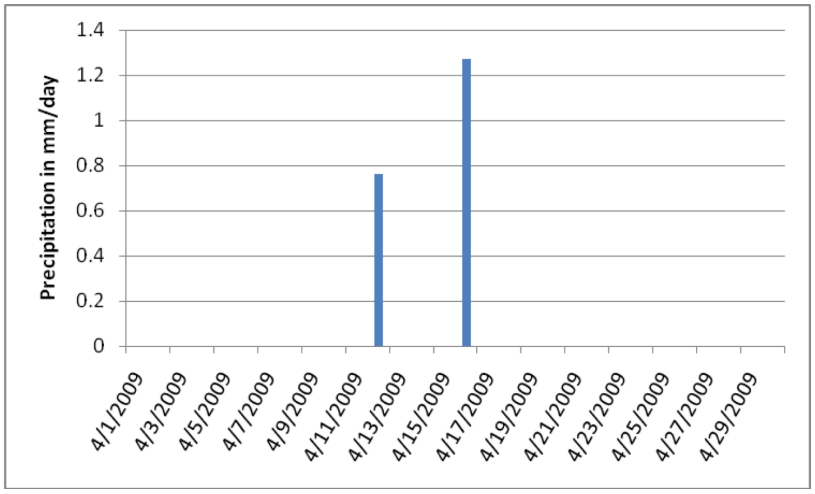

Figure A.13: Rainfall in April 2009

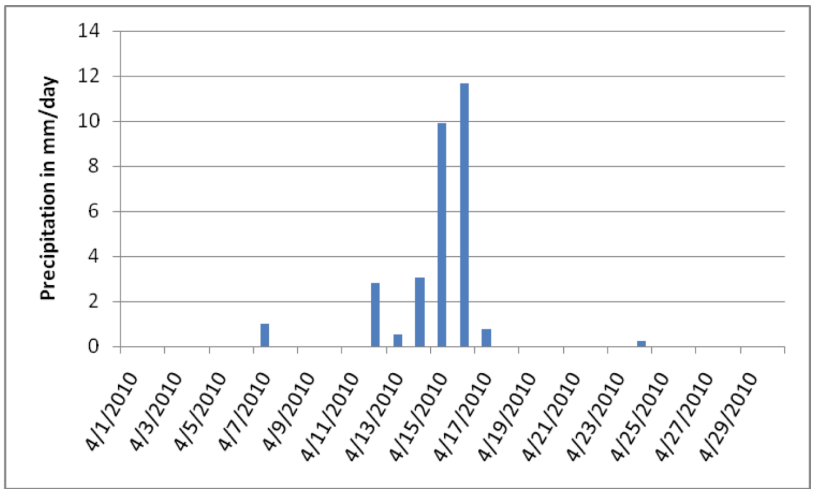

Figure A.14: Rainfall in April 2010

A.2.6 Salinity

The time-varying data used for the salinity at the tidal boundary condition was obtained from the salinity at gage SALT03 (q.v. Figure 2.4). The salinity for the inflow at the USGS gage 08211503 and for all pumped inflow is approximated as zero salinity.

A.2.7 Land Cover

The land cover data for the delta was gathered from the National Land Cover Dataset (NLCD) from the USGS Land Cover Institute. Manning's 'n' roughness coefficient associated with simulating flow across the 2001 NLCD were gathered from literature and translated to a matrix corresponding with bathymetry in the delta (Hossain, Jia and Chao 2009) provided in Table A.1. The impacts of piers and culverts under barriers are incorporated into the land cover matrix as adjusted Manning's roughness coefficients, as discussed in §A.1.3.

Table A.1: Manning's n values associated with various Land Cover types

Land Cover Description	Manning's n
Open water	0.025
Concrete/finished	0.015
Bare Earth	0.025
Trees	0.150
Heavy Brush	0.075
Light Brush	0.050
Pasture/Farmland	0.035

This page intentionally left blank for two-sided printing.

B Appendix: Additional information used in analysis

B.1 Inundated area based on cutoff depth

The inundated area can be defined based on different cutoff values for the minimum depth required. If the depth cutoff is defined as zero, trace values of water will be considered "inundated" and the entire marsh (including uplands) is likely to be considered inundated for even a small rainfall. Figure B.1 shows A_i for Scenario 6 (q.v. Table 2.3) with varying cutoffs for the minimum depth defining inundation. The cutoff values shown in the figure are given in meters. A value of 0.02 m (0.787 in) was chosen as the depth cutoff to define inundated area in the analysis

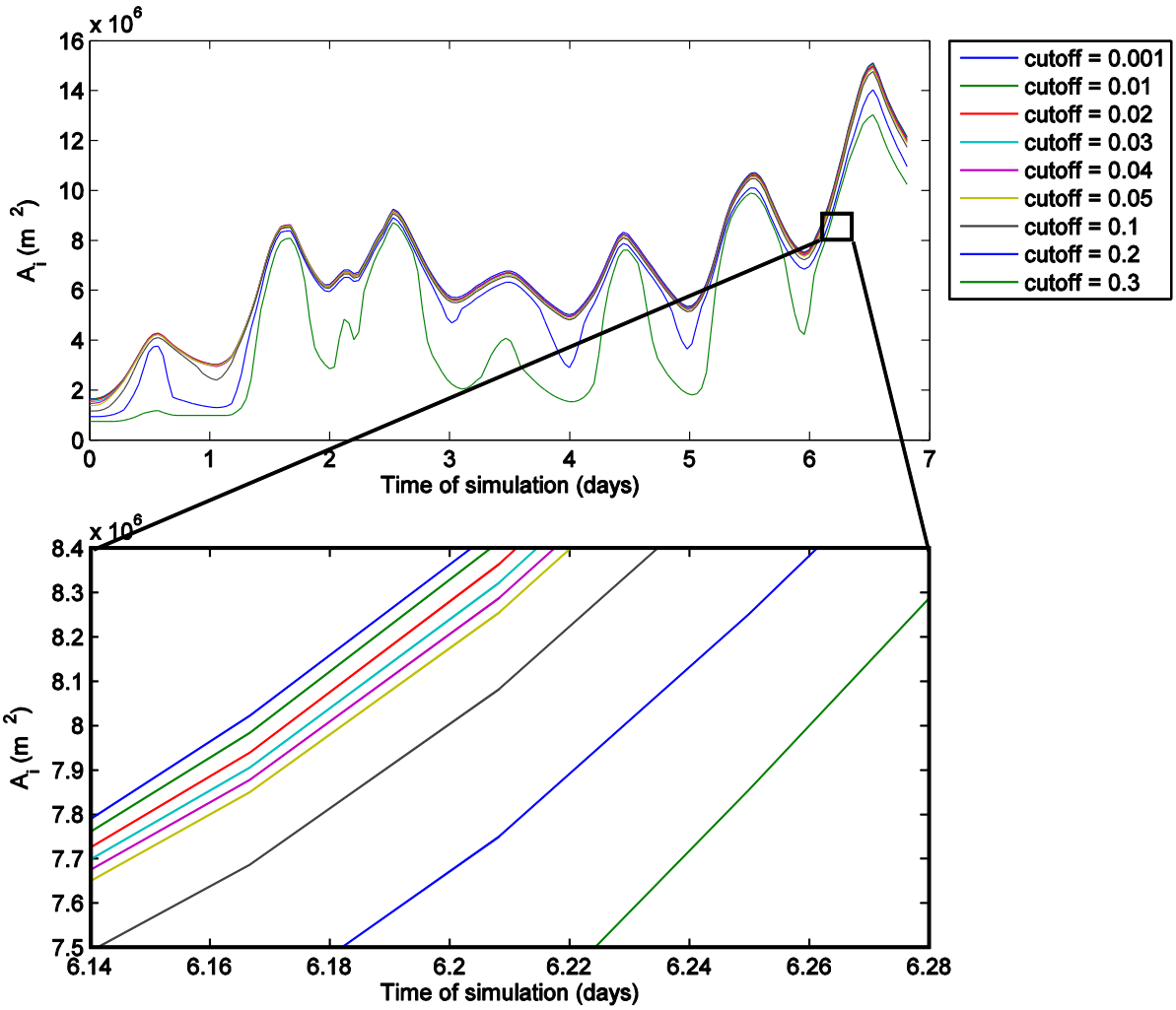

Figure B.1: Inundated area from Scenario 6 with varying cutoff values for minimum depth (in m)

B.2 Estimating vertical datum of monitoring stations

The SALT and NUDE stations used for qualitative validation were not georeferenced relative to NAVD88. To make a rough estimate of their elevation the monthly mean surface elevation at White Point was assumed to be equal to the mean surface elevation at these stations (i.e. any mean horizontal gradient was neglected). The general methodology is presented below:

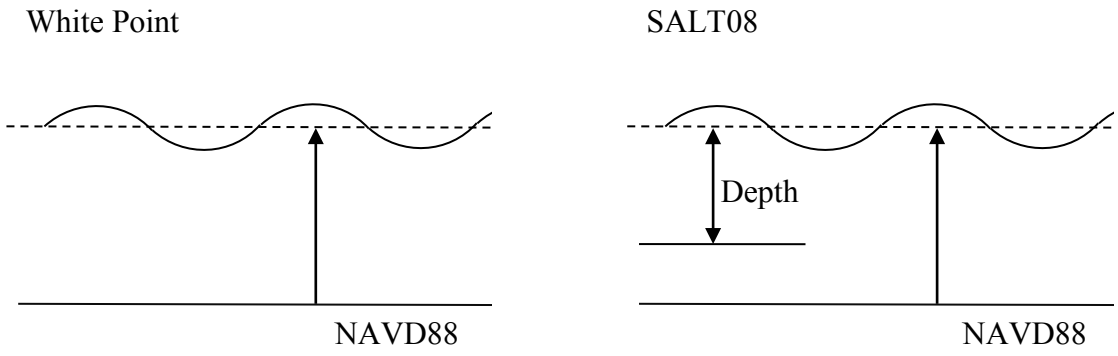

Figure B.2: Problem with the monitoring station vertical datum; depth measured at SALT08 is some unknown height above NAVD88

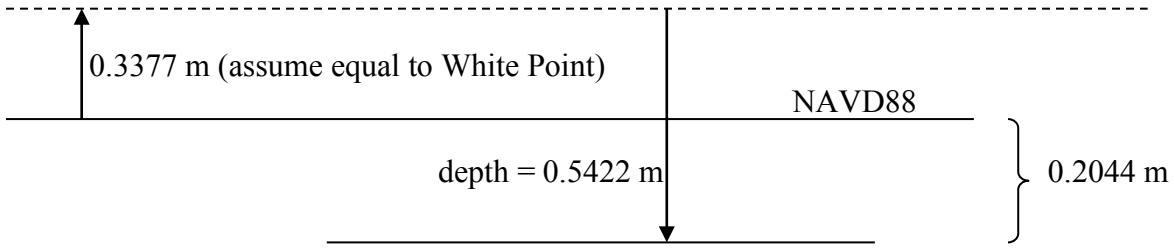

Figure B.3: Estimate for SALT08 reference if mean tidal elevation is identical to White Point value.

The monthly mean tidal elevation at White Point is 0.3377 m (primary water level with respect to NAVD88). The monthly mean depth at SALT08 is 0.5422 m (depth with respect to station datum). It follows that SALT08 is estimated to be 0.2044 m above NAVD88. This methodology is used for NUDE1, NUDE2, and NUDE3 as well as SALT08. Table B.1 displays the data used to approximate the calculations to transfer the depth data to surface elevations relative to a datum.

Table B.1: Values used to estimate the NAVD88 datums for the monitoring stations

Station	Monthly Avg Depth	Transfer data to Surface Elevation
SALT08	0.5422	0.2044
NUDE2	0.1654	-0.1723
NUDE3	0.3946	0.0569

B.3 Soil infiltration algorithm

The soil infiltration algorithm in the model incorporates a simple calculation that allows for depths to be absorbed at a constant rate. This algorithm is particularly important in the uplands surrounding the delta, where water depths are shallow. Development of more advanced models of soil moisture and infiltration are recommended.

B.4 Model's response to wind: percent change in volume

The impacts of changes in wind forcing on the model are investigated here as a percent change from the scenario with no wind, Simulation 8, and are displayed in Figure B.5. The wind substantially increases the total water volume in the Nueces Delta.

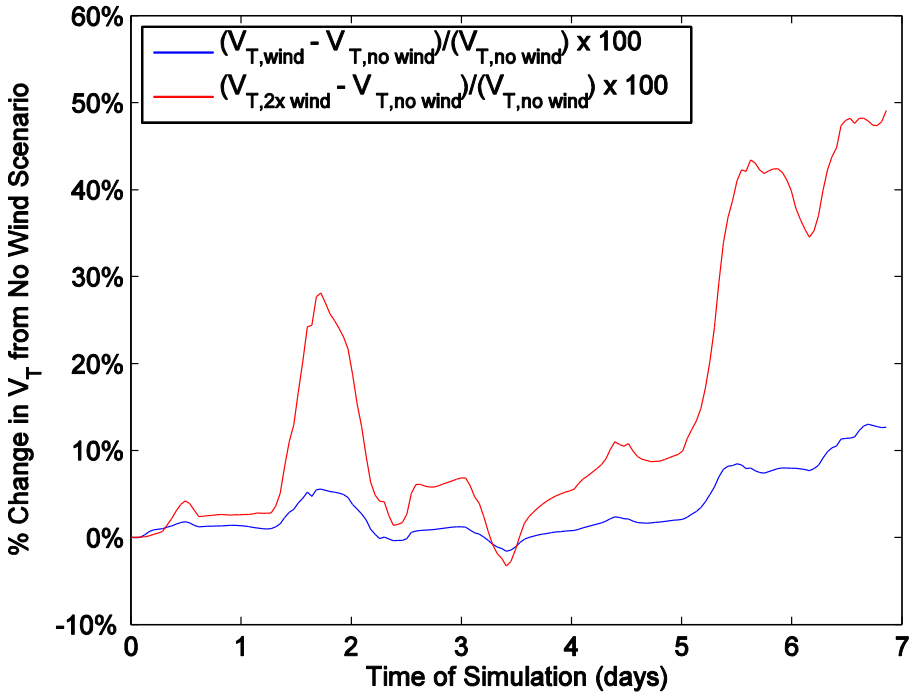

Figure B.5: Percent Change in VT for different wind scenarios

This page intentionally left blank for two-sided printing.

C Appendix: Additional information for future work

C.1 Culvert Data

Culverts allow flow beneath roadways that cross channels in the Nueces Delta a numer of locations. The main culvert is located at the road that crosses the Rincon Bayou just downstream of the Rincon Diversion Pipeline outfall. In the present version of the NDHM, the culverts are modeled as described in §A.1.3. This model could be improved by incorporating more accurate culvert hydraulics. There are three conditions for culvert flow that could be implemented: submerged outlet, a free outlet with submerged inlet, and free flow where both the inlet and outlet are unsubmerged (Figure C.1).

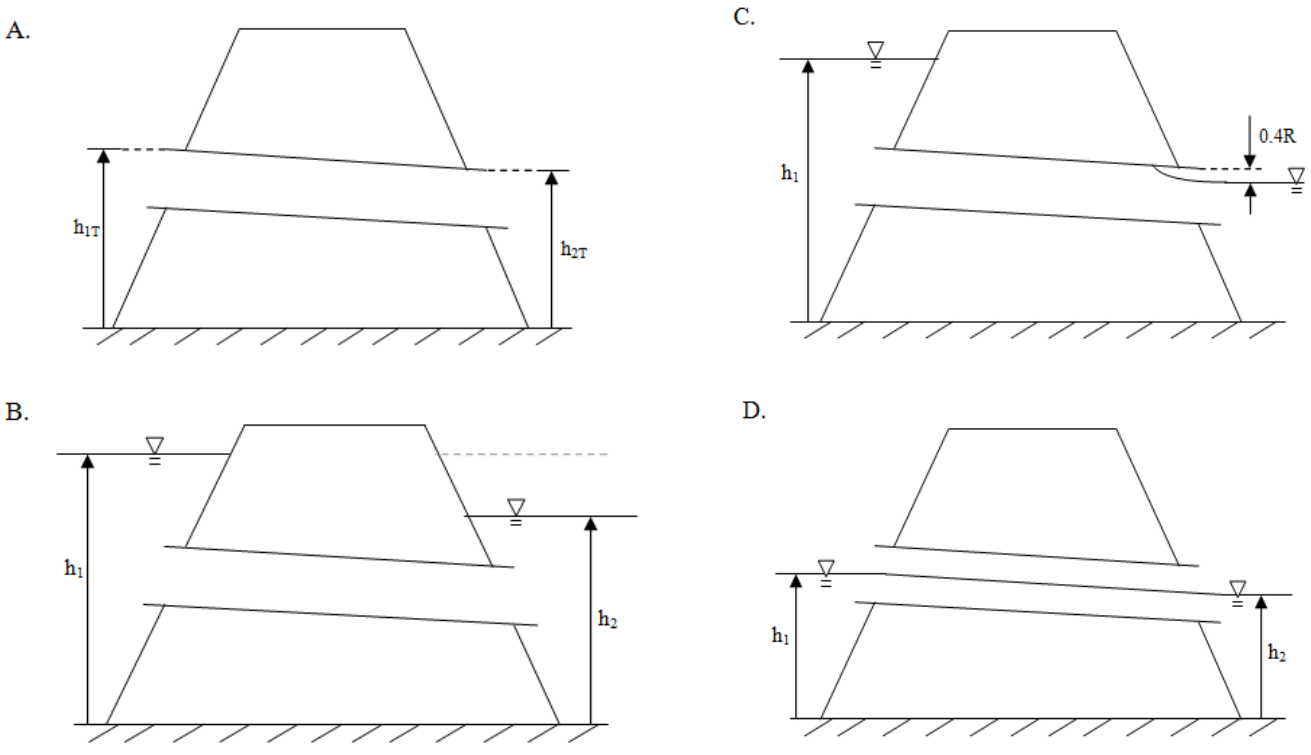

Figure C.1: Culvert flow conditions: A. culvert height definitions; B. submerged outlet; C. submerged inlet with free outlet; D. free flow.

Different hydraulic equations should be applied for these conditions. For a submerged outlet, Figure C.1.B, the flow rate is

$$Q = \frac{\pi\left(\frac{d}{2}\right)^2 \sqrt{2g\left(h_1 - h_2\right)}}{\sqrt{1.78 + L\left(\frac{1244522 \times n^2}{d^{4/3}}\right)}} \tag{C.1}$$

where:

d = diameter of the pipe

L = length of culvert barrel

n = Manning's n of the culvert barrel

h_1, h_2, h_{1T}, h_{2T} = as shown in Figure C.1.A and C.1.B

For the submerged inlet with free outlet, Figure C.1.C, we have

$$Q = \frac{\pi\left(\frac{d}{2}\right)^2 \sqrt{2g\left(h_1 - h_{2T} + 0.2d\right)}}{\sqrt{1.78 + L\left(\frac{1244522 \times n^2}{d^{4/3}}\right)}} \tag{C.2}$$

If both the inlet and outlet of the culvert barrel are unsubmerged, the flow is

$$Q = \frac{1}{n} A\, R^{2/3} S^{1/2} \tag{C.3}$$

where R is the hydraulic radius, S is the slope, and computation of R is conditional:

If $h_1 < \left(h_{1T} - \frac{d}{2}\right)$

$$P = r\,\theta$$

$$\theta = 2\arccos\left(\frac{r - y}{y}\right)$$

$$y = h_1 - (h_{1T} - d)$$

$$A = \frac{r^2(\theta - \sin\theta)}{2}$$

If $h_1 > \left(h_{1T} - \frac{d}{2}\right)$

$$P = 2\pi r - (r \times \theta)$$

$$\theta = 2\arccos\left(\frac{y-r}{y}\right)$$

$$y = h_1 - (h_{1T} - d)$$

$$A = \pi r^2 - \frac{r^2(\theta - \sin\theta)}{2}$$

C.2 Meteorological Data

Meteorological data may aid in accurately simulating heating and cooling in the Nueces Delta to evaluate evaporation and the salt balance. The PC2 Model has capabilities in progress to input shortwave radiation, cloud cover, relative humidity and air temperature data for these calculations.

Cloud cover, relative humidity and air temperature data can be obtained from weather data collected at Corpus Christi International Airport. Shortwave radiation can be calculated following Bisht et al (2005).

$$R_S^{\downarrow} - R_S^{\uparrow} = \frac{S_0\left(\cos\theta\right)^2}{d} \tag{C.4}$$

$$d = 1.085\cos\theta + e_0\left(2.7 + \cos\theta\right)\left(10^{-3}\right) + 0.1 \tag{C.5}$$

where:

S_0 = 1367 W/m2

θ = solar zenith angle

e_0 = screen level vapor pressure

The vapor pressure can be calculated using the Antoine Equation with parameters from the National Institute of Standards and Technology (U.S. Secretary of Commerce 2008).

$$\log_{10}\left(P\right) = A - \frac{B}{C+T} \tag{C.6}$$

where:

A = 5.40221

B = 1838.675

C = -31.737

The solar zenith angle can be obtained from the National Solar Radiation Database (NSRDB) from the National Climatic Data Center. Data from the NSRDB is only available up through 2005. The zenith angle at each hour in April varies by a maximum of 0.2 degrees from year to year from 1991-2005. Because the data is consistent from year to year, this data is considered reasonable for calculating the shortwave radiation for the dates simulated. To confirm that this data is accurate for possible input into the model, the solar zenith angle was calculated using equations for calculating the solar zenith angle at a particular latitude point based on the time of day and time of year (Sellers 1965, Wunderlich 1972). The calculations of the solar zenith angle on April 10

at the latitude of the Nueces Delta reveal that the measured solar zenith angles at the Corpus Christi Airport are comparable to the calculated values.

The calculated radiation values are reasonable when compared to solar radiation values measured directly in Sinton, TX, approximately 18 kilometers from the delta. This data was gathered by the Texas A&M AgriLife Extension TexasET system. This data is not appropriate for use as input for the model because varying measurement techniques for shortwave radiation can make data inconsistent in what is being measured.

C.3 Water temperature data

The water temperature data for the initial condition is available from TCOON at the salinity stations. As with the initial condition for salinity, the water temperature may be considered uniform from north to south across the delta and varies from east to west as a linear interpolation between the salinity gauging stations. The water temperature at the boundary condition of the incoming tide may be set equal to the water temperature at SALT03 through time. The water temperature for the inflow from at the USGS Station 08211503 is available as daily mean temperature data from USGS. This water temperature data can be used for the inflow at the USGS gage as well as the pumped water since it is pumped from the river. The temperature of rainfall might be considered equal to the average of the air temperature because rainfall temperature data is not available.

D Appendix: Matlab scripts

D.1 Analyzing spin-up

```
%% Compare 10 day & 17 day runs

load ('/Users/andrearyan/Documents/MATLAB/PC2
20110427/Analysis/Nueces_April2009_17days/OutData2D.mat');
OutData2D_17days = OutData2D; clear OutData2D;
disp ('*****Finished loading first variable*****')

load ('/Users/andrearyan/Documents/MATLAB/PC2
20110427/Analysis/Nueces_April2009_10days/OutData2D.mat');
OutData2D_10days = OutData2D; clear OutData2D;
disp ('*****Finished loading second variable*****')


%% Find volume of water in each time step
length1 = size(OutData2D_17days.depth_time);
mm = length1(2);

length2 = size(OutData2D_10days.depth_time);
length10 = length2(2);

sum_volume_17 = zeros(mm,1);
volume_17 = zeros(667,971,mm);
volume_17_nonan = zeros(667,971);

for n = 1:mm
    volume_17(:,:,n) = OutData2D_17days.depth(:,:,n);
    volume_17_nonan = volume_17(:,:,n);
    aa = isnan(volume_17_nonan);
    volume_17_nonan(aa) = 0; %get rid of nans
    volume_17(:,:,n) = volume_17_nonan;

    sum_volume_17(n,1) = sum(sum(volume_17(:,:,n)));
end

disp ('*****Finished Summing Volume for 17 day Scenario*****')

sum_volume_10 = zeros(length10,1);
volume_10 = zeros(667,971,length10);
volume_10_nonan = zeros(667,971);
for n = 1:length10
    volume_10(:,:,n) = OutData2D_10days.depth(:,:,n);
    volume_10_nonan = volume_10(:,:,n);
    aa = isnan(volume_10_nonan);
    volume_10_nonan(aa) = 0; %get rid of nans
    volume_10(:,:,n) = volume_10_nonan;

    sum_volume_10(n,1) = sum(sum(volume_10(:,:,n)));
end
```

```
disp ('*****Finished Summing Volume for the 10 day Scenario*****')

%% Find inundated area at each time step

depth_cutoff = 0.02; %this is the depth below which will not be included in
inundated area

sum_area_17 = zeros(mm,1);
area_17 = zeros(667,971,mm);

for n = 1:mm
    depth_17 = volume_17(:,:,n);
    cc = find(depth_17 < depth_cutoff);
    depth_17(cc) = 0;
    bb = find(depth_17 > 0);
    depth_17(bb) = 1;
    area_17(:,:,n) = depth_17;

    sum_area_17(n,1) = sum(sum(area_17(:,:,n))).*15.*15; %gives area inundated
at greater than 2 cm
end

disp ('*****Finished Finding Inundated Area for 17 day Scenario*****')

sum_area_10 = zeros(length10,1);
area_10 = zeros(667,971,length10);
for n = 1:length10
    depth_10 = volume_10(:,:,n);
    cc = find(depth_10 < depth_cutoff);
    depth_10(cc) = 0;
    bb = find(depth_10 > 0);
    depth_10(bb) = 1;
    area_10(:,:,n) = depth_10;

    sum_area_10(n,1) = sum(sum(area_10(:,:,n))).*15.*15; %gives area inundated
at greater than 2 cm
end

disp ('*****Finished Finding Inundated Area for 10 day Scenario*****')

%% Mean & Std. Dev of surface elevation through time

mean_elev_17 = zeros(mm,1);
stdev_elev_17 = zeros(mm,1);
elev_17 = zeros(667,971,mm);

diff = zeros(667,971,length10);
std_dev = zeros(length10,1);
mean_diff = zeros(length10,1);
max_diff = zeros(length10,1);

for n = 1:length10
    time_17 = n + (594000./90./40); %transfer time to work for 17 day scenario
```

```
    diff(:,:,n) = abs(volume_17(:,:,time_17) - volume_10(:,:,n));
    std_dev(n,1) = std(std(diff(:,:,n)));

    mean_diff(n,1) = mean(mean(diff(:,:,n)));
    max_diff(n,1) = max(max(diff(:,:,n)));
end

day = 24;

std_dev_day = [mean(std_dev(1:day,1));mean(std_dev(day+1:day*2,1));...
    mean(std_dev(day*2+1:day*3,1));mean(std_dev(day*3+1:day*4,1));...
    mean(std_dev(day*4+1:day*5,1));mean(std_dev(day*5+1:day*6,1));...
    mean(std_dev(day*6+1:day*7,1));mean(std_dev(day*7+1:day*8,1));...
    mean(std_dev(day*8+1:day*9,1));mean(std_dev(day*9+1:day*10,1))];

mean_diff_day = [mean(mean_diff(1:day,1));mean(mean_diff(day+1:day*2,1));...
    mean(mean_diff(day*2+1:day*3,1));mean(mean_diff(day*3+1:day*4,1));...
    mean(mean_diff(day*4+1:day*5,1));mean(mean_diff(day*5+1:day*6,1));...
    mean(mean_diff(day*6+1:day*7,1));mean(mean_diff(day*7+1:day*8,1));...
    mean(mean_diff(day*8+1:day*9,1));mean(mean_diff(day*9+1:day*10,1))];

% Inundated Area
stddev_diffarea_day =
[mean(diff_area2(1:day,1));mean(diff_area2(day+1:day*2,1));...
    mean(diff_area2(day*2+1:day*3,1));mean(diff_area2(day*3+1:day*4,1));...
    mean(diff_area2(day*4+1:day*5,1));mean(diff_area2(day*5+1:day*6,1));...
    mean(diff_area2(day*6+1:day*7,1));mean(diff_area2(day*7+1:day*8,1));...
    mean(diff_area2(day*8+1:day*9,1));mean(diff_area2(day*9+1:day*10,1))];

mean_diffarea_day =
[mean(diff_area2(1:day,1));mean(diff_area2(day+1:day*2,1));...
    mean(diff_area2(day*2+1:day*3,1));mean(diff_area2(day*3+1:day*4,1));...
    mean(diff_area2(day*4+1:day*5,1));mean(diff_area2(day*5+1:day*6,1));...
    mean(diff_area2(day*6+1:day*7,1));mean(diff_area2(day*7+1:day*8,1));...
    mean(diff_area2(day*8+1:day*9,1));mean(diff_area2(day*9+1:day*10,1))];

% Total Volume
stddev_diffvol_day =
[mean(diff_vol2(1:day,1));mean(diff_vol2(day+1:day*2,1));...
    mean(diff_vol2(day*2+1:day*3,1));mean(diff_vol2(day*3+1:day*4,1));...
    mean(diff_vol2(day*4+1:day*5,1));mean(diff_vol2(day*5+1:day*6,1));...
    mean(diff_vol2(day*6+1:day*7,1));mean(diff_vol2(day*7+1:day*8,1));...
    mean(diff_vol2(day*8+1:day*9,1));mean(diff_vol2(day*9+1:day*10,1))];

mean_diffvol_day = [mean(diff_vol2(1:day,1));mean(diff_vol2(day+1:day*2,1));...
    mean(diff_vol2(day*2+1:day*3,1));mean(diff_vol2(day*3+1:day*4,1));...
    mean(diff_vol2(day*4+1:day*5,1));mean(diff_vol2(day*5+1:day*6,1));...
    mean(diff_vol2(day*6+1:day*7,1));mean(diff_vol2(day*7+1:day*8,1));...
    mean(diff_vol2(day*8+1:day*9,1));mean(diff_vol2(day*9+1:day*10,1))];
```

D.2 Analyzing model response to rainfall

```
%% Compare rain vs no rain scenarios
```

```
% load Rain Scenarios for April 2009
load ('/Users/andrearyan/Documents/MATLAB/PC2
20110427/Analysis/Nueces_15x15_April2009_withrain/OutData2D_rain.mat');
disp ('*****Finished loading first variable*****')

load ('/Users/andrearyan/Documents/MATLAB/PC2
20110427/Analysis/NuecesApril2009_90s_7days/OutData2D_no_rain.mat');
disp ('*****Finished loading second variable*****')
OutData2D_no_rain = OutData2D; clear OutData2D;

load ('/Users/andrearyan/Documents/MATLAB/PC2
20110603/NuecesRuns_20110603/Nueces2009_WhR_7d_an_0p/OutData2D.mat');
OutData2D_hR = OutData2D; clear OutData2D;
disp ('*****Finished loading third variable*****')

%% Find volume of water in each time step
length1 = size(OutData2D_rain.depth_time);
mm = length1(2);

sum_volume_rain = zeros(mm,1);
volume_rain = zeros(667,971,mm);
for n = 1:mm
    volume_rain(:,:,n) = OutData2D_rain.depth(:,:,n);
    volume_rain_nonan = volume_rain(:,:,n);
    aa = isnan(volume_rain_nonan);
    volume_rain_nonan(aa) = 0; %get rid of NaNs
    volume_rain(:,:,n) = volume_rain_nonan;

    sum_volume_rain(n,1) = sum(sum(volume_rain(:,:,n)));
end

disp ('*****Finished Summing Volume for Rain Scenario*****')

sum_volume_norain = zeros(mm,1);
volume_norain = zeros(667,971,mm);
for n = 1:mm
    volume_norain(:,:,n) = OutData2D_no_rain.depth(:,:,n);
    volume_norain_nonan = volume_norain(:,:,n);
    aa = isnan(volume_norain_nonan);
    volume_norain_nonan(aa) = 0; %get rid of NaNs
    volume_norain(:,:,n) = volume_norain_nonan;

    sum_volume_norain(n,1) = sum(sum(volume_norain(:,:,n)));
end

disp ('*****Finished Summing Volume for No Rain Scenario*****')

sum_volume_hR = zeros(mm,1);
volume_hR = zeros(667,971,mm);
for n = 1:mm
    volume_hR(:,:,n) = OutData2D_hR.depth(:,:,n);
    volume_hR_nonan = volume_hR(:,:,n);
    aa = isnan(volume_hR_nonan);
```

```
    volume_hR_nonan(aa) = 0; %get rid of NaNs
    volume_hR(:,:,n) = volume_hR_nonan;

    sum_volume_hR(n,1) = sum(sum(volume_hR(:,:,n)));
end

disp ('*****Finished Summing Volume for Heavy Rain Scenario*****')

% When does it rain in 2009?
when_rain = ...
[174600 ,   0.762   ;...
531000  ,   1.27    ;...
534600  ,   0.508];

rain_amount = when_rain(:,2);

%% Find inundated area at each time step
depth_cutoff = 0.02; %this is the depth below which will not be included in
inundated area

sum_area_rain = zeros(mm,1);
area_rain = zeros(667,971,mm);

for n = 1:mm
    depth_rain = volume_rain(:,:,n);
    cc = find(depth_rain < depth_cutoff);
    depth_rain(cc) = 0;
    area_rain(:,:,n) = depth_rain;

    sum_area_rain(n,1) = sum(sum(area_rain(:,:,n))); %gives area inundated at
greater than 2 cm
end

disp ('*****Finished Finding Inundated Area for rain Scenario*****')

sum_area_norain = zeros(mm,1);
area_norain = zeros(667,971,mm);

for n = 1:mm
    depth_norain = volume_norain(:,:,n);
    cc = find(depth_norain < depth_cutoff);
    depth_norain(cc) = 0;
    area_norain(:,:,n) = depth_norain;

    sum_area_norain(n,1) = sum(sum(area_norain(:,:,n))); %gives area inundated
at greater than 2 cm
end

disp ('*****Finished Finding Inundated Area for no rain Scenario*****')

sum_area_hR = zeros(mm,1);
area_hR = zeros(667,971,mm);

for n = 1:mm
```

```
    depth_hR = volume_hR(:,:,n);
    cc = find(depth_hR < depth_cutoff);
    depth_hR(cc) = 0;
    area_hR(:,:,n) = depth_hR;

    sum_area_hR(n,1) = sum(sum(area_hR(:,:,n))); %gives area inundated at
greater than 2 cm
end

disp ('*****Finished Finding Inundated Area for no rain Scenario*****')

% difference in inundated area:
diff_area = sum_area_rain - sum_area_norain;
aa = find(diff_area < 0);
diff_area(aa) = 0;

diff_area2 = sum_area_hR - sum_area_norain;
aa = find(diff_area2 < 0);
diff_area2(aa) = 0;

%% Calculate percent diff for rain inundated area & total volume:
max_IA_hR = max(sum_area_hR(:,1));
max_IA_norain = max(sum_area_norain(:,1));
max_IA_rain = max(sum_area_rain(:,1));

diff_IA_hR = max_IA_hR - max_IA_norain
diff_IA_rain = max_IA_rain - max_IA_norain

max_vol_norain = max(sum_volume_norain(:,1));
max_vol_hR = max(sum_volume_hR(:,1));
max_vol_rain = max(sum_volume_rain(:,1));

perc_vol_hR = (max_vol_hR - max_vol_norain) / (max_vol_norain)
perc_vol_rain = (max_vol_rain - max_vol_norain) / (max_vol_norain)
```

D.3 Analyzing model response to wind

```
%% Load Variables for wind analysis

load ('/Users/andrearyan/Documents/MATLAB/PC2
20110603/NuecesRuns_20110603/Nueces2009_SR_7d_an_0p/OutData2D.mat');
OutData2D_nowind = OutData2D; clear OutData2D;
disp ('*****Finished loading first variable*****')

load ('/Users/andrearyan/Documents/MATLAB/PC2
20110427/Analysis/Nueces_15x15_April2009_withrain/OutData2D_rain.mat');
OutData2D_wind = OutData2D_rain; clear OutData2D_rain;
disp ('*****Finished loading second variable*****')

load ('/Users/andrearyan/Documents/MATLAB/PC2
20110603/NuecesRuns_20110603/Nueces2009_2WR_7d_an_0p/OutData2D.mat');
OutData2D_2xwind = OutData2D; clear OutData2D;
disp ('*****Finished loading third variable*****')
```

```
%% Find difference in mean depth
depth_cutoff = 0.02; %this is the depth below which will not be included in
inundated area

length1 = size(OutData2D_nowind.depth_time);
mm = length1(2);

% NO WIND
depth_nowind = zeros(667,971,mm);
depth_nonan = zeros(667,971);
area_nowind = zeros(667,971);
area_nowind_time = zeros(667,971,mm);
sum_area_nowind = zeros(mm,1);

for n = 1:mm
    %get rid of NaNs
    depth_nowind(:,:,n) = OutData2D_nowind.depth(:,:,n);
    depth_nonan = depth_nowind(:,:,n);
    aa = isnan(depth_nonan);
    depth_nonan(aa) = 0; %get rid of nans
    depth_nowind(:,:,n) = depth_nonan;

    area_nowind = depth_nonan;
    cc = find(area_nowind < depth_cutoff);
    area_nowind(cc) = 0;
    bb = find(area_nowind > 0);
    area_nowind(bb) = 1; % has 0's everywhere depth < cutoff & 1's elsewhere
    area_nowind_time(:,:,n) = area_nowind;

    sum_area_nowind(n,1) = sum(sum(area_nowind_time(:,:,n))).*15.*15; %gives
area inundated at greater than 2 cm
end

% WIND
depth_wind = zeros(667,971,mm);
depth_nan = zeros(667,971);
area_wind = zeros(667,971);
area_wind_time = zeros(667,971,mm);
sum_area_wind = zeros(mm,1);

for n = 1:mm
    depth_wind(:,:,n) = OutData2D_wind.depth(:,:,n); %get rid of NaNs
    depth_nonan = depth_wind(:,:,n);
    aa = isnan(depth_nonan);
    depth_nonan(aa) = 0; %get rid of nans
    depth_wind(:,:,n) = depth_nonan;

    area_wind = depth_nonan;
    cc = find(area_wind < depth_cutoff);
    area_wind(cc) = 0;
    bb = find(area_wind > 0);
    area_wind(bb) = 1; % has 0's everywhere depth < cutoff & 1's elsewhere
    area_wind_time(:,:,n) = area_wind;
```

```
    sum_area_wind(n,1) = sum(sum(area_wind_time(:,:,n))).*15.*15; %gives area
inundated at greater than 2 cm
end


% 2x WIND
depth_2xwind = zeros(667,971,mm);
depth_2xnan = zeros(667,971);
area_2xwind = zeros(667,971);
area_2xwind_time = zeros(667,971,mm);
sum_area_2xwind = zeros(mm,1);

for n = 1:mm
    %get rid of NaNs
    depth_2xwind(:,:,n) = OutData2D_2xwind.depth(:,:,n);
    depth_nonan = depth_2xwind(:,:,n);
    aa = isnan(depth_nonan);
    depth_nonan(aa) = 0; %get rid of nans
    depth_2xwind(:,:,n) = depth_nonan;

    area_2xwind = depth_nonan;
    cc = find(area_2xwind < depth_cutoff);
    area_2xwind(cc) = 0;
    bb = find(area_2xwind > 0);
    area_2xwind(bb) = 1; % has 0's everywhere depth < cutoff & 1's elsewhere
    area_2xwind_time(:,:,n) = area_2xwind;

    sum_area_2xwind(n,1) = sum(sum(area_2xwind_time(:,:,n))).*15.*15; %gives
area inundated at greater than 2 cm
end

%% Errorbar at last time step through 2D space (u_300D)

points = 48; %how many data points do you want
step = round(971/points)-1; %each point includes this many steps (rounds up to
nearest integer then minus one so we don't go over 971)

% NO WIND
mean_depth_nowind = zeros(points,1);
stddev_depth_nowind = zeros(points,1);

for jj = 1:points
    jj1 = (jj*step) - (step-1);
    jj2 = (jj*step);
    mean_depth_nowind(jj,1) = mean(mean(depth_nowind(:,jj1:jj2,mm)));
    stddev_depth_nowind(jj,1) = std(std(depth_nowind(:,jj1:jj2,mm)));
end

% NORMAL WIND
mean_depth_wind = zeros(points,1);
stddev_depth_wind = zeros(points,1);

for jj = 1:points
```

```
    jj1 = (jj*step) - (step-1);
    jj2 = (jj*step);
    mean_depth_wind(jj,1) = mean(mean(depth_wind(:,jj1:jj2,mm)));
    stddev_depth_wind(jj,1) = std(std(depth_wind(:,jj1:jj2,mm)));
end

% 2X WIND
mean_depth_2xwind = zeros(points,1);
stddev_depth_2xwind = zeros(points,1);

for jj = 1:points
    jj1 = (jj*step) - (step-1);
    jj2 = (jj*step);
    mean_depth_2xwind(jj,1) = mean(mean(depth_2xwind(:,jj1:jj2,mm)));
    stddev_depth_2xwind(jj,1) = std(std(depth_2xwind(:,jj1:jj2,mm)));
end

%% Calculate % increase in total volume of water on 7th day

vol_7_wind = sum(sum(depth_wind(:,:,168)));
vol_7_nowind = sum(sum(depth_nowind(:,:,168)));
vol_7_2xwind = sum(sum(depth_2xwind(:,:,168)));

perc_7_vol_wind = (vol_7_wind - vol_7_nowind) / (vol_7_nowind)
perc_7_vol_2xwind = (vol_7_2xwind - vol_7_nowind) / (vol_7_nowind)

%% Calculation % increase in total volume of water throughout time
vol_all_wind = zeros(mm,1);
vol_all_nowind = zeros(mm,1);
vol_all_2xwind = zeros(mm,1);
perc_all_vol_wind = zeros(mm,1);
perc_all_vol_2xwind = zeros(mm,1);

for n = 1:mm
    vol_all_wind(n,1) = sum(sum(depth_wind(:,:,n)));
    vol_all_nowind(n,1) = sum(sum(depth_nowind(:,:,n)));
    vol_all_2xwind(n,1) = sum(sum(depth_2xwind(:,:,n)));

    perc_all_vol_wind(n,1) = (vol_all_wind(n,1) - vol_all_nowind(n,1)) /
(vol_all_nowind(n,1)).*100;
    perc_all_vol_2xwind(n,1) = (vol_all_2xwind(n,1) - vol_all_nowind(n,1)) /
(vol_all_nowind(n,1)).*100;

end
```

D.4 Analyzing model response to surface roughness

```
%% Load Variables for Comparing Roughness (Manning's n)

load ('/Users/andrearyan/Documents/MATLAB/PC2
20110603/NuecesRuns_20110605/Nueces2010_WR_14d_an_0p/OutData2D.mat');
OutData2D_an = OutData2D; clear OutData2D;
```

```
load ('/Users/andrearyan/Documents/MATLAB/PC2
20110603/NuecesRuns_20110605/Nueces2010_WR_14d_bn_0p/OutData2D.mat');
OutData2D_bn = OutData2D; %this variable is manning's n * 10
clear OutData2D;

load ('/Users/andrearyan/Documents/MATLAB/PC2
20110603/NuecesRuns_20110605/Nueces2010_WR_14d_cn_0p/OutData2D.mat');
OutData2D_cn = OutData2D; %this variable is manning's n * 100
clear OutData2D;

load ('/Users/andrearyan/Documents/MATLAB/PC2
20110603/NuecesRuns_20110610_outdata/Nueces2010_WR_14d_dn_0p/OutData2D.mat');
OutData2D_dn = OutData2D; %this variable is manning's n * 2 for std dev areas
clear OutData2D;

load ('/Users/andrearyan/Documents/MATLAB/PC2
20110603/NuecesRuns_20110610_outdata/Nueces2010_WR_14d_en_0p/OutData2D.mat');
OutData2D_en = OutData2D; %this variable is manning's n * 10 for std dev areas
clear OutData2D;

%% Total Volume in the Delta for Runs with varying roughness

length1 = size(OutData2D_an.depth_time);
mm = length1(2)-1;%-1 since the OutData2D_dn & en are 1 less time step

sum_volume_an = zeros(mm,1);
volume_an = zeros(667,971,mm);
for n = 1:mm
    volume_an(:,:,n) = OutData2D_an.depth(:,:,n);
    volume_an_nonan = volume_an(:,:,n);
    aa = isnan(volume_an_nonan);
    volume_an_nonan(aa) = 0; %get rid of NaNs
    volume_an(:,:,n) = volume_an_nonan;

    sum_volume_an(n,1) = sum(sum(volume_an(:,:,n)));
end

disp ('*****Finished Summing Volume for Normal Roughness Scenario*****')

sum_volume_bn = zeros(mm,1);
volume_bn = zeros(667,971,mm);
for n = 1:mm
    volume_bn(:,:,n) = OutData2D_bn.depth(:,:,n);
    volume_bn_nonan = volume_bn(:,:,n);
    aa = isnan(volume_bn_nonan);
    volume_bn_nonan(aa) = 0; %get rid of NaNs
    volume_bn(:,:,n) = volume_bn_nonan;

    sum_volume_bn(n,1) = sum(sum(volume_bn(:,:,n)));
end

disp ('*****Finished Summing Volume for 10x Roughness Scenario*****')

sum_volume_cn = zeros(mm,1);
```

```
volume_cn = zeros(667,971,mm);
for n = 1:mm
    volume_cn(:,:,n) = OutData2D_cn.depth(:,:,n);
    volume_cn_nonan = volume_cn(:,:,n);
    aa = isnan(volume_cn_nonan);
    volume_cn_nonan(aa) = 0; %get rid of NaNs
    volume_cn(:,:,n) = volume_cn_nonan;

    sum_volume_cn(n,1) = sum(sum(volume_cn(:,:,n)));
end

disp ('*****Finished Summing Volume for 100x Roughness Scenario*****')

sum_volume_dn = zeros(mm,1);
volume_dn = zeros(667,971,mm);
for n = 1:mm
    volume_dn(:,:,n) = OutData2D_dn.depth(:,:,n);
    volume_dn_nonan = volume_dn(:,:,n);
    aa = isnan(volume_dn_nonan);
    volume_dn_nonan(aa) = 0; %get rid of NaNs
    volume_dn(:,:,n) = volume_dn_nonan;

    sum_volume_dn(n,1) = sum(sum(volume_dn(:,:,n)));
end

disp ('*****Finished Summing Volume for 2x std dev Roughness Scenario*****')

sum_volume_en = zeros(mm,1);
volume_en = zeros(667,971,mm);
for n = 1:mm
    volume_en(:,:,n) = OutData2D_en.depth(:,:,n);
    volume_en_nonan = volume_en(:,:,n);
    aa = isnan(volume_en_nonan);
    volume_en_nonan(aa) = 0; %get rid of NaNs
    volume_en(:,:,n) = volume_en_nonan;

    sum_volume_en(n,1) = sum(sum(volume_en(:,:,n)));
end

disp ('*****Finished Summing Volume for 10x std dev Roughness Scenario*****')

% compare total volume of water in the system
x_an = OutData2D_an.depth_time./3600./24;
x_bn = OutData2D_bn.depth_time./3600./24;
x_cn = OutData2D_cn.depth_time./3600./24;
x_dn = OutData2D_dn.depth_time./3600./24;
x_en = OutData2D_en.depth_time./3600./24;

y_an = sum_volume_an.*15*15;
y_bn = sum_volume_bn.*15*15;
y_cn = sum_volume_cn.*15*15;
y_dn = sum_volume_dn.*15*15;
y_en = sum_volume_en.*15*15;
```

```
% % difference in total volume:
diff_totalvol = y_an - y_bn;
diff_totalvol2 = y_an - y_cn;
diff_totalvol3 = y_an - y_dn;
diff_totalvol4 = y_an - y_en;

%% percent diff in total volume
perc_totalvol = (y_an - y_bn)./y_an.*100;
perc_totalvol2 = (y_an - y_cn)./y_an.*100;
perc_totalvol3 = (y_an - y_dn)./y_an.*100;
perc_totalvol4 = (y_an - y_en)./y_an.*100;

%% Find max total volume of water in the system:
max_an_vol = max(sum_volume_an(:,1)).*15*15;
max_bn_vol = max(sum_volume_bn(:,1)).*15*15;
max_cn_vol = max(sum_volume_cn(:,1)).*15*15;
max_dn_vol = max(sum_volume_dn(:,1)).*15*15;
max_en_vol = max(sum_volume_en(:,1)).*15*15;
```

D.5 Analyzing pumping

```
%% Compare Pump Scenarios
load ('/Users/andrearyan/Documents/MATLAB/PC2
20110427/Analysis/Nueces_15x15_April2008/OutData3D_0p.mat');
OutData3D_0p = OutData3D; clear OutData3D;
disp ('*****Finished loading first variable*****')


load ('/Users/andrearyan/Documents/MATLAB/PC2
20110427/Analysis/Nueces_15x15_April2008_1pump/OutData3D_1p.mat');
OutData3D_1p = OutData3D; clear OutData3D;
disp ('*****Finished loading second variable*****')

load ('/Users/andrearyan/Documents/MATLAB/PC2
20110427/Analysis/Nueces_15x15_April2008_2pumps/OutData3D_2p.mat');
OutData3D_2p = OutData3D; clear OutData3D;
disp ('*****Finished loading third variable*****')

load ('/Users/andrearyan/Documents/MATLAB/PC2
20110427/Analysis/Nueces_15x15_April2008_3pumps/OutData3D_3p.mat');
OutData3D_3p = OutData3D; clear OutData3D;
disp ('*****Finished loading fourth variable*****')

%% Find Ai at each time step - considering all spaces with any Blue = 1
length1 = size(OutData3D_1p.Blue_time);
mm = length1(2);

depth_cutoff = 0.02; %this is the depth below which will not be included in Ai

% 1 PUMP
sum_area_1p = zeros(mm,1);
blue_1p = zeros(667,971,mm);
```

```
for n = 1:mm
    blue_1p(:,:,n) = OutData3D_1p.Blue(:,:,1,n);
    blue_1p_nonan = blue_1p(:,:,n);
    aa = isnan(blue_1p_nonan);
    blue_1p_nonan(aa) = 0; %get rid of nans
    bb = find(blue_1p_nonan > 0);
    blue_1p_nonan(bb) = 1; %make all non-zero values = 1 (no fractions)
    blue_1p(:,:,n) = blue_1p_nonan; %blue_1p(:,:,n) now has 1's where there is
blue tracer and 0's elsewhere

    sum_area_1p(n,1) = sum(sum(blue_1p(:,:,n))).*15.*15; %gives area inundated
at greater than 2 cm
end

disp ('*****Finished Finding Inundated Area for 1 Pump Scenario*****')

% 2 PUMPS
sum_area_2p = zeros(mm,1);
blue_2p = zeros(667,971,mm);

for n = 1:mm
    blue_2p(:,:,n) = OutData3D_2p.Blue(:,:,1,n);
    blue_2p_nonan = blue_2p(:,:,n);
    aa = isnan(blue_2p_nonan);
    blue_2p_nonan(aa) = 0; %get rid of nans
    bb = find(blue_2p_nonan > 0);
    blue_2p_nonan(bb) = 1; %make all non-zero values = 1 (no fractions)
    blue_2p(:,:,n) = blue_2p_nonan; %blue_2p(:,:,n) now has 1's where there is
blue tracer and 0's elsewhere

    sum_area_2p(n,1) = sum(sum(blue_2p(:,:,n))).*15.*15; %gives area inundated
at greater than 2 cm
end

disp ('*****Finished Finding Inundated Area for 2 Pump Scenario*****')

% 3 PUMPS

sum_area_3p = zeros(mm,1);
blue_3p = zeros(667,971,mm);

for n = 1:mm
    blue_3p(:,:,n) = OutData3D_3p.Blue(:,:,1,n);
    blue_3p_nonan = blue_3p(:,:,n);
    aa = isnan(blue_3p_nonan);
    blue_3p_nonan(aa) = 0; %get rid of nans
    bb = find(blue_3p_nonan > 0);
    blue_3p_nonan(bb) = 1; %make all non-zero values = 1 (no fractions)
    blue_3p(:,:,n) = blue_3p_nonan; %blue_1p(:,:,n) now has 1's where there is
blue tracer and 0's elsewhere

    sum_area_3p(n,1) = sum(sum(blue_3p(:,:,n))).*15.*15; %gives area inundated
at greater than 2 cm
end
```

```
disp ('*****Finished Finding Inundated Area for 3 Pump Scenario*****')

%% Find inundated area at each time step - with cutoff
length1 = size(OutData3D_1p.Blue_time);
mm = length1(2);

cutoff = 0.4; %this is the fraction of blue tracer required to be included in
Ai

% 1 PUMP
sum_area_1p_cutoff = zeros(mm,1);
blue_1p_cutoff = zeros(667,971,mm);

for n = 1:mm
    blue_1p_cutoff(:,:,n) = OutData3D_1p.Blue(:,:,1,n);
    blue_1p_clean = blue_1p_cutoff(:,:,n);
    aa = isnan(blue_1p_clean);
    blue_1p_clean(aa) = 0; %get rid of nans
    bb = find(blue_1p_clean > cutoff);
    blue_1p_clean(bb) = 1; %make all more than cutoff = 1
    cc = find(blue_1p_clean < cutoff);
    blue_1p_clean(cc) = 0; %make all less than cutoff = 0
    blue_1p_cutoff(:,:,n) = blue_1p_clean; %blue_1p(:,:,n) now has 1's where
there is blue tracer greater than cutoff and 0's elsewhere

    sum_area_1p_cutoff(n,1) = sum(sum(blue_1p_cutoff(:,:,n))).*15.*15; %gives
area inundated at greater than 2 cm
end

disp ('*****Finished Finding Cutoff Inundated Area for 1 Pump Scenario*****')

% 2 PUMP
sum_area_2p_cutoff = zeros(mm,1);
blue_2p_cutoff = zeros(667,971,mm);

for n = 1:mm
    blue_2p_cutoff(:,:,n) = OutData3D_2p.Blue(:,:,1,n);
    blue_2p_clean = blue_2p_cutoff(:,:,n);
    aa = isnan(blue_2p_clean);
    blue_2p_clean(aa) = 0; %get rid of nans
    bb = find(blue_2p_clean >= cutoff);
    blue_2p_clean(bb) = 1; %make all more than cutoff = 1
    cc = find(blue_2p_clean < cutoff);
    blue_2p_clean(cc) = 0; %make all less than cutoff = 0
    blue_2p_cutoff(:,:,n) = blue_2p_clean; %blue_1p(:,:,n) now has 1's where
there is blue tracer greater than cutoff and 0's elsewhere

    sum_area_2p_cutoff(n,1) = sum(sum(blue_2p_cutoff(:,:,n))).*15.*15; %gives
area inundated at greater than 2 cm
end

disp ('*****Finished Finding Cutoff Inundated Area for 2 Pump Scenario*****')
```

```
% 3 PUMP
sum_area_3p_cutoff = zeros(mm,1);
blue_3p_cutoff = zeros(667,971,mm);

for n = 1:mm
    blue_3p_cutoff(:,:,n) = OutData3D_3p.Blue(:,:,1,n);
    blue_3p_clean = blue_3p_cutoff(:,:,n);
    aa = isnan(blue_3p_clean);
    blue_3p_clean(aa) = 0; %get rid of nans
    bb = find(blue_3p_clean >= cutoff);
    blue_3p_clean(bb) = 1; %make all more than cutoff = 1
    cc = find(blue_3p_clean < cutoff);
    blue_3p_clean(cc) = 0; %make all less than cutoff = 0
    blue_3p_cutoff(:,:,n) = blue_3p_clean; %blue_1p(:,:,n) now has 1's where
there is blue tracer greater than cutoff and 0's elsewhere

    sum_area_3p_cutoff(n,1) = sum(sum(blue_3p_cutoff(:,:,n))).*15.*15; %gives
area inundated at greater than 2 cm
end

disp ('*****Finished Finding Cutoff Inundated Area for 3 Pump Scenario*****')

%% Pumping at each hour
ypump_1p = zeros(mm,1);
for bb = 1:mm
    ypump_1p(bb,1) = (0.5).*bb*3600;  % flow=0.5 cms/pump & bb is saved hourly
end

ypump_2p = zeros(mm,1);
for bb = 1:mm
    ypump_2p(bb,1) = (1.0).*bb*3600;
end

ypump_3p = zeros(mm,1);
for bb = 1:mm
    ypump_3p(bb,1) = (1.5).*bb*3600;
end

%% Compare Cutoff Scenarios for 2 Pump Scenario
% 2 PUMP
sum_area_2p_cutoff1_multiple = zeros(mm,1);
blue_2p_cutoff_multiple = zeros(667,971,mm);
area_with_cutoff_multiple = zeros(10,mm,1);

for j = 1:10
    cutoff = j.*0.1;
    for n = 1:mm
        blue_2p_cutoff_multiple(:,:,n) = OutData3D_2p.Blue(:,:,1,n);
        blue_2p_clean_multiple = blue_2p_cutoff_multiple(:,:,n);
        aa = isnan(blue_2p_clean_multiple);
        blue_2p_clean_multiple(aa) = 0; %get rid of nans
        bb = find(blue_2p_clean_multiple >= cutoff);
        blue_2p_clean_multiple(bb) = 1; %make all more than cutoff = 1
        cc = find(blue_2p_clean_multiple < cutoff);
```

```
        blue_2p_clean_multiple(cc) = 0; %make all less than cutoff = 0
        blue_2p_cutoff_multiple(:,:,n) = blue_2p_clean_multiple;
%blue_1p(:,:,n) now has 1's where there is blue tracer greater than cutoff and
0's elsewhere

        sum_area_2p_cutoff1_multiple(n,1) =
sum(sum(blue_2p_cutoff_multiple(:,:,n))).*15.*15; %gives area inundated at
greater than 2 cm
    end
    area_with_cutoff_multiple(j,:,1) = sum_area_2p_cutoff1_multiple;
end

disp ('*****Finished Finding Ai for various cutoffs for 2 Pump Scenario*****')

%% Compare Salinities

%% Find matrix at each time step for salinity less than salinity cutoff
(brackish water)
length1 = size(OutData3D_1p.Salinity_time);
mm = length1(2);

SAL_cutoff = 15; %this is the salinity cutoff

% 0 PUMP
sal_0p = zeros(667,971,mm);

for n = 1:mm
    sal_0p(:,:,n) = OutData3D_0p.Salinity(:,:,1,n);
    sal_0p_nonan = sal_0p(:,:,n);
    aa = isnan(sal_0p_nonan);
    sal_0p_nonan(aa) = SAL_cutoff+1; %get rid of nans - make NaN > cutoff
    cc = find(sal_0p_nonan <= SAL_cutoff);
    sal_0p_nonan(cc) = 1; %make all values <= 15ppt  = 1 (no fractions)
    bb = find(sal_0p_nonan > SAL_cutoff); %(this includes the NaNs)
    sal_0p_nonan(bb) = 0; %make all values > 15ppt  = 0 (no fractions)
    sal_0p(:,:,n) = sal_0p_nonan; % 1's where there is sal<=15 & 0's elsewhere
end

disp ('*****Finished Finding Salinity matrix for salinity < 15 for 1 Pump
Scenario*****')

% 1 PUMP
sal_1p = zeros(667,971,mm);

for n = 1:mm
    sal_1p(:,:,n) = OutData3D_1p.Salinity(:,:,1,n);
    sal_1p_nonan = sal_1p(:,:,n);
    aa = isnan(sal_1p_nonan);
    sal_1p_nonan(aa) = SAL_cutoff+1; %get rid of nans - make NaN > cutoff
    cc = find(sal_1p_nonan <= SAL_cutoff);
    sal_1p_nonan(cc) = 1; %make all values <= 15ppt  = 1 (no fractions)
    bb = find(sal_1p_nonan > SAL_cutoff);
    sal_1p_nonan(bb) = 0; %make all values > 15ppt  = 0 (no fractions)
    sal_1p(:,:,n) = sal_1p_nonan; % 1's where there is sal<=15 & 0's elsewhere
```

```
end

disp ('*****Finished Finding Sal matrix for sal < 15 for 1 Pump Scenario*****')

% 2 PUMPS
sal_2p = zeros(667,971,mm);

for n = 1:mm
    sal_2p(:,:,n) = OutData3D_2p.Salinity(:,:,1,n);
    sal_2p_nonan = sal_2p(:,:,n);
    aa = isnan(sal_2p_nonan);
    sal_2p_nonan(aa) = SAL_cutoff + 1; %get rid of nans - make NaN > cutoff
    cc = find(sal_2p_nonan <= SAL_cutoff);
    sal_2p_nonan(cc) = 1; %make all values <= 15ppt  = 1 (no fractions)
    bb = find(sal_2p_nonan > SAL_cutoff);
    sal_2p_nonan(bb) = 0; %make all values > 15ppt  = 0 (no fractions)
    sal_2p(:,:,n) = sal_2p_nonan; % 1's where there is sal<=15 & 0's elsewhere
end

disp ('*****Finished Finding Sal matrix for sal < 15 for 2 Pump Scenario*****')

% 3 PUMPS

sal_3p = zeros(667,971,mm);

for n = 1:mm
    sal_3p(:,:,n) = OutData3D_3p.Salinity(:,:,1,n);
    sal_3p_nonan = sal_3p(:,:,n);
    aa = isnan(sal_3p_nonan);
    sal_3p_nonan(aa) = 120; %get rid of nans - make NaN > cutoff
    cc = find(sal_3p_nonan <= SAL_cutoff);
    sal_3p_nonan(cc) = 1; %make all values <= 15ppt  = 1 (no fractions)
    bb = find(sal_3p_nonan > SAL_cutoff);
    sal_3p_nonan(bb) = 0; %make all values > 15ppt  = 0 (no fractions)
    sal_3p(:,:,n) = sal_3p_nonan; % 1's where there is sal<=15 & 0's elsewhere
end

disp ('*****Finished Finding Sal matrix for sal < 15 for 3 Pump Scenario*****')

%% Find matrix for fraction of freshwater
ref = 30; %reference level of 30 ppt

% 0 PUMP
frac_0p = zeros(667,971,mm);

for n = 1:mm
    frac_0p(:,:,n) = OutData3D_0p.Salinity(:,:,1,n);
    frac_0p_nonan = frac_0p(:,:,n);
    aa = isnan(frac_0p_nonan);
    frac_0p_nonan(aa) = ref + 3; %to get rid of nans – make NaN > ref
    F = (ref - frac_0p_nonan)./ref;
    bb = find(F < 0); %anywhere there was higher sal than ref, F < 0
    F(bb) = 0; %make all values > ref or NaN  = 0 (no fractions)
```

```
    frac_0p(:,:,n) = F;
end

disp ('*****Finished Finding FW fraction matrix for 0 Pump Scenario*****')

% 1 PUMP
frac_1p = zeros(667,971,mm);

for n = 1:mm
    frac_1p(:,:,n) = OutData3D_1p.Salinity(:,:,1,n);
    frac_1p_nonan = frac_1p(:,:,n);
    aa = isnan(frac_1p_nonan);
    frac_1p_nonan(aa) = ref + 3; %get rid of nans - make NaN > ref
    F = (ref - frac_1p_nonan)./ref;
    bb = find(F < 0); %anywhere there was higher sal than ref, F < 0
    F(bb) = 0; %make all values > ref or NaN  = 0 (no fractions)
    frac_1p(:,:,n) = F;
end

disp ('*****Finished Finding FW fraction matrix for 1 Pump Scenario*****')

% 0 PUMP
frac_2p = zeros(667,971,mm);

for n = 1:mm
    frac_2p(:,:,n) = OutData3D_2p.Salinity(:,:,1,n);
    frac_2p_nonan = frac_2p(:,:,n);
    aa = isnan(frac_2p_nonan);
    frac_2p_nonan(aa) = ref + 3; %get rid of nans - make NaN > ref
    F = (ref - frac_2p_nonan)./ref;
    bb = find(F < 0); %anywhere there was higher sal than ref, F < 0
    F(bb) = 0; %make all values > ref or NaN  = 0 (no fractions)
    frac_2p(:,:,n) = F;
end

disp ('*****Finished Finding FW fraction matrix for 2 Pump Scenario*****')

% 0 PUMP
frac_3p = zeros(667,971,mm);

for n = 1:mm
    frac_3p(:,:,n) = OutData3D_3p.Salinity(:,:,1,n);
    frac_3p_nonan = frac_3p(:,:,n);
    aa = isnan(frac_3p_nonan);
    frac_3p_nonan(aa) = ref + 3; %get rid of nans - make NaN > ref
    F = (ref - frac_3p_nonan)./ref;
    bb = find(F < 0); %anywhere there was higher sal than ref, F < 0
    F(bb) = 0; %make all values > ref or NaN  = 0 (no fractions)
    frac_3p(:,:,n) = F;
end

disp ('*****Finished Finding FW fraction matrix for 3 Pump Scenario*****')

%% Load OutData2D's for Depth
```

```
load ('/Users/andrearyan/Documents/MATLAB/PC2
20110427/Analysis/Nueces_15x15_April2008/OutData2D_0p.mat');
OutData2D_0p = OutData2D; clear OutData2D;
disp ('*****Finished loading first variable*****')

load ('/Users/andrearyan/Documents/MATLAB/PC2
20110427/Analysis/Nueces_15x15_April2008_1pump/OutData2D_1p.mat');
OutData2D_1p = OutData2D; clear OutData2D;
disp ('*****Finished loading second variable*****')

load ('/Users/andrearyan/Documents/MATLAB/PC2
20110427/Analysis/Nueces_15x15_April2008_2pumps/OutData2D_2p.mat');
OutData2D_2p = OutData2D; clear OutData2D;
disp ('*****Finished loading third variable*****')

load ('/Users/andrearyan/Documents/MATLAB/PC2
20110427/Analysis/Nueces_15x15_April2008_3pumps/OutData2D_3p.mat');
OutData2D_3p = OutData2D; clear OutData2D;
disp ('*****Finished loading fourth variable*****')

%% Calculate Volume of Brackish water (volume < SAL_cutoff)

% 0 Pumps:
vol_brack_0p = zeros(mm,1);

for n = 1:mm
    depth_0p = OutData2D_0p.depth(:,:,n);
    gg = isnan(depth_0p);
    depth_0p(gg) = 0;
    brackish_0p = sum(sum(sal_0p(:,:,n).*depth_0p)).*15.*15;
   %this multiplies the depth by 1 for any cell with salinity < 15ppt and 0 for
any cell > 15ppt and also takes the sum to find the volume (sum up all the
depths & multiply by 225)
   vol_brack_0p(n,1) = brackish_0p;
end

% 1 Pumps:
vol_brack_1p = zeros(mm,1);

for n = 1:mm
    depth_1p = OutData2D_1p.depth(:,:,n);
    gg = isnan(depth_1p);
    depth_1p(gg) = 0;
   brackish_1p = sum(sum(sal_1p(:,:,n).*depth_1p)).*15.*15;
   %this multiplies the depth by 1 for any cell with salinity < 15ppt and 0 for
any cell > 15ppt and also takes the sum to find the volume (sum up all the
depths & multiply by 225)
   vol_brack_1p(n,1) = brackish_1p;
end

% 2 Pumps:
vol_brack_2p = zeros(mm,1);
```

```
for n = 1:mm
    depth_2p = OutData2D_2p.depth(:,:,n);
    gg = isnan(depth_2p);
    depth_2p(gg) = 0;
   brackish_2p = sum(sum(sal_2p(:,:,n).*depth_2p)).*15.*15;
   %this multiplies the depth by 1 for any cell with salinity < 15ppt and 0 for
any cell > 15ppt and also takes the sum to find the volume (sum up all the
depths & multiply by 225)
   vol_brack_2p(n,1) = brackish_2p;
end

% 3 Pumps:
vol_brack_3p = zeros(mm,1);

for n = 1:mm
    depth_3p = OutData2D_3p.depth(:,:,n);
    gg = isnan(depth_3p);
    depth_3p(gg) = 0;
    brackish_3p = sum(sum(sal_3p(:,:,n).*depth_3p)).*15.*15;
   %this multiplies the depth by 1 for any cell with salinity < 15ppt and 0 for
any cell > 15ppt and also takes the sum to find the volume (sum up all the
depths & multiply by 225)
   vol_brack_3p(n,1) = brackish_3p;
end

%% Calculate V_FW in the system (assuming 30 as the ref salinity)

% 0 Pumps
frac_0p(:,:,n);
vol_fresh_0p = zeros(mm,1);

for n = 1:mm
    depth_0p = OutData2D_0p.depth(:,:,n);
    gg = isnan(depth_0p);
    depth_0p(gg) = 0;
   fresh_0p = sum(sum(frac_0p(:,:,n).*depth_0p)).*15.*15;
    % this multiplies the fraction of freshwater in each cell by the depth
    % and area to find the volume of freshwater
   vol_fresh_0p(n,1) = fresh_0p;
end

% 1 Pumps
frac_1p(:,:,n);
vol_fresh_1p = zeros(mm,1);

for n = 1:mm
    depth_1p = OutData2D_1p.depth(:,:,n);
    gg = isnan(depth_1p);
    depth_1p(gg) = 0;
    fresh_1p = sum(sum(frac_1p(:,:,n).*depth_1p)).*15.*15;
    % this multiplies the fraction of freshwater in each cell by the depth
    % and area to find the volume of freshwater
   vol_fresh_1p(n,1) = fresh_1p;
end
```

```
% 2 Pumps
frac_2p(:,:,n);
vol_fresh_2p = zeros(mm,1);

for n = 1:mm
    depth_2p = OutData2D_2p.depth(:,:,n);
    gg = isnan(depth_2p);
    depth_2p(gg) = 0;
    fresh_2p = sum(sum(frac_2p(:,:,n).*depth_2p)).*15.*15;
    % this multiplies the fraction of freshwater in each cell by the depth
    % and area to find the volume of freshwater
    vol_fresh_2p(n,1) = fresh_2p;
end

% 3 Pumps
frac_3p(:,:,n);
vol_fresh_3p = zeros(mm,1);

for n = 1:mm
    depth_3p = OutData2D_3p.depth(:,:,n);
    gg = isnan(depth_3p);
    depth_3p(gg) = 0;
   fresh_3p = sum(sum(frac_3p(:,:,n).*depth_3p)).*15.*15;
    % this multiplies the fraction of freshwater in each cell by the depth
    % and area to find the volume of freshwater
   vol_fresh_3p(n,1) = fresh_3p;
end
```

This page intentionally left blank for two-sided printing.

E References

Adams, John S., and Jace Tunnell, (2010). *Rincon Bayou Salinity Monitoring Project.*. Technical Report, Coastal Bend Bays & Estuaries Program. Corpus Christi.

Alan Plummer Associates, Inc. (2007). *City of Corpus Christi Water Supply Project*. Technical Report.

Alber, Merryl, (2002). "A Conceptual Model of Estuarine Freshwater Inflow Management." *Estuaries* 25:6B:1262-1274.

Alexander, Heather D., and Kenneth H. Dunton, (2002). "Freshwater Inundation Effects on Emergent Vegetation of a Hypersaline Salt Marsh." *Estuaries*, 25:6B:1426-1425.

Alexander, Heather D., and Kenneth H. Dunton, (2006). "Treated Wastewater Effluent as an Alternative Freshwater Source in a Hypersaline Salt Marsh: Impacts on Salinity, Inorganic Nitrogen, and Emergent Vegetation." *Journal of Coastal Research,* 22:2:377-392.

Battjes, Jurjen A., (2006). "Developments in coastal engineering research." *Coastal Engineering,* 53:121-132.

Bisht, Gautam, Virginia Venturini, and Shafiqul Isl. (2005). "Estimation of the net radiation using MODIS (Moderate Resolution Imaging Spectroradiometer) data for clear sky days." *Remote Sensing of Environment,* 97:52-67.

Bureau of Reclamation. (2000a). *Concluding Report: Rincon Bayou Demonstration Project. Volume I: Executive Summary.* United States Department of the Interior, Bureau of Reclamation, Oklahoma-Texas Area Office, Austin, Texas.

Bureau of Reclamation, (2000b). *Concluding Report: Rincon Bayou Demonstration Project. Volume II: Findings.* United States Department of the Interior, Bureau of Reclamation, Oklahoma-Texas Area Office, Austin, Texas.

Casulli, V., and E. Cattani, (1994). "Stability, Accuracy and Efficiency of a Semi-Implicit Method for Three-Dimensional Shallow Water Flow." *Computers & Mathematics with Applications,* 27:4:99-112.

Casulli, V., and P. Zanolli, (2002). "Semi-Implicit Numerical Modeling of Nonhydrostatic Free-Surface Flows for Environmental Problems." *Mathematical and Computer Modelling,* 36:1131-1149.

Casulli, Vincenzo, and Ralph T. Cheng, (1992). "Semi-Implicit Finite Difference Methods for Three-Dimensional Shallow Water Flow." *International Journal for Numerical Methods in Fluids,* 15:629-648.

Charbeneau, Randall J., and Edward R. Holley, (2001). *Backwater Effects of Bridge Piers in Subcritical Flow.* Project Summary Report, Center for Transportation Research, University of Texas at Austin.

Chen, Changsheng, Hedong Liu, and Robert C. Beardsley, (2003). "An Unstructured Grid, Finite-Volume, Three-Dimensional, Primitive Equations Ocean Model: Application

to Coastal Ocean and Estuaries." *Journal of Atmospheric and Oceanic Technology,* 20:159-186.

Copeland, B.J., (1996). "Effects of Decreased River Flow on Estuarine Ecology." *Water Pollution Control Federation,* 38:11:1831-1839.

Cunningham, Atlee M., (1999). *Corpus Christi Water Supply Documented History 1852-1997. Second Edition.* Texas A&M University-Corpus Christi,.

Gibeaut, J., (2003). "LiDAR: Mapping a Shoreline by Laser Light." *Geotimes,* 48:11:22-27.

Heilman, J.L., F.A. Heinsch, D.R. Cobos, and K.J. McInnes, (2000). "Energy Balance of a High Marsh on the Texas Gulf Coast: Effect of Water Availability." *Journal of Geophysical Research,* 105:D17:22371-22377.

Hodges, Ben R., (2004). "Accuracy Order of Crank–Nicolson Discretization for Hydrostatic Free-Surface Flow." *Journal oF Engineering Mechanics-ASCE,* 130:8:904-910.

Hodges, Ben R., Bernard Laval, and Bridget M. Wadzuk, (2006). "Numerical error assessment and a temporal horizon for internal waves in a hydrostatic model." *Ocean Modelling,* 13:44-64.

Hodges, Ben R., and Francisco J. Rueda (2008). "Semi-implicit two-level predictor-corrector methods for non-linearly coupled, hydrostatic, barotropic/baroclinic flows." *International Journal of Computational Fluid Dynamics*, 22:9:593-607.

Hossain, AKMA, Yafei Jia, and Xiabo Chao, (2009). "Estimation of Manning's Roughness Coefficient Distribution for Hydrodynamic Model Using Remotely Sensed Land Cover Features." *2009 17th International Conference on Geoinformatics,* George Mason University. pp. 635-638.

Irlbeck, M.J., and G.H. Ward, (2000). "Analysis of the historic flow regime of the Nueces River into the upper Nueces Delta, and of the potential restoration value of the Rincon Bayou Demonstration Project." In *Concluding Report: Rincon Bayou Demonstration Project, Appendix C.* (United States Department of the Interior, Bureau of Reclamation),.

Ji, Z.-G., M.R. Morton, and J.M. Hamrick, (2001). "Wetting and Drying Simulation of Estuarine Processes." *Estuarine, Coastal and Shelf Science,* 53:683-700.

Montagna, P.A., E.M. Hill, and B. Moulton, (2009). "Role of Science-based and Adaptive Management in Allocating Environmental Flows to the Nueces Estuary, Texas, USA." *WIT Transactions on Ecology and the Environment,* 122:559-570.

Montagna, Paul A., Alber Merryl, Doering Peter, and Connor S. Michael, (2002). "Freshwater Inflow: Science, Policy, Management." *Estuaries,* 25:6B:1243-1245.

Montagna, Paul A., Richard D. Kalke, and Christine Ritter, (2002). "Effect of Restored Freshwater Inflow on Macrofauna and Meiofauna in Upper Rincon Bayou, TX, USA." *Estuaries,* 25:6B:1436-1447.

Nicolau, Brien A., John Jr. W. Tunnell, John S. Adams, and Barbara F. Ruth, (1996). "Long-Term Monitoring of Estuarine Faunal Use in the Nueces Delta Mitigation Project,

Corpus Christi, Texas: 1989 Through 1995." *Annual Ecosystem Restoration Conference.* Tampa, Florida.

Nicolau, Terri, et al. (2002). *Nueces Estuary Advisory Council Recommended Monitoring Plan For Rincon Bayou*, *Nueces Delta.*

Ockerman, D.J., (2001). *Water Budget for the Nueces Estuary, Texas, May-October 1998.* Fact Sheet, U.S. Department of the Interior, U.S. Geological Survey.

Oey, Lie-Yauw, (2006). "An OGCM with movable land-sea boundaries." *Ocean Modelling* 13:176-195.

Palmer, Terry A., Paul A. Montagna, and Richard D. Kalke, (2002). "Downstream Effects of Restored Freshwater Inflow to Rincon Bayou, Nueces Delta, Texas, USA." *Estuariesc* 25:6B:1448-1456.

Pulich, Warren, (2006). *Texas Coastal Bend*. USGS.

Rasser, Michael Kevin, (2009). *The Role of Biotic and Abiotic Processes in the Zonation of Salt Marsh Plants in the Nueces River Delta, Texas.* Dissertation, The University of Texas at Austin.

Roman, Charles T., Richard W. Garvine, and John W. Portnoy, (1995). "Hydrologic Modeling as a Predictive Basis for Ecological Restoration of Salt Marshes." *Environmental Management* 19:4:559-566.

Rueda, F.J., E. Sanmiguel-Rojas, and B.R. Hodges, (2007). "Baroclinic stability for a family of two-level semi-implicit numerical methods for the 3D shallow water equations." *International Journal for Numerical Methods in Fluids* 54:3:237-268.

Ryan, A.J., (2011). *Modeling Hydrodynamic Fluxes in the Nueces River Delta*. M.S. Thesis, Department of Civil, Architectural and Environmental Engineering, University of Texas at Austin, 116 pgs.

Sellers, William, (1965). *Physical Climatology.* The University of Chicago Press.

Spillman, C.M., Hamilton, D.P., Hipsey, M.R., Imberger J., (2008). "A spatially resolved model of seasonal variations in phytoplankton and clam (Tapes philippinarum) biomass in Barbamarco Lagoon, Italy." *Estuarine Coastal and Shelf Science,* 79:2:2:187-203.

Stelling, G.S., H.W.J. Kernkamp, and M.M. Laguzzi, (1998). "Delft Flooding System: A powerful tool for inundation assessment based upon a positive flow simulation." *Hydroinformatics*. 449-456.

Tolan, J.M., (2007). "El Nino-Southern Oscillation impacts translated to the watershed scale: Estuarine salinity patterns along the Texas Gulf Coast, 1982 to 2004." *Estuarine Coastal and Shelf Science,* 72,:1-2:247-260.

U.S. Secretary of Commerce (2008). *National Institute of Standards and Technology Chemistry WebBook.*. http://webbook.nist.gov/chemistry/ (accessed 2011).

Veilleux, Vicki, (2011). *National Geodetic Survey: Frequently Asked Questions.* January. http://www.ngs.noaa.gov/faq.shtml.

Ward, George H., (1997). *Processes and Trends of Circulation within the Corpus Christi Bay National Estuary Program Study Area.* Corpus Christi: Texas National Resource Conservation Commission.

Ward, George H., Michael J. Irlbeck, and Paul A. Montagna, (2002). "Experimental River Diversion for Marsh Enhancement." *Estuaries* 25:6B:1416-1425.

Wunderlich, Walter O. (1972). *Heat and Mass Transfer Between a Water Surface and the Atmosphere.* Laboratory Report No. 14, Tennessee Valley Authority,.

Xia, Junqiang, Roger A. Falconer, and Binliang Lin, (2010). "Hydrodynamic impact of a tidal barrage in the Severn Estuary, UK." *Renewable Energy,* 35:1455–1468.

Yang, Zhaoqing, and Tarang Khangaonkar, (2009). "Modeling tidal circulation and stratification in Skagit River estuary using an unstructured grid ocean model." *Ocean Modelling,* 28:34-49.

Zhang, Yinglong, Antonio M. Baptista, and Edward P. III Myers, (2004). "A cross-scale model for 3D baroclinic circulation in estuary-plume-shelf systems: I. Formulation and skill assessment." *Continental Shelf Research,* 24:2187-2214.

Zheng, Lianyuan, Changsheng Chen, and Frank Y. Zhang, (2004). "Development of water quality model in the Satilla River Estuary, Georgia." *Ecological Modelling,* 178:457-482.